

2020

Synthesis and Design of Novel Polymer Grafted Nanoparticles Relevant to Drug Delivery Vehicles for Biomedical Application

Maan Abduldiyem Hassan Al-Ali

Follow this and additional works at: <https://scholarcommons.sc.edu/etd>



Part of the [Chemistry Commons](#)

Recommended Citation

Al-Ali, M. A.(2020). *Synthesis and Design of Novel Polymer Grafted Nanoparticles Relevant to Drug Delivery Vehicles for Biomedical Application*. (Doctoral dissertation). Retrieved from <https://scholarcommons.sc.edu/etd/6088>

This Open Access Dissertation is brought to you by Scholar Commons. It has been accepted for inclusion in Theses and Dissertations by an authorized administrator of Scholar Commons. For more information, please contact digres@mailbox.sc.edu.

SYNTHESIS AND DESIGN OF NOVEL POLYMER GRAFTED
NANOPARTICLES RELEVANT TO DRUG DELIVERY VEHICLES
FOR BIOMEDICAL APPLICATIONS

by

Maan Abduldiyem Hassan Al-Ali

Bachelor of Science
University of Basrah, 2000

Master of Science
University of Basrah, 2007

Submitted in Partial Fulfillment of the Requirements

For the Degree of Doctor of Philosophy in

Chemistry

College of Arts and Sciences

University of South Carolina

2020

Accepted by:

Brian C. Benicewicz, Major Professor

Chuanbing Tang, Committee Member

Andrew B. Greytak, Committee Member

Alan W. Decho, Committee Member

Cheryl L. Addy, Vice Provost and Dean of the Graduate School

© Copyright by Maan Abduldiyem Hassan Al-Ali, 2020
All Rights Reserved.

DEDICATION

To the soul of my beloved father, my first ideal.

To the source of tenderness that illuminates my life, my dear mother.

To my soulmate who supported me and stood with me in hardness days, my wife,
Ayat.

To my adorable children, Nooran, Fatima, Sarah, and Yousuf.

To my brothers and sisters.

ACKNOWLEDGMENTS

First and foremost, it is a great honor and a big privilege to get my degree mentored by my research advisor, Dr. Brian C. Benicewicz. I would like to express my sincere gratitude to such an enthusiastic and knowledgeable person. Also, I would like to thank him for all of his guidance and support for my research projects. With his knowledge and enthusiasm for polymer science and chemistry, I experienced a diverse, productive, and stimulating environment in my career. I eagerly appreciate his advice and guidance, and I am sincerely grateful for all of the opportunities that I have had while working in his group.

I would like to thank my doctoral committee members, Dr. Chuanbing Tang, Dr. Andrew B. Greytak, and Dr. Alan W. Decho, for their contributions and encouragement, and suggestions on my research. I want to thank Dr. Decho and his student Savannah Chandler for their collaborations with our group.

I would like to thank the Benicewicz group members, both past and present, for all of their help, suggestions, and friendship. Especially, I would like to thank Dr. Kayley Hayat and Dr. Michel Bell for their help when I first joined the group. Great thanks to Susan Hipp, Warren Steckle, for their help during my study in Horizon building. Also, I would like to thank Dr. Julia Pribyl, Dr. Andrew

Pingitore, Dr. Yucheng Huang, Dr. Mohammad Khani, Dr. Yang Zheng, Dr. Zaid Alajeely, Laura Murdock, Dr. Fei Huang, Dr. Lihui Wang, Karl Golian, Caroline Rohlfing, Richard Ly, and many others. Thanks for all your help and suggestions!

Next, I would like to thank my family, my wife, our daughters, and our son, who, without their lovely emotional support and encouragement, I could not be here. I would love to thank my brothers and sisters for always supporting and encouraging me. Thanks and great gratitude for both my first inspirational and teacher in my life, my dear father, and my dear mother, who will be more proud of me than myself.

Finally, I would like to thank the Iraqi Ministry of Higher Education and Scientific Research for funding me for the first five years in my Ph.D. program.

ABSTRACT

The modification of inorganic nanoparticles with organic polymer chains has become a significant field of study for the engineering of advanced nanocomposite materials. This dissertation presents the design, synthesis, and characterization of novel polymer grafted silica nanoparticles as new strategies to combat bacterial resistance. Described herein is the synthesis of monomers that have been graft polymerized onto silica nanoparticles that can be used as a delivery drug vehicle for biomedical applications. The polymerization of these monomers was performed via reversible addition-fragmentation chain transfer (RAFT) polymerization. The molecular design of the RAFT agents that are attached to the surfaces of the nanoparticles has the main role in controlling the molecular weight and dispersity of the polymer chains grafted to the surface of the nanoparticles. The method of attachment of the RAFT agents additionally controls the surface graft density. The important properties of nanocomposites can be exploited in many different areas, such as biomedical applications.

In the first chapter of this work, the overall background of antimicrobial polymers, the functionalization of nanoparticles using RAFT polymerization, and

the concept of the modification of silica nanoparticles to afford a bimodal brush system is described. The second chapter focuses on designing a new type of stimulus-responsive polymer that can work as antibiotic-delivery carriers in biomedical applications. We reported pH-responsive “controlled release” polymers that were grafted on silica nanoparticles using reversible addition-fragmentation chain transfer (RAFT) polymerization. Two monomers 2-((2-(propionyloxy) propanoyl)oxy)ethyl methacrylate (HEMA-LA) and 4-(2-(methacryloyloxy)ethoxy)-4-oxobutanoic acid (HEMA-SA), containing hydrolytically sensitive ester linkages were synthesized to functionalize on the surface of silica nanoparticles. The degradation rate was monitored by attaching dyes at the end of these monomers in each repeat unit to study the release rate, thus assessing the use of these monomers as delivery vehicles for anti-bacterial applications.

In the following chapter, bimodal polymer chains grafted on the surface of silica nanoparticles was developed via RAFT polymerization to create water-dispersible nanoparticles that have additional advantages as antibiotic-delivery vehicles in biomedical applications. Two different polymer chains populations were attached to silica nanoparticles; the first population is high graft density with low molecular weight, which is a pH-responsive controlled release polymer derived from two possible monomers (HEMA-LA) and (HEMA-SA), both

containing a hydrolytically sensitive ester linkage: the second population is a water-dissolvable polymer of methacrylic acid (MAA) at low graft density with high molecular weight. Fluorescent dyes were conjugated to the controlled release polymers to monitor the nanoparticles in biological systems.

Finally, in the fourth chapter, we described a new approach using two different RAFT agents, 4-cyano-4-(phenylcarbonothioylthio)pentanoic acid (CPDB), and 4-cyano-4-[(dodecylsulfanylthiocarbonyl)sulfanyl]pentanoic acid (CDSS) to create bimodal polymer brush grafted nanoparticle. These novel bimodal brush silica nanoparticles were designed successfully to combat antibiotic-resistant bacteria. The first population polymer brush is based on two potential “controlled release” monomers 2-((2-((2-hydroxy propanoyl)oxy) propanoyl)oxy) ethyl methacrylate (HEMA-LA), 2-(methacryloyloxy)ethyl succinate (HEMA-SA) containing a hydrolytically sensitive ester linkage as a high graft density, short brush to work as antibiotic-delivery carriers. However, the second population polymer brush was based on a sugar-containing monomer, 2-methacrylamido glucopyranose (MAG), as a low graft density, long brush to enhance bacterial uptake of nanoparticles.

TABLE OF CONTENTS

DEDICATION	iii
ACKNOWLEDGEMENTS.....	iv
ABSTRACT	vi
LIST OF TABLES.....	xii
LIST OF FIGURES.....	xiii
LIST OF SCHEMES.....	xviii
LIST OF ABBREVIATIONS.....	xxi
CHAPTER 1: INTRODUCTION	1
1.1 RAFT Polymerization	2
1.2 Mechanism of RAFT polymerization.....	3
1.3 Polymer Grafted Nanoparticles	5
1.4 Nanoparticles as delivery vehicles	9
1.5 Bimodal Nanocomposites	10
1.6 References.....	11

CHAPTER 2: POLYMERIZATION OF “CONTROLLED RELEASE” MONOMERS CONTAINING A HYDROLYTICALLY SENSITIVE ESTER LINKAGE VIA RAFT POLYMERIZATION.....	16
2.1 Abstract.....	17
2.2 Introduction	18
2.3 Experimental.....	20
2.4 Results and Discussion.....	31
2.5 Conclusions.....	49
2.6 References	50
CHAPTER 3: ENGINEERING WATER-DISPERSIBLE BIMODAL POLYMER GRAFTED SILICA NANOPARTICLES AS ANTIBIOTIC-CARRIERS	54
3.1 Abstract.....	55
3.2 Introduction	56
3.3 Materials and Methods.....	58
3.4 Results and Discussion.....	72
3.5 Conclusions.....	88
3.6 References	89
CHAPTER 4: DESIGNING “SWEET-NANOPARTICLES” AS A NOVEL STRATEGY TO COMBAT ANTIBIOTIC-RESISTANT BACTERIA.....	95
4.1 Abstract.....	96
4.2 Introduction	97
4.3 Materials and Methods.....	100

4.4 Results and Discussion.....	114
4.5 Conclusions.....	134
4.6 References	135
CHAPTER 5: CONCLUSION AND FUTURE WORK	143
5.1 Conclusions.....	144
5.2 Future Work.....	147
BIBLIOGRAPHY	153

LIST OF TABLES

Table 2.1 Various molecular weights and chain densities of SiO ₂ @P(HEMA-LA) and SiO ₂ @P(HEMA-SA) using RAFT polymerization.....	38
Table 3.1 Grafting densities and molecular weights of bimodal nanoparticles, SiO ₂ @P(HEMA-LA-dye)-PMAA, and SiO ₂ @P(HEMA-SA-dye)-PMAA.....	84
Table 4.1 Polymerization of the glycomonomer (MAG-TMS) using CDSS as RAFT agent and AIBN as an initiator at 65°C.....	128
Table 4.2 Molecular weights and grafting densities of bimodal nanoparticles, SiO ₂ @P(HEMA-LA-dye)-PMAG, and SiO ₂ @P(HEMA-SA-dye)-PMAG.....	129

LIST OF FIGURES

Figure 1.1 The three main CRP methods.....	3
Figure 1.2 Generalized dithioester RAFT agent and polymer formed using a RAFT agent.....	4
Figure 1.3 General mechanism of RAFT polymerization.....	5
Figure 1.4 Bare nanoparticles vs. polymer grafted nanoparticles in a polymer matrix	6
Figure 1.5 Techniques of polymer attachment A) physisorption, B) grafting-to approach, C) grafting-from approach	8
Figure 1.6 Polymer morphologies resulting from various grafting densities	8
Figure 1.7 Illustration of various architectures of core-shell nanoparticles: (a) single shell and (b) double shell, both of which are classified as monomodal core-shell nanoparticles, and (c) bimodal core-shell nanoparticles	11
Figure 2.1 ¹ H-NMR (300 MHz, CDCl ₃) spectrum of HEMA-LA monomer	23
Figure 2.2 ¹ H-NMR (300 MHz, CDCl ₃) spectrum of HEMA-SA monomer.....	25
Figure 2.3 Images of serial dilutions, UV spectrum of various concentrations, and the resultant calibration curves of (a) NBD-COOH, (b) NBD-NH ₂ dyes	30

Figure 2.4 (a) Pseudo first-order kinetic plots of HEMA-LA with free CPDB (black solid circle); CPDB grafted nanoparticles with 0.1 ch./nm² density (black solid square) (b) dependence of molecular weight of HEMA-LA (red squares and circles), (solid black line, theoretical Mn), and the dispersity (blue squares and circles) on the conversion for the RAFT polymerization of HEMA-LA with ratio between species [CPDB]/[HEMA-LA]/[AIBN]=500:1:0.1 with free CPDB (squares); CPDB grafted nanoparticles with 0.1 ch./nm² density (circles) (c) pseudo first-order kinetic plots of HEMA-SA with free CPDB (black solid circle); CPDB grafted nanoparticles with 0.1 ch./nm² density (black solid square) (d) dependence of molecular weight of HEMA-SA (red squares and circles), (solid black line, theoretical Mn), and the dispersity (blue squares and circles) on the conversion for the RAFT polymerization of HEMA-SA with ratio between species [CPDB]/[HEMA-SA]/[AIBN]=500:1:0.1 with free CPDB (squares); CPDB grafted nanoparticles with 0.1 ch./nm² density (circles)34

Figure 2.5 GPC traces of (a) SiO₂@P(HEMA-LA) and (b) SiO₂@P(HEMA-SA) in THF using ratio 500:1:0.1 of [monomer]: [CTA]:[initiator] at different times38

Figure 2.6 UV-vis, FT-IR spectrums of SiO₂-g-P(HEMA-LA)-dye (red curve), and SiO₂-g-P(HEMA-SA)-dye (black curve).....41

Figure 2.7 TGA trace of (a) SiO₂-g-HEMA-LA-dye and (b) SiO₂-g-HEMA-SA-dye nanoparticles.....43

Figure 2.8 UV-vis spectra of SiO₂@P(HEMA-LA)-NBD-COOH at (a) 25°C and (b) 37°C for 58 days.....45

Figure 2.9 UV-vis spectra of SiO₂@P(HEMA-SA)-NBD-NH₂ at (a) 25°C and (b) 37°C for 58 days.....45

Figure 2.10 Cumulative release rate of (a) SiO ₂ @P(HEMA-LA-dye) and (b) SiO ₂ @P(HEMA-SA-dye), at 25°C and 37°C for 58 days.....	46
Figure 2.11 Cumulative release rate of SiO ₂ @P(HEMA-LA-dye) and SiO ₂ @P(HEMA-SA-dye) at 25°C and 37°C for 58 days	48
Figure 3.1 ¹ H NMR (300 MHz, CDCl ₃) spectrum of HEMA-LA monomer	62
Figure 3.2 ¹ H NMR (300 MHz, CDCl ₃) spectrum of HEMA-SA monomer.....	63
Figure 3.3 (a)Pseudo first-order kinetic plot of HEMA-LA. (b) dependence of molecular weight of HEMA-LA (red circle), theoretical molecular weight (solid line), and the dispersity (blue circle) on the conversion for the surface-initiated RAFT polymerization of HEMA-LA on modified silica nanoparticles with CPDB density: 0.1 chains/nm ² ([CPDB]/[HEMA-LA]/[AIBN]=500:1:0.1). (c) Pseudo first-order kinetic plot of HEMA-SA and (d) Dependence of molecular weight of HEMA-SA (red circle), theoretical molecular weight (solid line), and the dispersity (blue circle) on the conversion for the surface-initiated RAFT polymerization of HEMA-SA on modified silica nanoparticles with CPDB density: 0.1 chains/nm ² ([CPDB]/[HEMA-SA]/[AIBN]=500:1:0.1).....	74
Figure 3.4 Thermogravimetric analysis of (a) SiO ₂ -g-P(HEMA-LA), and (b) SiO ₂ -g-P(HEMA-SA) nanoparticles.....	76
Figure 3.5 UV-vis spectra of prepared NBD-dyes NBD-COOH, NBD-NH ₂ and commercially available dye, NBD-NHS.....	79
Figure 3.6 GPC analysis of bimodal grafted nanoparticles (a) SiO ₂ -g-P(HEMA-LA-dye)-PMAA, and (b) SiO ₂ -g-P(HEMA-SA-dye)-PMAA	85

Figure 3.7 TGA analysis of (a) Bare SiO ₂ , Monomodal NP's SiO ₂ -g-P(HEMA-LA), and Bimodal NP's SiO ₂ -g-P(HEMA-LA)-(PMAA), (b) Bare SiO ₂ , Monomodal NP's SiO ₂ -g-P(HEMA-SA), and Bimodal NP's SiO ₂ -g-P(HEMA-SA)-(PMAA).....	87
Figure 4.1 UV absorption spectra of polymer grafted nanoparticles with cleaved CDSS RAFT agent (red line), and with CDSS attached to the polymers on the surface of silica nanoparticles (black line).....	119
Figure 4.2 UV-vis, FT-IR spectrums of MA 200: SiO ₂ @P(HEMA-LA)-NBD-COOH, and MA 195: SiO ₂ @P(HEMA-SA)-NBD-NH ₂	122
Figure 4.3 The dispersion of dye labeled polymer grafted nanoparticles (SiO ₂ -g-P(HEMA-SA)-dye) and the fluorescence under UV-vis light.....	117
Figure 4.4 ¹ H-NMR spectrums of CDSS RAFT agent, CDSS-OH, and CDSS-Phosphate and (b) ³¹ P-NMR spectrum of CDSS-Phosphate.....	124
Figure 4.5 UV-vis, FT-IR spectrums of synthesized RAFT agent (CDSS-Phosphate).....	124
Figure 4.6 UV-vis of the CDSS-Phosphate grafted on the surface of monomodal nanoparticles.....	126
Figure 4.7 ¹ H-NMR of the glucomonomer TMS-MAG.....	127
Figure 4.8 ¹³ C-NMR of the glucomonomer TMS-MAG.....	127

Figure 4.9 GPC traces of bimodal grafted silica nanoparticles

a) bimodal grafted nanoparticles $\text{SiO}_2\text{-g-P(HEMA-LA-dye)-P(TMS-MAG)}$ (blue line), deconvoluted peaks of monomodal nanoparticles $\text{SiO}_2\text{-g-P(HEMA-LA-dye)}$ (green line), and $\text{SiO}_2\text{-g-P(TMS-MAG)}$ (red line), measured monomodal grafted nanoparticles $\text{SiO}_2\text{-g-P(HEMA-LA)}$ (black line). b) bimodal grafted nanoparticles $\text{SiO}_2\text{-g-P(HEMA-SA-dye)-P(TMS-MAG)}$ (blue line), deconvoluted peaks of monomodal nanoparticles $\text{SiO}_2\text{-g-P(HEMA-SA-dye)}$ (green line), and $\text{SiO}_2\text{-g-P(TMS-MAG)}$ (red line), measured monomodal grafted nanoparticles $\text{SiO}_2\text{-g-P(HEMA-SA)}$ (black line).....130

Figure 4.10 The fluorescence under UV-vis of the “Sweet Bimodal nanoparticles, (a) $\text{SiO}_2\text{@P(HEMA-LA-dye)-PMAG}$, and (b) $\text{SiO}_2\text{@P(HEMA-SA-dye)-PMAG}$142

LIST OF SCHEMES

Scheme 2.1 Synthesis of HEMA-LA monomer	23
Scheme 2.2 Synthesis of HEMA-SA monomer	24
Scheme 2.3 Polymerization of (a) HEMA-LA and (b) HEMA-SA mediated by free CPDB RAFT agent	33
Scheme 2.4 Synthetic scheme for the functionalization of SiO ₂ nanoparticles with CPDB RAFT agents	36
Scheme 2.5 Synthesis of the dyes, 6-aminohexanoic acid (NBD-COOH), and NBD-hexamethylenediamine (NBD-NH ₂)	39
Scheme 2.6 Synthesis of dye-labeled on SiO ₂ @HEMA-LA, and SiO ₂ @HEMA-SA grafted-nanoparticles	40
Scheme 3.1 Synthesis of HEMA-LA monomer	61
Scheme 3.2 Synthesis of HEMA-SA monomer	63
Scheme 3.3 Grafting-from Polymerization of HEMA-LA and HEMA-SA mediated by anchored CPDB on silica nanoparticles	73
Scheme 3.4 Synthesis and attachment of the fluorescence dyes on silica nanoparticles	80
Scheme 3.5 The proposed approach to grafting the second population of polymer chains on the surface of the nanoparticles	81
Scheme 3.6 Modification of RAFT agent (CPDB) with a phosphate group	82
Scheme 3.7 Synthetic strategy for synthesizing the bimodal grafted nanoparticles	83
Scheme 4.1 Initially proposed synthesis of bimodal brush nanoparticles using two different RAFT agents	115
Scheme 4.2 Proposed strategy to synthesis bimodal brush nanoparticles using two different RAFT agents	117

Scheme 4.3 Attaching (a) NBD-COOH dye to the SiO ₂ @ P(HEMA-LA) and (b)NBD-NH ₂ dye to the SiO ₂ @ P(HEMA-SA).....	120
Scheme 4.4 Synthesis of phosphate-containing CDSS agent.....	123
Scheme 4.5 Synthesis of the glecomonomer TMS-MAG.....	126
Scheme 4.6 Total synthesis of bimodal “sweet nanoparticles” SiO ₂ -g-P(HEMA-LA-dye)-P(MAG).....	132
Scheme 4.7 Total synthesis of bimodal “sweet nanoparticles” SiO ₂ -g-P(HEMA-SA-dye)-P(MAG).....	133
Scheme 5.1 Synthesis various kinds of monomers HEMA-GL, HEMA-DO, and HEMA-DA.....	141
Scheme 5.2 The proposal new synthesis of bimodal nanoparticles SiO ₂ -g-P(MAA)-P(HEMA-LA-dye), and SiO ₂ -g-P(MAA)-P(HEMA-SA-dye).	151

LIST OF ABBREVIATIONS

AIBN	Azobisisobutyronitrile
ATRP	Atom Transfer Radical Polymerization
CDSS	4-cyano-4-[(dodecylsulfanylthiocarbonyl)sulfanyl]pentanoic acid
CPDB.....	4-cyanopentanoic acid dithiobenzoate
CRP.....	Controlled Radical Polymerization
CTA	Chain transfer agent
DCC.....	N, N'-Dicyclohexylcarbodiimide
DDS	Drug delivery system
DLS.....	Dynamic Light Scattering
DMAP	4-Dimethylaminopyridine
DSC	Differential scanning calorimetry
FT-IR	Fourier-transform infrared spectroscopy
GPC	Gel permeation chromatography
HEMA	Hydroxyethyl Methacrylate
HEMA-LA	2-((2-(propionyloxy) propanoyl)oxy)ethyl methacrylate
HEMA-SA	4-(2-(methacryloyloxy)ethoxy)-4-oxobutanoic acid
HF	Hydrofluoric acid
MAA.....	Methacrylic acid
MAG.....	2-methacrylamido glucopyranose

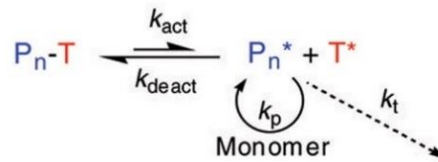
Mn	Number-average of molecular weight
NBD-Cl	4-Chloro-7-nitrobenzo-2-oxa-1,3-diazole
NBD-NHS.....	N-[2-{N-(7'-Nitrobenz- 2'-oxa-1',3'-diazol-4'-yl) amino} ethyl- carbonyloxy] succinimide
NMP	Nitroxide-Mediated Polymerization
NMR.....	Nuclear Magnetic Resonance
NP.....	Nanoparticle
PBS.....	Phosphate-buffered saline
PDI.....	Polydispersity index
RAFT	Reversible Addition-Fragmentation Chain Transfer Polymerization
SI-RAFT	Surface-initiated RAFT
TEM.....	Transmission electron microscopy
TFA.....	Trifluoroacetic acid
Tg.....	Glass Transition Temperature
TGA	Thermogravimetric Analysis
THF.....	Tetrahydrofuran
TMS-MAG.....	2-deoxy-2-methacrylamido tetra-(O-trimethylsilyl) D- glucopyranose
UV-vis	Ultraviolet-visible spectroscopy

CHAPTER 1
INTRODUCTION

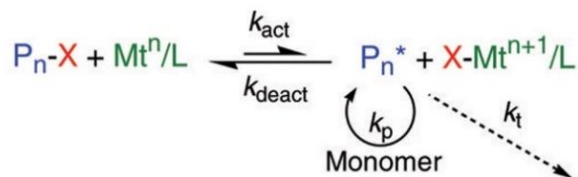
1.1 RAFT Polymerization:

Since 40 years ago, novel controlled polymerization techniques have been discovered in polymer chemistry.¹ Reversible addition-fragmentation chain transfer (RAFT) polymerization is considered one of the controlled radical polymerization (CRP) techniques that give living characteristics to free radical polymerization.²⁻⁵ Living polymerization has emerged where the propagation of polymerization is continued by all chains and its process in the absence of chain termination.⁶ The RAFT polymerization technique can be used to improve the properties of polymers such as precise control over polymer molecular weights with narrow polydispersity and the abilities to create well-defined molecular architectures.⁷ Controlled radical polymerization techniques are generally classified by three major methods (Figure 1.1); nitroxide-mediated polymerization (NMP)⁸ which requires high reaction temperature, atom transfer radical polymerization (ATRP)⁹ that requires a metal catalyst, and reversible addition-fragmentation chain transfer polymerization (RAFT).^{1,10} RAFT together with ATRP are the most widely used CRP techniques to date. RAFT is often preferred for its simplicity and versatility, usage with a wide range of monomers, lack of metal catalyst, and low polymerization temperatures.^{7,11}

1) SFRP or NMP
Thermal dissociation of dormant species (k_{act}) provides a low concentration of radicals



2) ATRP
Transition metal activation (k_{act}) of a dormant species with a radically transferable atom



3) Degenerative Transfer or RAFT
Majority of chains are dormant species that participate in transfer reactions (k_{exch}) with a low concentration of active radicals

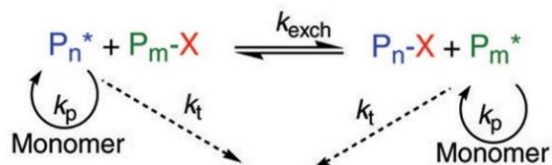


Figure 1.1: The three main CRP methods.¹²

1.2 Mechanism of RAFT Polymerization:

The RAFT technique employs a chain transfer agent (CTA), which works to control the polymerization due to its ability to create and participate in a chain equilibrium. Common CTAs are dithioester, dithiocarbamate, or trithiocarbonate compounds that referred to as RAFT agents and contain Z and R groups that are responsible for controlling the polymerization (Figure 1.2). Monomer structure and the structure of the R and Z group of the CTA are the main factors that affect control of the polymerization.¹³

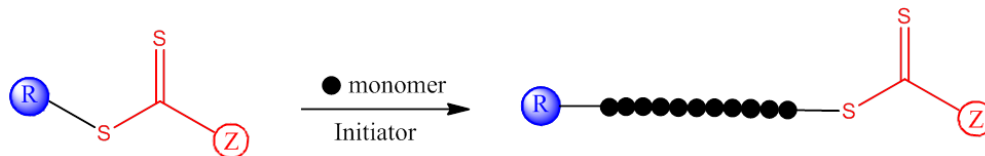


Figure 1.2: Generalized dithioester RAFT agent and polymer formed using a RAFT agent.

The general proposed mechanism for RAFT polymerization is shown in Figure 1.3. Initiation begins due to the conventional initiation process by the homolysis of a free radical initiator. After the initiator attacks the monomer, propagating radical species (P_n^*) will be created. (P_n^*) will react with the RAFT agent (A) to form the intermediate (I), which can then fragment into dithioester (B) and a new radical (R^*). The new radical (R^*) will re-initiate the free monomer and form a new propagating radical species (P_m^*). The equilibrium between two propagating radical species (P_n^* , P_m^*) will be established. The chain end of RAFT CTA will remain active, allowing for more additions for the synthesis of block copolymers or other advanced polymer architectures.¹⁴⁻²⁰ High ratio of RAFT agent to the initiator in the polymerization is important to maintain the equilibrium between active radical species, and to avoid having a large number of active species which leads to termination between propagating radical species (P_n^* , P_m^*).

The Z and R groups of the RAFT agent are responsible for controlling the equilibrium between active radical species CTA, and the rate of monomer addition. The Z group works to stabilizing the radical species that leads to

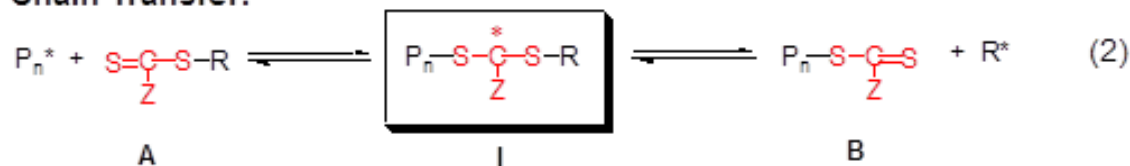
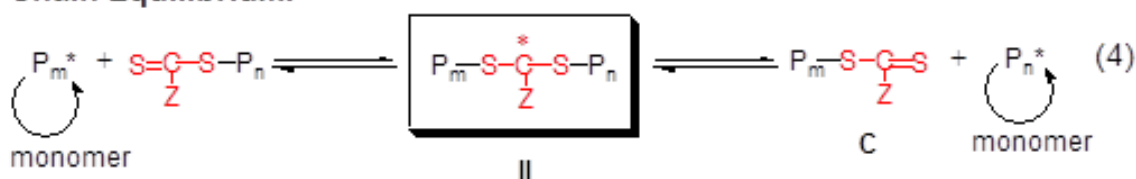
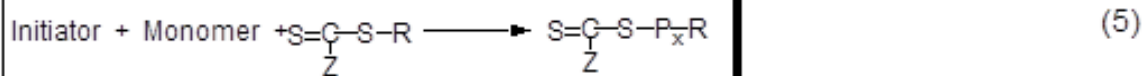
Initiation:**Chain Transfer:****Reinitiation:****Chain Equilibrium:****Overall Process:**

Figure 1.3: General mechanism of RAFT polymerization.

control of the reactivity of CTA while the R group acts as an excellent leaving group with respect to (P_n^*) .¹⁰

1.3 Polymer Grafted Nanoparticles:

RAFT polymerization has a significant role in the development of nanoparticles for polymer nanocomposites due to the surface modification of nanoparticles.²¹ Properties of a polymer matrix can be significantly enhanced by using nanoparticles as fillers. Usually, preventing the agglomeration of nanoparticles is a necessary requirement for improving polymer nanocomposite

properties. Ungrafted bare nanoparticles do not have favorable interactions with their environment.²² Therefore, a successful approach to overcome agglomerations caused by surface tension among nanoparticles is through surface modification with polymer chains, which can increase the dispersion of particles (Figure 1.4).

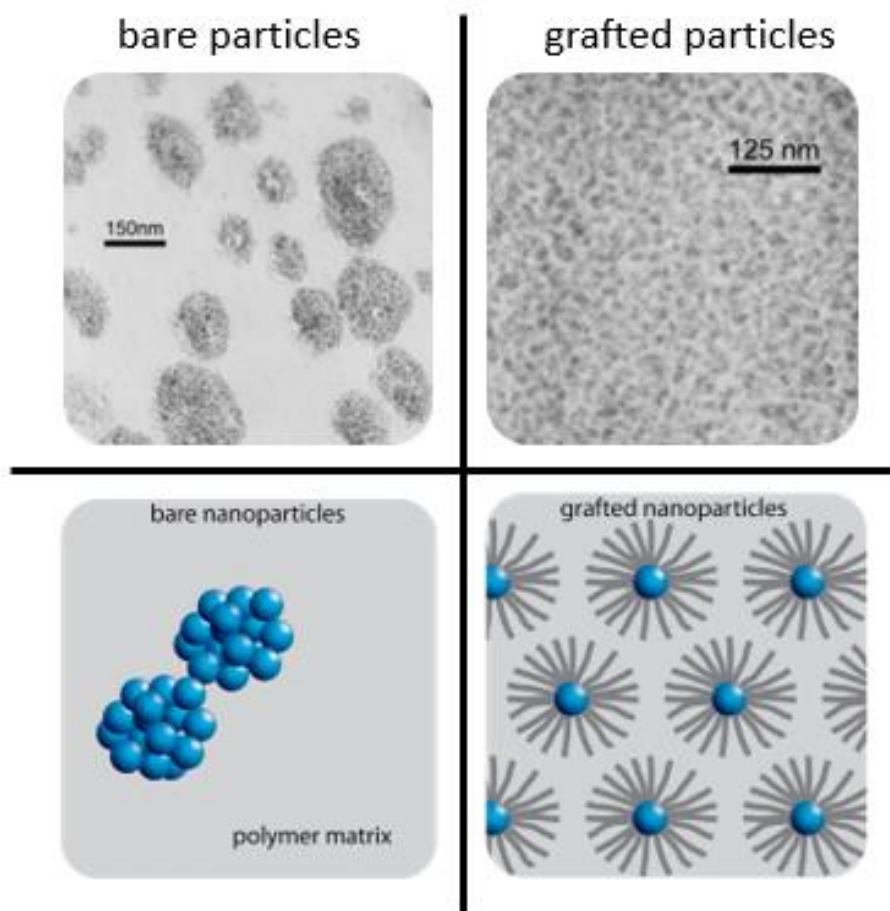


Figure 1.4: Bare nanoparticles vs. polymer grafted nanoparticles in a polymer matrix.

RAFT polymerization provides an excellent method to attach well-defined polymer chains to the surface of nanoparticles.²¹⁻²³ Polymer chains can be created

following two methods: (i) Non-covalent attachment (physisorption) and (ii) Covalent attachment (chemisorption). Physisorption experimentally is very straightforward, but it has several limitations, such as desorption or weak linkage, that limits its applications. Furthermore, chemisorption attachment is more widely used due to its strong attachment between introduced polymer chains and the surface of nanoparticles.²⁴

The covalent attachment of chains can be achieved by two main strategies: *grafting-to* and *grafting-from*. The *grafting-to* technique covalently attaches polymer chains which have reactive end groups to the surface of nanoparticles. Grafting-to does not provide high graft density of polymer chains because of the steric repulsions between them. Furthermore, the reaction between the end group on polymer chains and the reactive group on the surface of the nanoparticles will be less efficient with increasing the molecular weight of the polymer. On the other hand, the *grafting-from* technique directly initiates the polymerization from initiator functionalized surfaces, which are covalently linked to the surface. Grafting-from is advantageous in that it achieves nanoparticles with higher graft densities because steric interactions are avoided (Figure 1.5).^{24,25}

The morphology of the polymer chains that are attached to the substrate surface of nanoparticles depends on grafting density. Higher graft densities do not allow for more distance between polymer chains. Therefore, steric hindrance leads

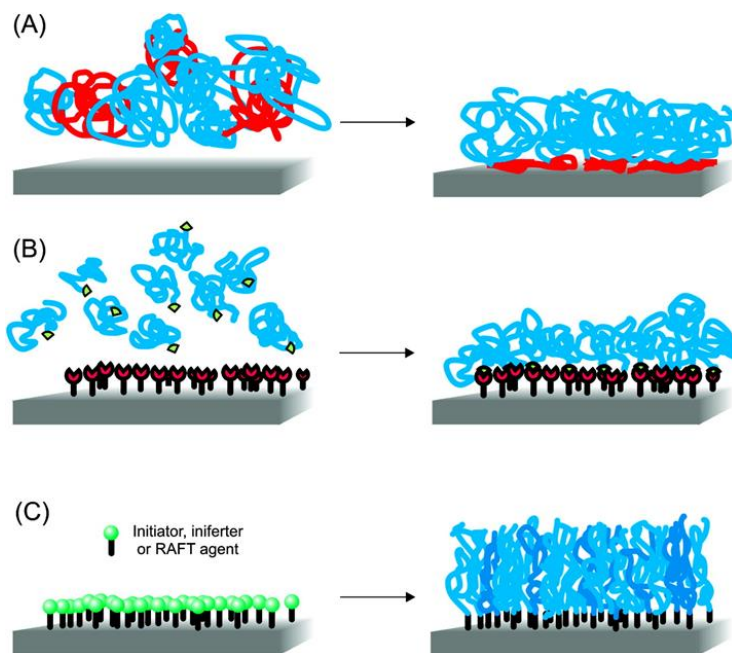


Figure 1.5: Techniques of polymer attachment A) physisorption, B) grafting-to approach, C) grafting-from approach.

to brushes with more extended chain conformations. In contrast, low graft densities provide the polymer chain space to stretch back towards the substrate surface of nanoparticles and adopt various conformations such as mushroom structures (Figure 1.6). Therefore, graft density plays a significant role that affects matrix interactions.^{26,27}

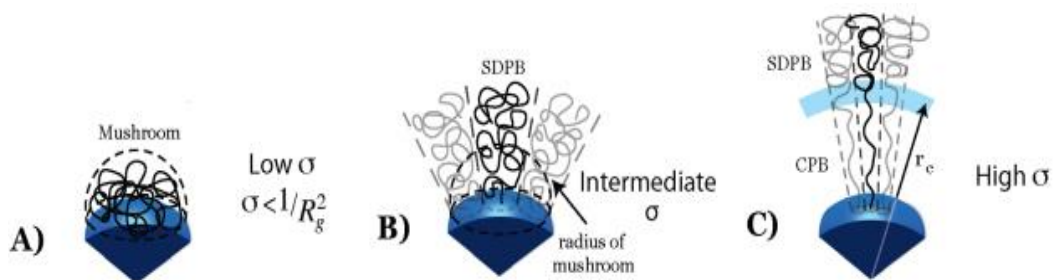


Figure 1.6: Polymer morphologies resulting from various grafting densities.²⁸

1.4 Nanoparticles As Delivery Vehicles:

The widespread use of antibiotic drugs that become essential for many medical interventions to reduce bacterial growth and to treat bacterial infections specifically, combined with the adapt-ability of bacterial types, has led to appearance a new phenomenon, antibacterial resistance, which has become a global issue. Antibacterial resistance is one of the issues that has gathered remarkable attention during the past three decades.²⁹ Bacteria have developed their abilities to become more resistant to traditional antibiotics. β -lactam antibiotics are the common conventional antibiotics that have widely used and have a long history. Bacteria gradually started to develop resistance against these antibiotics by creating β -lactamase enzymes which work to deactivate antibiotics through hydrolyzing the β -lactam ring efficiently.³⁰ Therefore, one of the significant approaches that are used to inhibit β -lactamase and overcome bacteria-resistance is developing antibacterial nanoparticles where the antibiotic linkage to the surface of nanoparticles will enhance their effectiveness against bacteria.³¹ Antibacterial nanoparticles have been developed and investigated as therapeutic delivery vehicles. Nanoparticles can offer variable and structured surfaces having various types and densities of antibiotics.³² Consequently, this will permit the specificity of the quantities of antibiotic molecules that will be carried by nanoparticles that will reach infectious bacterial cells. Overcoming bacterial

resistance may occur by releasing antibiotics slowly into the system while preserving an effective antibiotic concentration for extended times.³³ One of the synthetic strategies that can be used is the design of new monomers, containing an ester linkage which can be easily hydrolyzed. The slow degradation of the side chains will occur, resulting in the slow release of antibiotics from the surface of nanoparticles.

1.5 Bimodal Nanocomposites:

A novel architecture of grafting bimodal polymer brushes on nanoparticles can significantly improve the entanglement of nanoparticle fillers and matrix polymers. Improving the properties of polymers/ matrices will lead to the wider application of polymer nanocomposites. Extensive research has been done to understand the relationship between the polymer brushes on the nanoparticles and their matrices.³⁴ However, controlling the graft densities of brushes and the interface of the brush/matrix are significant issues that need to be addressed to fully understand the structure-property relationship in polymer nanocomposites. Typically, the aggregation process of monomodal brush grafted nanoparticles is addressed by a delicate equilibrium between enthalpic and entropic interfacial interactions.^{35,36} Therefore, using a bimodal polymer brush architecture on nanoparticles is considered an improved approach currently to overcome the aggregation of nanoparticles that occurs in polymer nanocomposites. A bimodal

polymer brush is created by attaching two populations of polymer chains with different lengths to the surface of nanoparticles (Figure 1.7).³⁷ Both approaches, grafting-from, and grafting-to are successfully used to prepare bimodal polymer brushes.

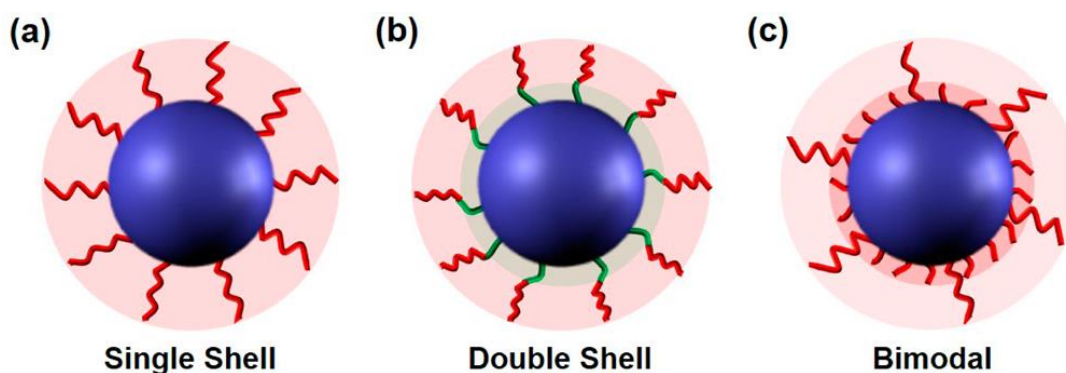


Figure 1.7: Illustration of various architectures of core-shell nanoparticles: (a) single shell and (b) double shell, both of which are classified as monomodal core-shell nanoparticles, and (c) bimodal core-shell nanoparticles.³⁸

1.6 References:

- (1) Chiefari, J.; Chong, Y. K.; Ercole, F.; Krstina, J.; Jeffery, J.; Le, T. P. T.; Mayadunne, R. T. A.; Meijs, G. F.; Moad, C. L.; Moad, G.; Rizzardo, E.; Thang, S. H. *Macromolecules* **1998**, *31* (16), 5559–5562.
- (2) Ilgach, D. M.; Meleshko, T. K.; Yakimansky, A. V. *Polym. Sci. Ser. C* **2015**, *57* (1), 3–19.

- (3) Moad, Graeme, Ezio Rizzardo, and S. H. T. *Acc. Chem. Res.* **2008**, *41* (9), 1133–1142.
- (4) Moad, G.; Rizzardo, E.; Thang, S. H. *Aust. J. Chem.* **2005**, *58* (6), 379–410.
- (5) Moad, G.; Rizzardo, E.; Thang, S. H. *Aust. J. Chem.* **2012**, *65* (8), 985–1076.
- (6) Vazaios, A.; Lohse, D. J.; Hadjichristidis, N. *Macromolecules* **2005**, *38* (13), 5468–5474.
- (7) Li, C.; Benicewicz, B. C. *Macromolecules* **2005**, *38*, 5929–5936.
- (8) Hawker, C. J.; Bosman, A. W.; Harth, E. *Chem. Rev.* **2001**, *101* (12), 3661–3688.
- (9) Wang, J. S.; Matyjaszewski, K. *J. Am. Chem. Soc.* **1995**, *117* (20), 5614–5615.
- (10) Moad, G.; Rizzardo, E.; Thang, S. H. *Aust. J. Chem.* **2006**, *59* (10), 669–692.
- (11) Perrier, S. *Macromolecules* **2017**, *50* (19), 7433–7447.
- (12) Spanswick, J.; Matyjaszewski, K.; Spanswick, J. *Mater. Today* **2005**, *8* (3), 26–33.
- (13) Barner-Kowollik, C. *Handbook of RAFT Polymerization*; WILEY-VCH Verlag GmbH & Co., 2008.

- (14) Keddie, D. J.; Moad, G.; Rizzardo, E.; Thang, S. H. *Macromolecules* **2012**, *45* (13), 5321–5342.
- (15) Harvison, M. A.; Roth, P. J.; Davis, T. P.; Lowe, A. B. *Aust. J. Chem.* **2011**, *64* (8), 992–1006.
- (16) Moad, G.; Rizzardo, E.; Thang, S. H. *Polym. Int.* **2011**, *60* (1), 9–25.
- (17) Gregory, A.; Stenzel, M. H. *Prog. Polym. Sci.* **2012**, *37* (1), 38–105.
- (18) Roth, P. J.; Boyer, C.; Lowe, A. B.; Davis, T. P. *Macromol. Rapid Commun.* **2011**, *32* (15), 1123–1143.
- (19) Moad, G.; Chong, Y. K.; Mulder, R.; Rizzardo, E.; Thang, S. H. *ACS Symp. Ser.* **2009**, *1024*, 3–18.
- (20) Moad, G. *ACS Symp. Ser. 1187*, **2015**, 211–246.
- (21) Li, C.; Han, J.; Ryu, C. Y.; Benicewicz, B. C. *Macromolecules* **2006**, *39* (9), 3175–3183.
- (22) Fu, S. Y.; Feng, X. Q.; Lauke, B.; Mai, Y. W. *Compos. Part B Eng.* **2008**, *39* (6), 933–961.
- (23) Ranjan, R.; Brittain, W. J. *Macromolecules* **2007**, *40* (17), 6217–6223.

- (24) Barbey, R.; Lavanant, L.; Paripovic, D.; Schüwer, N.; Sugnaux, C.; Tugulu, S.; Klok, H. A. *Chem. Rev.* **2009**, *109* (11), 5437–5527.
- (25) Dai, Xiao-Hui, D. C.-M. *J. Polym. Sci. Part A Polym. Chem.* **2008**, *46* (September 2010), 817–829.
- (26) Brittain, W. J.; Minko, S. J. *J. Polym. Sci. Part A Polym. Chem.* **2007**, *45* (16), 3505–3512.
- (27) Schadler, L. S.; Kumar, S. K.; Benicewicz, B. C.; Lewis, S. L.; Harton, S. E. *MRS Bull.* **2007**, *32* (4), 335–340.
- (28) Dukes, D.; Li, Y.; Lewis, S.; Benicewicz, B.; Schadler, L.; Kumar, S. K. *Macromolecules* **2010**, *43* (3), 1564–1570.
- (29) Deng, H.; McShan, D.; Zhang, Y.; Sinha, S. S.; Arslan, Z.; Ray, P. C.; Yu, H. *Environ. Sci. Technol.* **2016**, *50* (16), 8840–8848.
- (30) Li, W.; Dong, K.; Ren, J.; Qu, X. *Angew. Chemie - Int. Ed.* **2016**, *55* (28), 8049–8053.
- (31) Wang, L.; Chen, Y. P.; Miller, K. P.; Cash, B. M.; Jones, S.; Glenn, S.; Benicewicz, B. C.; Decho, A. W. *Chem. Commun.* **2014**, *50* (81), 12030–12033.
- (32) Wang, L.; Benicewicz, B. C. *ACS Macro Lett.* **2013**, *2* (2), 3–6.

- (33) Tamizharasi, S.; Rathi, V.; Rathi, J. C. *Syst. Rev. Pharm.* **2011**, *2* (1), 19–29.
- (34) Rungta, A.; Natarajan, B.; Neely, T.; Dukes, D.; Schadler, L. S.; Benicewicz, B. C. *Macromolecules* **2012**, *45* (23), 9303–9311.
- (35) Meldal, M. *Macromol. Rapid Commun.* **2008**, *29* (12–13), 1016–1051.
- (36) Kumar, S. K.; Krishnamoorti, R. *Annu. Rev. Chem. Biomol. Eng.* **2010**, *1* (1), 37–58.
- (37) Skvortsov, A. M.; Gorbunov, A. A.; Leermakers, F. A. M.; Fleer, G. J. *Macromolecules* **1999**, *32* (6), 2004–2015.
- (38) Qiao, Y.; Yin, X.; Wang, L.; Islam, M. S.; Benicewicz, B. C.; Ploehn, H. J.; Tang, C. *Macromolecules* **2015**, *48* (24), 8998–9006.

CHAPTER 2

POLYMERIZATION OF “CONTROLLED RELEASE” MONOMERS CONTAINING A HYDROLYTICALLY SENSITIVE ESTER LINKAGE VIA RAFT POLYMERIZATION¹

¹Al-Ali, M.A. and Benicewicz B. C. To be submitted to Journal of Polymer Science.

2.1 Abstract:

The aim of this work was to develop a novel type of drug-delivery carrier consisting of a pH-responsive “controlled release” polymer containing an antibacterial drug grafted onto the surface of a nanoparticle. Herein, we describe the first report of pH-responsive biodegradable polymers grafted from the surface of silica nanoparticles. Grafted “controlled release” polymers containing a hydrolytically sensitive ester linkage on silica nanoparticles were successfully prepared via reversible addition-fragmentation chain transfer (RAFT) polymerization. Two potential “controlled release” monomers, 2-((2-(propionyloxy) propanoyl)oxy)ethyl methacrylate (HEMA-LA) and 4-(2-(methacryloyloxy)ethoxy)-4-oxobutanoic acid (HEMA-SA), were synthesized by the ring-opening reaction of L-lactide and succinic anhydride with 2-hydroxyethyl methacrylate (HEMA), respectively. The polymerization of the methacrylate monomers was carried out using 4-cyanopentanoic acid dithiobenzoate (CPDB) as a RAFT agent. Both polymers poly(HEMA-LA) and poly(HEMA-SA) were characterized by NMR spectroscopy and gel permeation chromatography (GPC). The degradation rates of these two polymers were investigated using phosphate buffer solution (PBS, pH = 7.4) at 25°C and 37°C as a function time using conjugated dyes (NBD-aminohexanoic acid, NBD-hexamethylenediamine). The pH-dependence of dye-loaded polymer grafted nanoparticles was confirmed by the

evaluation of the cumulative release rate at two temperatures 25°C, 37°C. Such polymer grafted nanoparticles are being developed for use as delivery vehicles for antibacterial applications.

2.2. Introduction:

Drug delivery of pharmaceutical compounds is considered the key to achieving a significant therapeutic effect, whether for humans or animals.¹ Nanotechnology methods have more significant potential in drug delivery systems (DDS) as the desired drug could be released using biodegradable polymers.² For the ideal drug delivery system(DDS), preserving the drug level within a desired therapeutic range is the main aim because there is a toxic and ineffective plasma level for each drug.³ The design of a “Controlled Release” drug delivery technique using nanotechnology is one of the significant strategies to overcome various diseases.⁴ Globally, different stimuli-sensitive polymeric systems have attracted considerable attention in recent years that show a response to an external stimulus such as pH, temperature, specific ion, and electric field.⁵ pH-sensitive nanopolymers, among the different types of stimuli-responsive polymers, have been advanced and most widely used to develop sensitive nano-systems in which the drug will release in different pH environments.⁶ The use of polymers containing a pH-sensitive ester linkage on silica nanoparticles has gained significant importance during recent decades.⁷

Several strategies/ approaches of pH-responsive drug release have been studied. For instance, one of the important strategies is to introduce ionizable functional groups, such as esters, amides, phosphoric acids, and carboxylic acids with nanomaterials. These ionizable functional groups are biodegradable, which can result in the drug release through the mechanism of a pH-stimulus environment.⁸ pH-sensitive polymers with ionizable groups that are considered a class of polyelectrolytes that can be ionized and change their conformation. Several pH-sensitive polymers have been developed by using acidic or basic groups that accept or release protons in response to changes in the pH environment. Esters linkages have been preferred when engineering polymeric materials for controlled release compared to amides, carbonates, and carbamates because of their relative ease of hydrolysis at physiological pH (7.4).⁹ At pH 7.4, the esters groups that have a carbonyl adjacent to an ether linkage can be readily hydrolyzed to alcohol and carboxylic acid derivatives.¹⁰

However, the current study is focused on the designing of pH-sensitive polymers grafted onto silica nanoparticles (SiO₂@HEMA-LA, SiO₂@HEMA-SA). Controlled release pH-responsive monomers containing ester linkage were synthesized. The Grafting-from RAFT polymerization technique was used to polymerize these controlled release monomers onto the surface of silica nanoparticles to get controlled and high loading capacity.¹¹ The controlled release

study was investigated by attaching labeled-dyes to the pH-sensitive polymers to monitor the degradation rate. Furthermore, loading drugs or antibiotics could be attached to pH-sensitive polymers grafted on silica nanoparticles and study their release rate.

2.3 Experimental:

2.3.1 Materials:

L-lactide (Sigma Aldrich, 95%) and succinic anhydride (Acros Organics, 99%) were used as received. 2-Hydroxyethyl methacrylate (HEMA, Sigma Aldrich, 99%) was purified by passing through a column of basic aluminum oxide (Alfa Aesar, 99%) to remove the inhibitor, methyl ether hydroquinone (MEHQ). Colloidal silica nanoparticles (SiO_2 , spherical 14 ± 4 nm, 30 wt% in MEK) were purchased from Nissan Chemical Co. The RAFT agent 4-cyanopentanoic acid dithiobenzoate (CPDB) was purchased from Boron Molecular and used as received. 3-Aminopropyldimethylethoxysilane and dimethylmethoxy-n-octylsilane were purchased from Gelest, Inc. (95%) and used as received. Azobisisobutyronitrile (AIBN) was used after purification by recrystallization in methanol. The catalysts, tin (II) 2-ethylhexanoate and 4-dimethylaminopyridine (DMAP), were purchased from Alfa Aesar and Chem-Impex Int'l Inc respectively. All other reagents and solvents were used as received unless otherwise noted.

2.3.2 Instrumentation:

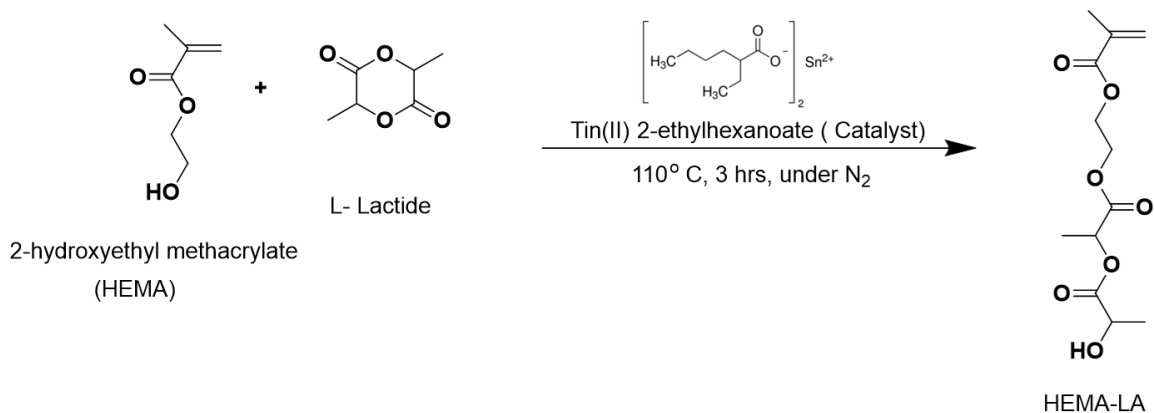
¹H-NMR spectra were recorded with a Bruker Avance III-HD spectrometer (300 MHz) using CDCl₃ as a solvent and measured with tetramethylsilane (TMS) as an internal reference. Gel permeation chromatography (GPC) was used to measure the molecular weights (M_n) and dispersity index (Đ) using a Varian 290-LC pump, a Varian 390-LC refractive index detector, and three Styragel columns (HR1, HR3 and HR4, molecular weight range of 100-5000, 500-30000, and 5000-500000) calibrated with polystyrene and poly(methylmethacrylate) standards obtained from Polymer Laboratories. Tetrahydrofuran (THF) was used as an eluent at 30°C and a flow rate of 1.0 mL/min. Thermogravimetric analysis (TA Instruments Q5000) was used to obtain TGA characterization after preheating to 100°C for 10 min to remove residual solvents for all the samples. After cooling to 50°C, the samples were reheated to 800°C with a heating rate of 10°C/min under nitrogen flow. FT-IR spectra were recorded using a BioRad Excalibur FTS 3000. UV-vis absorption spectra were taken on a Shimadzu UV-2450 spectrophotometer.

2.3.2 Synthesis of “Controlled Release” Monomers:

Two methacrylate monomers were synthesized via the ring-opening reaction of the corresponding cyclic lactone compound, L-lactide, or succinic anhydride with hydroxyethyl methacrylate (HEMA) catalyzed by stannous 2-ethylhexanoate and DMAP, respectively.

2.3.2.1 Synthesis of 2-((2-(Propionyloxy) Propanoyl)oxy)ethyl Methacrylate (HEMA-LA) (Scheme 2.1):

L-lactide (2.99 g, 20.7 mmol) was placed in round flask and dried overnight under vacuum at rt. HEMA (2.8 mL, 23 mmol) and tin(II) 2-ethylhexanoate (52 μ L, 0.16 mmol) were then added to the flask, and the reaction was deoxygenated by a repeated vacuum nitrogen cycle. Subsequently, the mixture was heated to 115°C under vacuum for 3 hours with stirring. The crude product was dissolved in anhydrous chloroform and washed with 1 M HCl. Then, the organic phase was washed with deionized water, isolated, and residual chloroform removed using a rotary evaporator operating under vacuum. Yields varied from 70-75% based on the added amount of L-lactide. $^1\text{H-NMR}$ (300 MHz, CDCl_3): δ =1.38–1.63 ppm (6H, CH–CH₃), δ = 1.94 ppm (3H, CH₂=CCH₃), δ = 2.79 ppm (1H, OH), δ = 4.26–4.39 ppm (4H, OCH₂–CH₂), δ = 4.39–4.51 ppm (1H, CH-(OH)CH₃), δ = 5.08–5.29 ppm (1H, C(=O)–CH), δ = 5.58 ppm (1H, CH₂=C), δ = 6.10 ppm (1H, CH₂=C) (Figure 2.1). HRMS (EI) (m/z) calcd for C₁₂H₁₈O₇: 274.1149; found: 274.1167.^{12,13}



Scheme 2.1: Synthesis of HEMA-LA monomer.

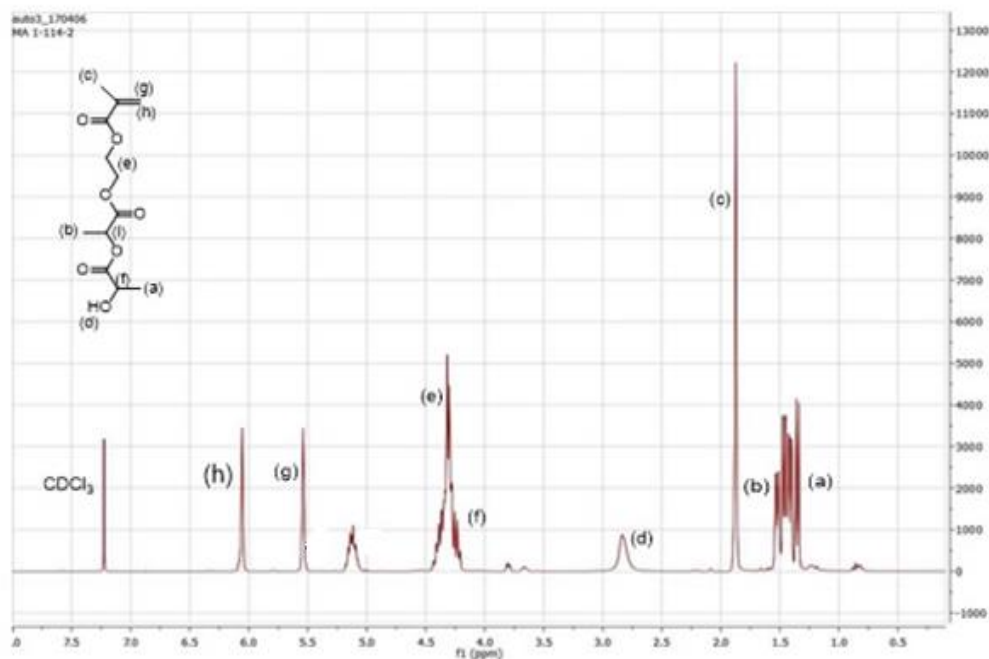
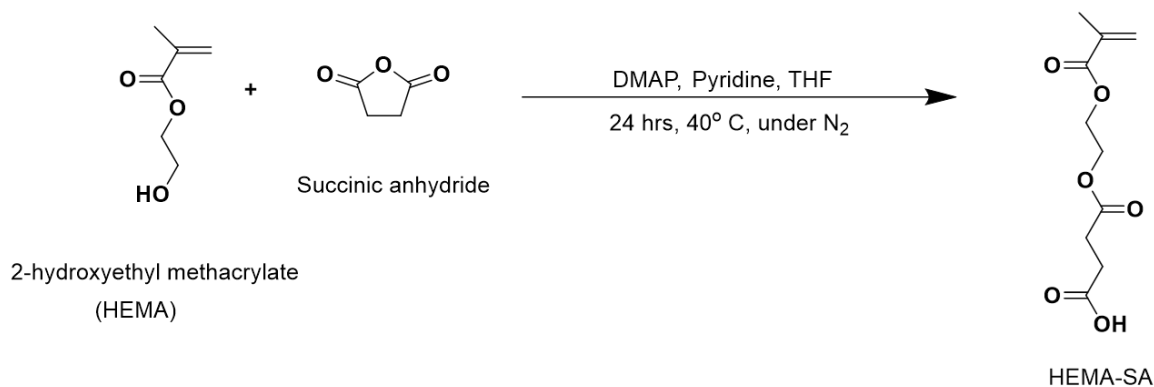


Figure 2.1: ¹H-NMR (300 MHz, CDCl₃) spectrum of HEMA-LA monomer.

2.3.2.2 Synthesis of 4-(2-(Methacryloyloxy)ethoxy)-4-oxobutanoic Acid (HEMA-SA) (Scheme 2.2):

2-Hydroxyethyl methacrylate (HEMA; 6.1 mL, 50 mmol) was dissolved in anhydrous THF in a Schlenk flask (250 mL) at room temperature under nitrogen.

Succinic anhydride (6 g, 0.06 mol), 12 mL of pyridine, and 4-dimethylaminopyridine (0.49 g, 4.0 mmol) were added to the flask. Then, the reaction mixture was stirred for 24 h at 40°C under nitrogen. The reaction was cooled to the room temperature, and the solvent was evaporated under vacuum. The residue was dissolved in DCM, followed by washing three times with 0.1 M HCl solution. The organic phase was dried over anhydrous magnesium sulfate overnight and filtered. After evaporation of the solvent, the remaining HEMA-COOH product was dried under vacuum at room temperature. A viscous liquid was obtained (yield 60%, 6.9 g). ¹H NMR (300 MHz, CDCl₃): δ = 6.13 (s, 1H, HCH=C(CH₃-), 5.54 (s, 1H, HCH=C(CH₃-), 4.36 (t, 4H, -OOC(CH₂)₂OCO-), 2.68 (t, 4H, HOOC(CH₂)₂COO-), 1.85 (s, 3H, H₃CC(COO-)CH₂) (Figure 2.2). HRMS (EI) (m/z) calcd for C₁₀H₁₄O₆: 230.0842; found: 230.0873.^{14,15}



Scheme 2.2: Synthesis of HEMA-SA monomer.

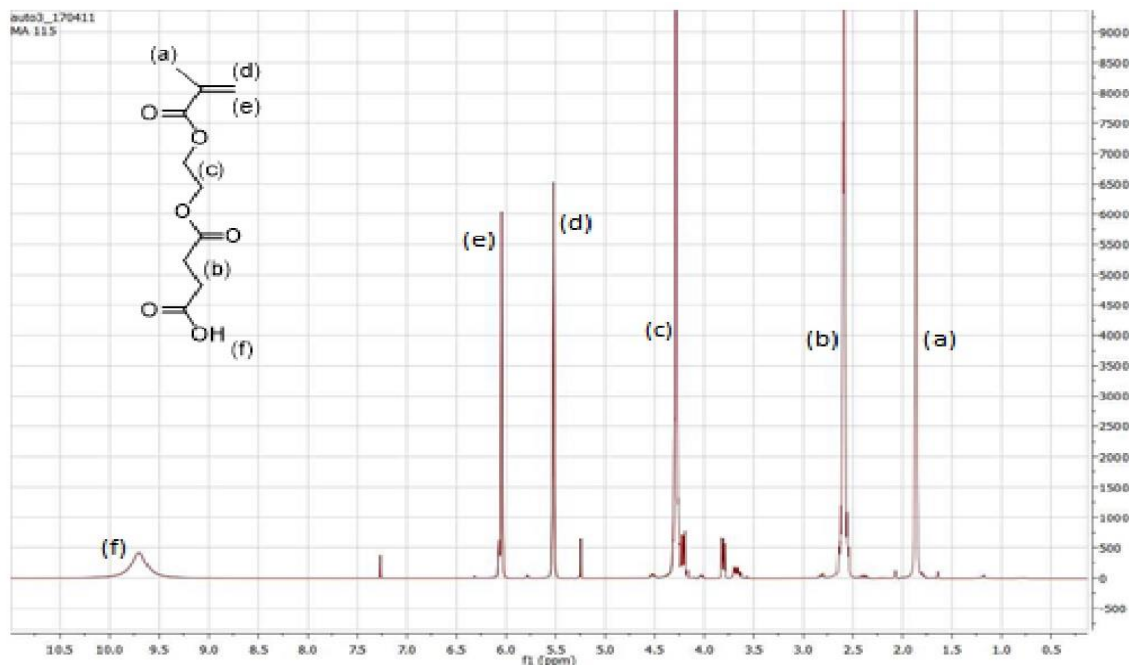


Figure 2.2: ¹H-NMR (300 MHz, CDCl₃) spectrum of HEMA-SA monomer.

2.3.3 Activation of 4-cyano-4-(thiobenzoylthio)pentanoic acid (CPDB):

Dimethylamino pyridine (DMAP) (122 mg, 1.0 mmol) was added slowly to the solution of CPDB (2.80 g, 10.0 mmol), 2-mercaptothiazoline (1.2 g, 10.0 mmol), and dicyclohexylcarbodiimide (DCC) (2.5 g, 12.0 mmol) in 40 ml of dichloromethane. Then, the solution was stirred (6 h) at room temperature. The solids were removed from the solution by filtration. The solution was evaporated to remove the solvent, and silica gel column chromatography (5:4 hexane: ethyl acetate) was used to obtain activated CPDB as a red oil (80% yield, 4 g). ¹H-NMR (300 MHz, CDCl₃): δ (ppm) 7.90 (d, 2H), 7.56 (t, 1H), 7.38 (t, 2H), 4.58 (t, 2H, NCH₂CH₂S), 3.60-3.66 (m, 2H, (CN)C(CH₃)-CH₂CH₂CON), 3.31 (t, 2H,

NCH₂CH₂S), 2.50-2.56 (m, 2H, (CN)C(CH₃)CH₂CH₂CON), 1.95 (s, 3H, (CH₃)C(CN)S).¹⁶ HRMS (EI) (m/z) calcd for C₁₆H₁₆N₂OS₄: 380.0193; found: 380.0203.

2.3.4 Attachment of activated CPDB onto silica nanoparticles (SiO₂@CPDB):

Silica nanoparticles (10.0 g, 30 wt % in MEK) were added to a round bottom flask with 30 mL THF and 350 μ L 3-aminopropyldimethylethoxy silane was added. After purging with N₂ for more than 30 min, the solution was refluxed in a 75°C overnight. Then, the solution was cooled to r.t and precipitated into a large amount of hexanes. The solution was centrifuged at 3,500 rpm for 8 minutes and the solvent decanted. The precipitation-dissolution process was then repeated for another two times. The amine-functionalized nanoparticles were dispersed in 30 mL of dry THF, which was added dropwise into a THF solution of 1.47 mL activated CPDB (0.19 M) at r.t. and stirred for 6 hours. The solution was precipitated into a large amount of hexane (approx. 500 ml), and the nanoparticles were recollected by centrifugation at 3500 rpm for 8 min. This precipitation-dissolution process was repeated until the supernatant solution was colorless. The nanoparticles were dried under vacuum at r.t. The grafting density of CPDB anchored silica nanoparticles (0.3 ch/nm²) was determined using a calibration curve of made from standard solutions of free CPDB via UV-vis a spectrometer.¹⁷

2.3.5 RAFT Polymerization of “Controlled Release” Monomers From CPDB Functionalized Silica Nanoparticles:

CPDB-anchored silica nanoparticles (1g, 56.18 $\mu\text{mol/g}$) were dispersed in THF (8 ml). HEMA-LA (7.7 g, 28.07 mmol) or HEMA-SA (6.5 g, 28.23 mmol), AIBN (0.562 ml of 10 mM THF solution) were added to the Schlenk tube, where the ratio between species of [CPDB]:[monomer]:[AIBN] was 1:500:0.1. The Schlenk tube was degassed by three freeze–pump–thaw cycles, filled with nitrogen, and then the Schlenk tube was placed in an oil bath at 65°C for the desired time. The Schlenk tube was quenched in ice water to stop the polymerization. The polymer-grafted silica nanoparticles were precipitated by pouring into 500 ml of hexanes and centrifuged at 3500 rpm for 8 min. The nanoparticles were dispersed back into THF. Polymer chains were cleaved from the nanoparticles by dissolving 50 mg of polymer-grafted nanoparticles in 3 ml of THF and treating with 0.2 ml aqueous HF (49%). The solution was stirred overnight, and the cleaved polymer chains were analyzed by GPC.¹⁸

2.3.6 Cleavage of CPDB Agents From The Polymeric Chain Ends Of The Silica Nanoparticles:

Polymer-grafted nanoparticles (1 g, SiO₂-g-HEMA-LA, SiO₂-g-HEMA-SA) were dispersed in 40 ml THF, and solid AIBN (0.12 g) was added at the ratio of ([CTA]:[AIBN]= 1:20). The solution was heated under nitrogen at 65°C for 1 h. The

solution was poured into 500 ml of hexanes and centrifuged at 3500 rpm for 8 min to recover the nanoparticles.¹⁷

2.3.7 Preparation Of NBD-Labelled Amino Acid:

A solution of 6-aminohexanoic acid (1.2 eq, 3 mmol) and NaHCO₃ (3 eq, 7.5 mmol) in MeOH (30 mL) were stirred at room temperature for 30 min and refluxed at 65°C for 15 min. Then, 4-chloro-7-nitrobenzofurazan (NBD-Cl, 1 eq, 2.5 mmol) was dissolved in MeOH (5 mL) and added dropwise to the solution. After two hours, the reaction was cooled to room temperature and acidified to approximately pH=2 with 1M HCl. Subsequently, the mixture was extracted three times with EtOAc (20 mL), washed with brine, dried with MgSO₄, filtered, and the solvent removed using a rotary evaporator. The resultant NBD-labelled amino acid was then recrystallized from aqueous MeOH.¹⁹ The product was yield as bright orange crystals (yield: 80%, 0.59 g). T_m= 156-158°C, UV (MeOH) λ_{max}: 335, 458. FT-IR ν_{max}/cm⁻¹ 1700 (strong, sharp C=O). MS (EI+) m/z: [M]⁺ 294.

2.3.8 Preparation Of NBD-Labelled Hexamethylenediamine:

Hexamethylenediamine-NBD dye was synthesized in two steps, first preparing N-Boc-hexamethylenediamine-NBD that was converted to the hexamethylenediamine-NBD. A solution of 4-chloro-7-nitrobenzofurazan (NBD-Cl) (1 eq, 2.5 mmol) and mono-Boc-hexamethylenediamine (1.1 eq, 2.76 mmol) was prepared in ethanol (30 mL). Pyridine (catalytic, 260 μL) was added to the stirred

solution and allowed to stir for 30 min. The mixture was concentrated and purified by column chromatography (toluene: ethyl acetate 7:3) to obtain the product as a red foam. Next, the Boc-protected dye was dissolved in a mixture of solvent (1:1 of trifluoroacetic acid (TFA): dichloromethane (DCM)) and then stirred for one hour. The solution was concentrated and resuspended in acetonitrile. The final product was obtained as golden crystals after the solution was precipitated into cold diethyl ether (yield 81%, 0.6 g).²⁰ UV (MeOH) λ_{max} : 336, 460. FT-IR $\nu_{\text{max}}/\text{cm}^{-1}$ 3380 (medium, sharp N-H). HRMS (EI) (m/z) calcd for $\text{C}_{12}\text{H}_{17}\text{N}_5\text{O}_3$: 279.1382; found: 279.3014.

2.3.9 Amino hexanoic Acid-NBD Conjugate On HEMA-LA-g-SiO₂ And Hexamethylenediamine-NBD Conjugate On HEMA-SA-g-SiO₂:

Polymer-g-SiO₂ (1 equiv.) (HEMA-LA-g-SiO₂ or HEMA-SA-g-SiO₂), dye-labeled NBD (1 equiv.) (amino hexanoic acid-NBD or hexamethylenediamine-NBD, respectively), and dicyclohexylcarbodiimide (DCC) (1.2 equiv.) were dissolved in 30 mL of THF. (Dimethylamino) pyridine (DMAP) (0.1 equiv.) was added slowly to the solution. Subsequently, the solution was stirred at r.t. for 6 h. The solution was filtered, and the solvent was concentrated using a rotary evaporator. The solution was then precipitated by pouring into hexane (400 ml) and centrifuged at 3500 rpm for 8 min to recover the nanoparticles. The

precipitation-dissolution process was repeated twice until the supernatant layer after centrifugation was colorless to ensure the removal of free dyes.

2.3.10 In Vitro Quantification Of Dye:

The calibration curves for the dyes were achieved by preparing a standard solution of dye using 27 mg of dye dissolved in 50 ml THF. Then, various concentrations were prepared (13.6, 6.8, 4.3, 1.7, 0.8, 0.4) in 50 ml THF to obtain serial dilutions and assayed at 457- 460 nm using UV spectrophotometry. The data were plotted to obtain a straight lines for the quantification of the dyes (Figure 2.3 a,b).²¹

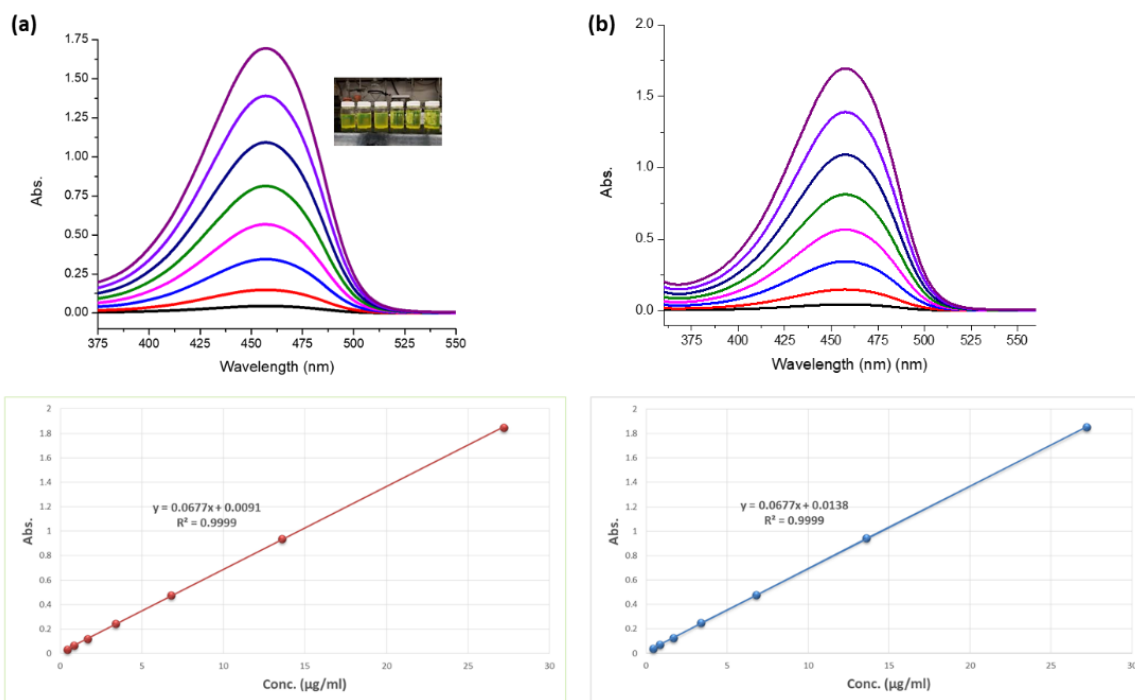


Figure 2.3: Images of serial dilutions, UV spectrum of various concentrations, and the resultant calibration curves of (a) NBD-COOH, (b) NBD-NH₂ dyes.

2.3.11 Dye Release Rate Studies:

Dye release kinetics were determined using pH = 7.4 phosphate-buffered saline solution (PBS) at pH = 7.4 at 25°C and 37°C for the dye attached polymer grafted nanoparticles. HEMA-SA-dye-g-SiO₂ or HEMA-LA-dye-g-SiO₂ (200 mg) were immersed in 250 ml of PBS solution at pH 7.4 using a dialysis membrane bag (MWCO 3500, Fisherbrand), which was tied at the ends after filling with 5 ml of the PBS buffer solution. The systems were incubated at different temperatures, 25°C and 37°C, and provided with gentle shaking at 40 rpm over the test periods. PBS solution (5 ml) was sampled out and assayed for released dye at 480 nm using a (Shimadzu UV-2450) spectrophotometer, at predetermined time points. The UV-vis was measured for these withdrawn samples at 25°C and 37°C, at determined intervals, and replaced with fresh buffer solution (PBS) following every sampling point to keep the same concentration during the full release period. The study was continued until the released amount reached an equilibrium.²²

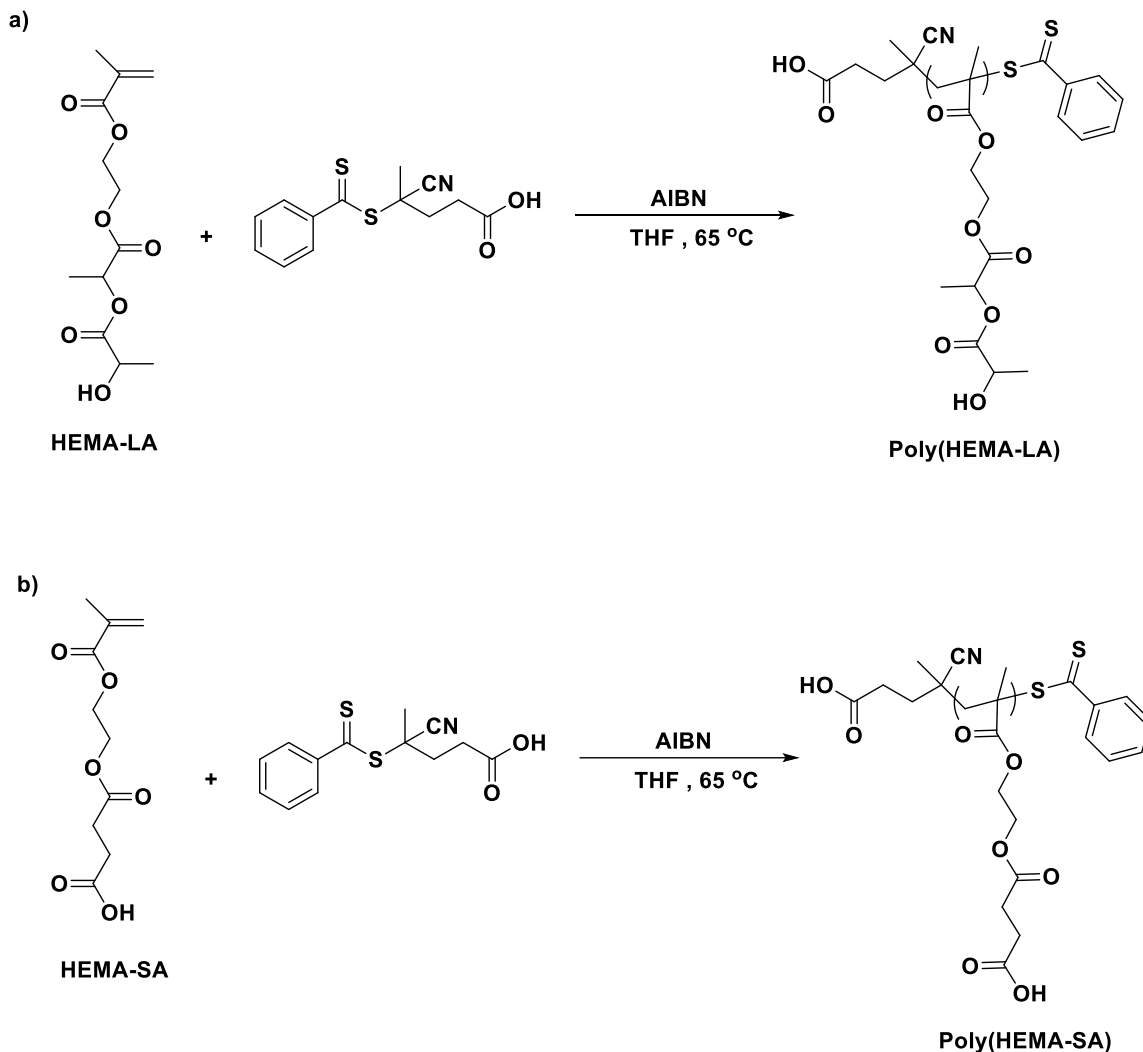
2.4 Results And Discussion:

2.4.1 Polymerization Of The "Controlled Release" (HEMA-LA, HEMA-SA) Monomers Mediated By Free CPDB:

To praper for grafting HEMA-LA and HEMA-SA on the surface of silica nanoparticles via RAFT polymerization, the polymerization behavior of both monomers mediated by free CPDB RAFT agent was investigated. Generally, the

initial and significant aspect when using the RAFT technique is choosing a suitable RAFT agent which is compatible with the monomer which will provide successful control.²³ In this work, we investigated two types of RAFT agents. A trithiocarbonate derivative 4-cyano-4-[(dodecylsulfanylthiocarbonyl) sulfanyl] pentanoic acid (CDSS) and a dithiobenzoate derivative 4-cyanopentanoic acid dithiobenzoate (CPDB) were tested at 65°C. Both monomers could be polymerized with the trithiocarbonate derivative CDSS. However, the polymerizations resulted in low monomer conversions and produced polymers with broad polydispersity. However, we found that the dithiobenzoate derivative CPDB RAFT agent provided a controlled polymerization, where was compatible with both monomers HEMA-LA and HEMA-SA.

The synthetic procedure for the RAFT polymerization of both HEMA-LA and HEMA-SA monomers via free CPDB in solution is shown in Scheme 2.3. The feed ratio $[CTA]/[Monomer]/[Initiator]$ of polymerization was 500: 1: 0.1 at 65°C under inert gas conditions. Figure 2.4 shows the results of the kinetic study for the free RAFT polymerization and surface-initiated RAFT polymerization of both monomers HEMA-LA and HEMA-SA. By observing the consumption $\ln(M_0/M_t)$ of each monomer (HEMA-LA, HEMA-SA; individually), which increased concurrently with the time and the conversion of the polymerizations, we found a



Scheme 2.3: Polymerization of (a) HEMA-LA and (b) HEMA-SA mediated by free CPDB RAFT agent.

good linear relationship. Increasing the molecular weight of both monomers gradually versus increasing the monomer conversion will indicate a constant radical concentration throughout the reaction and the living character of the polymerizations.²⁴ Moreover, the SI-RAFT polymerization of both monomers (HEMA-LA, HEMA-SA) was faster than the free RAFT agent-mediated

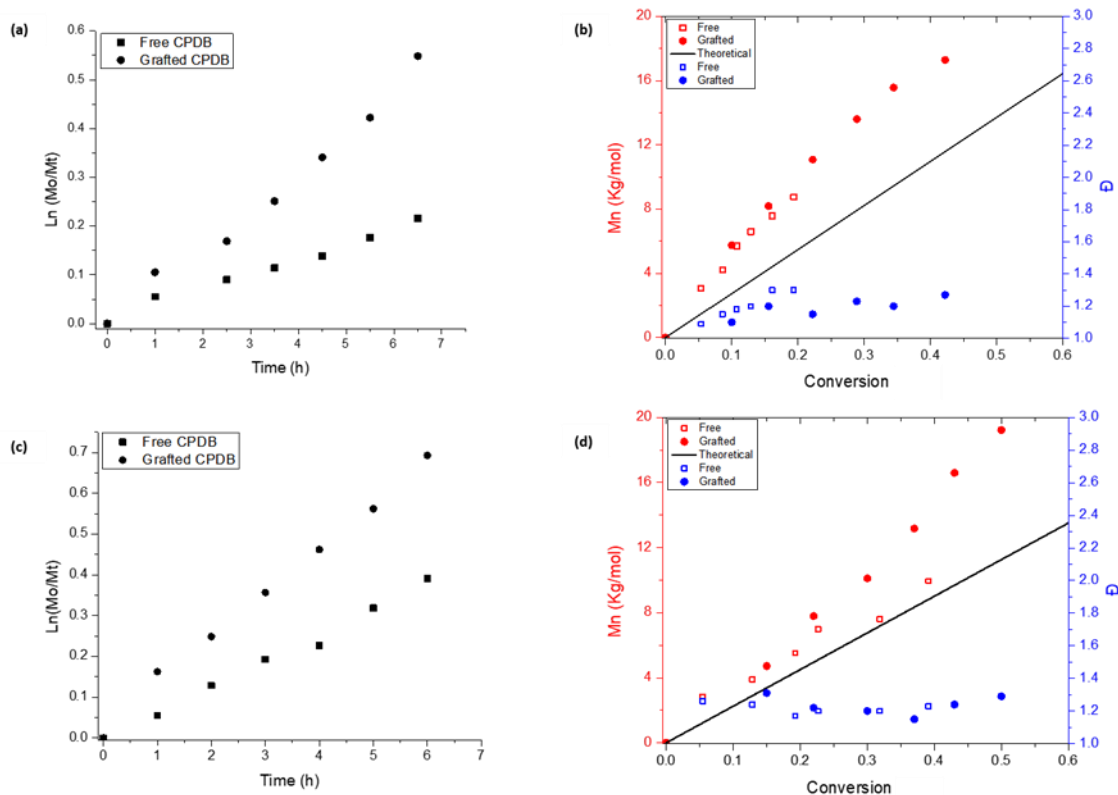
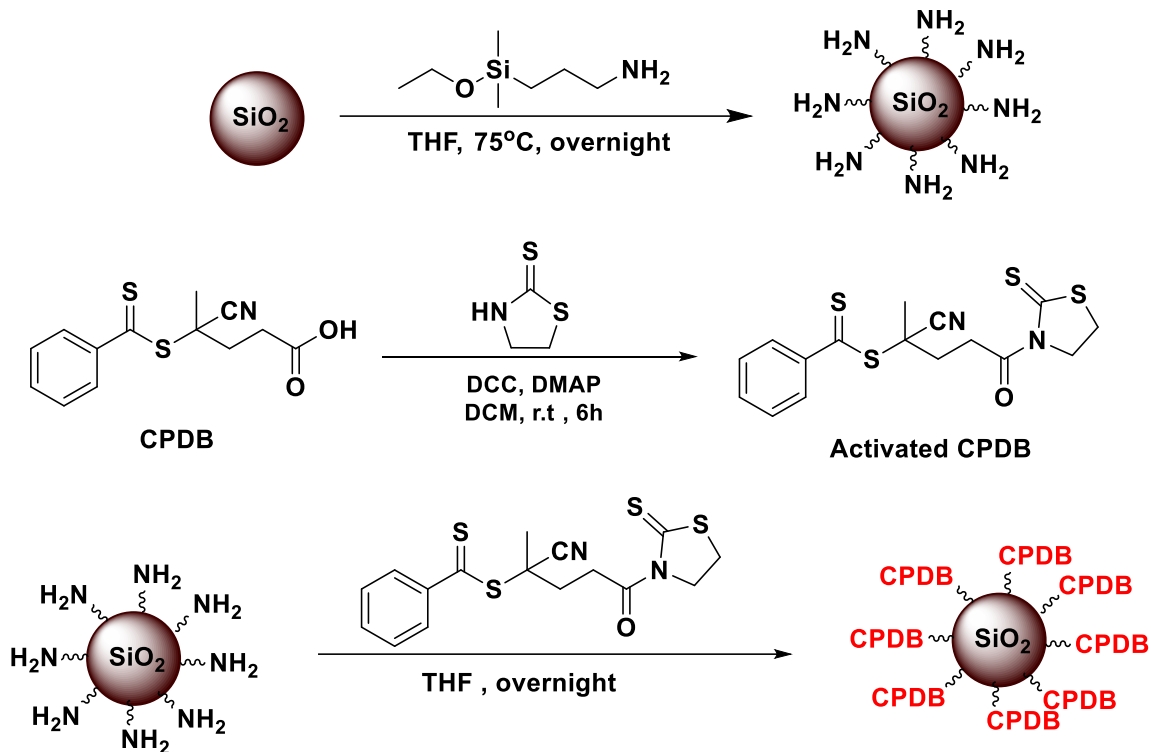


Figure 2.4 (a) Pseudo first-order kinetic plots of HEMA-LA with free CPDB (black solid circle); CPDB grafted nanoparticles with 0.1 ch/nm² density (black solid square) (b) dependence of molecular weight of HEMA-LA (red squares and circles), (solid black line, theoretical Mn), and the dispersity (blue squares and circles) on the conversion for the RAFT polymerization of HEMA-LA with ratio between species [CPDB]/[HEMA-LA]/[AIBN]=500:1:0.1 with free CPDB (squares); CPDB grafted nanoparticles with 0.1 ch/nm² density (circles) (c) pseudo first-order kinetic plots of HEMA-SA with free CPDB (black solid circle); CPDB grafted nanoparticles with 0.1 ch/nm² density (black solid square) (d) dependence of molecular weight of HEMA-SA (red squares and circles), (solid black line, theoretical Mn), and the dispersity (blue squares and circles) on the conversion for the RAFT polymerization of HEMA-SA with ratio between species [CPDB]/[HEMA-SA]/[AIBN]=500:1:0.1 with free CPDB (squares); CPDB grafted nanoparticles with 0.1 ch/nm² density (circles).

polymerization. The molecular weight distribution (\bar{M}_w/\bar{M}_n) of HEMA-LA was generally narrow no more than (1.30) compared with the molecular weight distribution (\bar{M}_w/\bar{M}_n) of the monomer HEMA-SA which is (1.31). At this time, the reasons for these trends are unclear, although this study adds more data to understand these relationships as new monomers are evaluated.

2.4.2 RAFT Polymerization of HEMA-LA and HEMA-SA from CPDB-Functionalized On Silica Nanoparticles:

Both HEMA-LA and HEMA-SA polymer-grafted nanoparticles via RAFT polymerization were prepared using the grafting-from approach using nanoparticles having CPDB RAFT agents covalently attached to the surface of the nanoparticles. The surface of the nanoparticles was modified by attachment of 3-aminopropyl dimethylethoxysilane onto the surface. CPDB chain transfer agents were anchored onto the surface of silica nanoparticles by reacting a mercaptothiazoline activated-CPDB (4-cyano-4-(phenylcarbonylthioylthio)pentanoate) with amine-functionalized silica nanoparticles (Scheme 2.4).²⁵ Controlling the ratio of silica nanoparticles to 3-aminopropyl dimethylethoxysilane provides good control to prepare the CPDB-grafted silica nanoparticles (CPDB-g-SiO₂) with various graft densities from 0.01–0.7 chains/nm².²⁶ The grafting density of the RAFT agents attached to the surface of silica nanoparticles was confirmed using UV-Vis spectrometry.



Scheme 2.4: Synthetic scheme for the functionalization of SiO₂ nanoparticles with CPDB RAFT agents.

Comparing the UV absorption at 302.5 nm of CPDB agents anchored onto silica nanoparticles (SiO₂-g-CPDB) to a standard absorption curve for known amounts of free CPDB was performed to determine the amount of the RAFT agents attached to the surface of nanoparticles before polymerization.¹⁷ RAFT polymerization of "controlled release" monomers HEMA-LA and HEMA-SA was studied in solution and on the surface of silica nanoparticles. Both polymers, Poly(HEMA-LA) brush anchored silica nanoparticles (HEMA-LA-g-SiO₂), and Poly(HEMA-SA) brush anchored silica nanoparticles (HEMA-SA-g-SiO₂), were

prepared via surface-initiated polymerization of HEMA-LA and HEMA-SA, respectively, from the surface of CPDB-g-SiO₂. In all RAFT polymerizations, we used azobisisobutyronitrile (AIBN) as the initiator for the polymerization at a molar ratio of [AIBN]/[CPDB] =1/10. An initiator to RAFT ratio of 0.1 was maintained in all polymerizations. We observed that the graft polymerization of HEMA-LA and HEMA-SA was affected by the ratio of [initiator]/[CTA]. When a polymerization was conducted at a higher ratio of an initiator, e.g., 0.2 or 0.3, partial and complete gelation of the polymerization solution, respectively, was observed after 12 h when we used a molar ratio of ([Monomer]:[CPDB] =1000:1). All polymerization reactions were carried out under similar conditions using AIBN as the initiator at 65°C and with the ratio of ([CTA]:[monomer]:[initiator]= 1:500:0.1). The molecular weight (M_n) and the dispersity (Đ) of HEMA-LA and HEMA-SA polymeric chains were evaluated using the gel permeation chromatography (GPC) analysis (Figure 2.5). HEMA-LA and HEMA-SA chains were cleaved from the surface of silica nanoparticles (50 mg) by stirring overnight in 4 mL of THF and 0.2 mL hydrofluoric acid.²⁷ The GPC traces of both (HEMA-LA, HEMA-SA) are shown from different polymerization times. All the curves are unimodal and continuously shifted to lower elution times with increasing polymerization time, which indicates an increase in the molecular weights. Table 1 summarizes some of the RAFT polymerizations that used to synthesize various

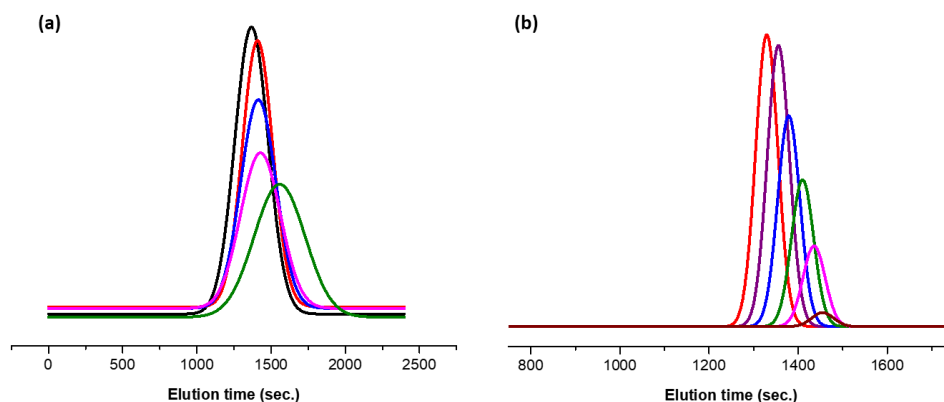


Figure 2.5: GPC traces of (a) SiO₂@P(HEMA-LA) and (b) SiO₂@P(HEMA-SA) in THF using ratio 500:1:0.1 of [monomer]:[CTA]:[initiator] at different times.

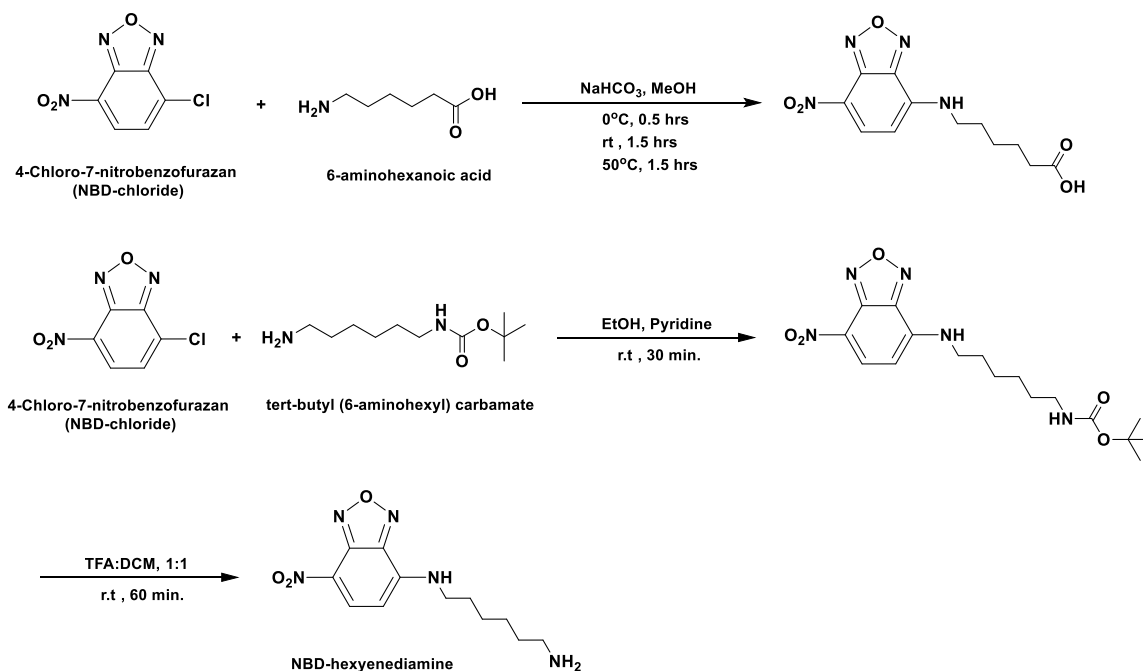
Table 2.1: Various molecular weights and chain densities of SiO₂@P(HEMA-LA) and SiO₂@P(HEMA-SA) using RAFT polymerization.

Sample	Ratio [RAFT]:[M] :[I]	Time (hrs)	GD (ch./nm ²)	Mn (KDa)	Đ
MA 149 SiO ₂ @P(HEMA-LA)	1: 500: 0.1	24	0.14	35.182	1.5
MA 159 SiO ₂ @P(HEMA-LA)	1: 500: 0.1	12	0.068	14.154	1.35
MA 161 SiO ₂ @P(HEMA-LA)	1: 500: 0.1	25	0.068	29.328	1.4
MA 170 SiO ₂ @P(HEMA-LA)	1: 500: 0.1	24	0.1	21.980	1.4
MA 160 SiO ₂ @P(HEMA-SA)	1: 500: 0.1	26	0.068	42.336	1.45
MA 169 SiO ₂ @P(HEMA-SA)	1: 500: 0.1	9	0.1	6.249	1.15
MA 181 SiO ₂ @P(HEMA-SA)	1: 1000: 0.1	9	0.1	10.755	1.2

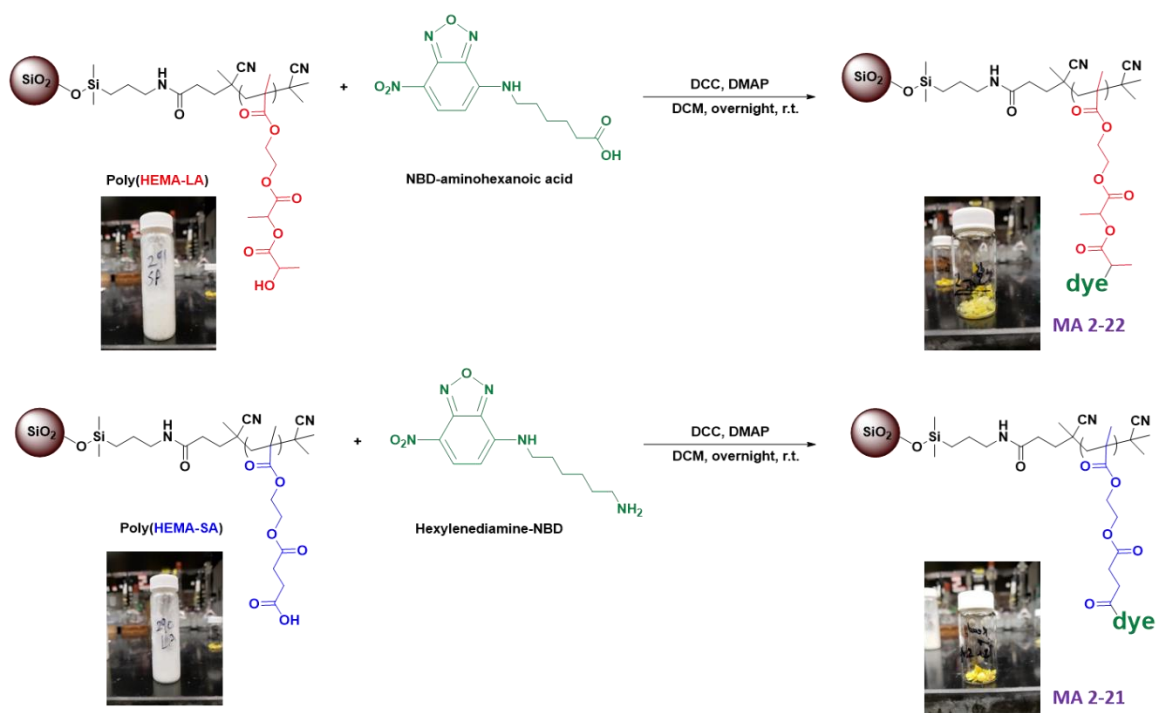
chain densities and molecular weights of polymer-grafted silica nanoparticles. Both HEMA-LA and HEMA-SA grafted silica nanoparticles were prepared at a constant RAFT/monomer ratio, (1:500) with targeted molecular weights less than 50 (kDa). Higher ratios and longer polymerization times will often result in gelation of the polymerization solutions.

2.4.3 Dye Labelling On Polymer-g-Nanoparticles (HEMA-SA-g-SiO₂, HEMA-LA-g-SiO₂):

Two different dyes (aminohexanoic acid-NBD, hexamethylenediamine-NBD) were synthesized (Scheme 2.5) and conjugated to the polymer grafted nanoparticles (HEMA-LA-g-SiO₂, HEMA-SA-g-SiO₂) (Scheme 2.6). After cleavage



Scheme 2.5: Synthesis of the dyes, 6-aminohexanoic acid (NBD-COOH), and NBD-hexamethylenediamine (NBD-NH₂).



Scheme 2.6: Synthesis of dye-labelled SiO₂@HEMA-LA, and SiO₂@HEMA-SA grafted-nanoparticles.

of the RAFT agent from the polymeric chain ends of the silica nanoparticles, both dyes were conjugated to the polymers via the Steglich esterification reaction using DCC/DMAP as the reagent and catalyst.²⁸ The synthetic schemes show that two different conjugation chemistries were used to link the dyes to the polymer on the surface of nanoparticles. The conjugation of nanoparticles (SiO₂-g-HEMA-LA, SiO₂-g-HEMA-SA) with dyes (aminohexanoic acid-NBD, hexyldiamine-NBD) was made through the ester and amide bonds, respectively, and it was confirmed using UV-vis and FT-IR spectroscopy (Figure 2.6). The UV-vis analysis of the NBD-dye attached to polymer grafted nanoparticles was showed an absorption at 460 nm

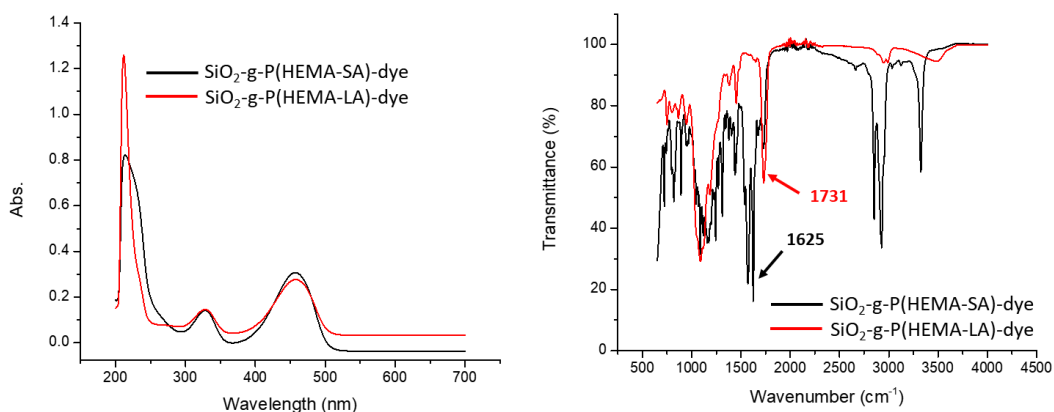


Figure 2.6: UV-vis, FT-IR spectrums of SiO₂-g-P(HEMA-LA)-dye (red curve), and SiO₂-g-P(HEMA-SA)-dye (black curve).

for both dyes that indicated the successful attachment. Moreover, the FT-IR analysis for SiO₂-g-P(HEMA-LA)-dye showed the ester group peak as a medium, sharp C=O stretching vibration peak at $\sim 1731\text{ cm}^{-1}$. Additionally, the amide group in SiO₂-g-P(HEMA-SA)-dye appeared as a strong, sharp C=O stretching vibration peak at $\sim 1625\text{ cm}^{-1}$.

The grafting density of the dye-attached polymer grafted nanoparticles could be estimated by comparing the graft density of the nanoparticles prior to and after attaching the dyes. The free dye showed an absorption at 460 nm. The amount of NBD-dyes on the polymer grafted silica nanoparticles was determined quantitatively by comparing the absorption at 480 nm for the dyes attached to silica nanoparticles to a standard calibration curve made from the free NBD-dyes. The amount of NBD-dye attached to the surface of the nanoparticles,

SiO₂@PHEMA-LA, SiO₂@PHEMA-SA (0.1 ch/nm² as determined by the RAFT agent) was calculated to be (22, 19.44 μmol/g, respectively) as determined by UV-vis spectroscopy. The graft densities (0.093, 0.082 ch/nm²) of dye-attached polymer grafted nanoparticles (SiO₂@PHEMA-LA-NBD-COOH, SiO₂@PHEMA-SA-NBD-NH₂, respectively) were comparable to that of polymer grafted nanoparticles (SiO₂@PHEMA-LA, SiO₂@PHEMA-SA) (0.1 ch/nm²) as determined by the RAFT agent measurement. The small differences may be due to the incomplete conversion of the amine and acid groups into dye-labeled groups.

Figure 2.7 shows the TGA analysis of the SiO₂-g-HEMA-LA-dye and SiO₂-g-HEMA-SA-dye nanoparticles, where the weight gain was observed after the polymerization. Compared with the bare silica nanoparticles, the polymer-grafted nanoparticles showed a higher weight loss of approximately (82.01%, 81.69%) for HEMA-LA, and HEMA-SA, respectively. When measured over the temperature range of 50–800°C, we observed increasing weight loss related to the increase in grafting organic materials on the surface of nanoparticles, such as unfunctionalized nanoparticles, amino-functionalized silica nanoparticles, CPDB-functionalized silica nanoparticles, polymer-grafted silica nanoparticles (PHEMA-LA, PHEMA-SA). That was clear by attaching the NBD-dyes to the polymer-grafted silica nanoparticles. Where the TGA traces were showed a higher weight

loss of approximately (97.38%, 94.71%) for dye-labeled polymer-grafted silica nanoparticles (PHEMA-LA-dye, PHEMA-SA-dye, respectively).

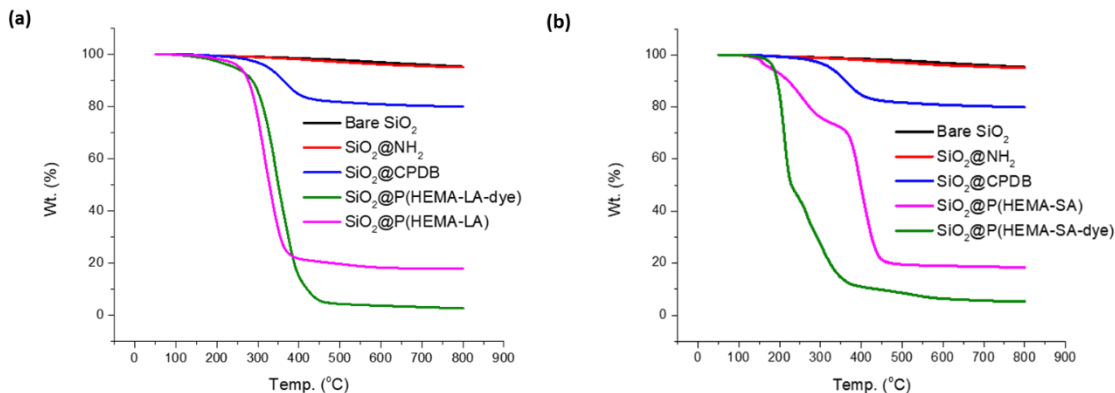


Figure 2.7: TGA trace of (a) SiO₂-g-HEMA-LA-dye and (b) SiO₂-g-HEMA-SA-dye nanoparticles.

2.4.4 Releasing Of Loaded Dyes From Nanoparticles (HEMA-LA-dye-g-SiO₂, HEMA-SA-dye-g-SiO₂):

To evaluate the controlled release properties of both polymer grafted silica nanoparticles that could be used for applications in drug delivery, the cumulative release rates of the dye-attached grafted nanoparticles were determined in-vitro.²⁹ Dye release from both polymer grafted nanoparticles was studied in phosphate-buffered saline (PBS) media with a pH value of 7.4 at two different temperatures, 25°C and 37°C, to evaluate the thermo-responsive nature of the polymers. The dye-attached grafted nanoparticles (HEMA-LA-dye-g-SiO₂, HEMA-SA-dye-g-SiO₂) were dispersed in 10 mL of dissolution media and placed in dialysis bags

(molecular weight cutoff of 3500; Thermo Fisher Scientific, USA). The dissolution media used in this study were 200 mL phosphate-buffered saline (PBS), pH 7.4, under continuous stirring (100 rpm rotation speed) at 25°C, 37°C. The dye released into the PBS buffer medium from HEMA-LA-dye-g-SiO₂ and HEMA-SA-dye-g-SiO₂ was collected, and the medium was replaced by fresh PBS at pre-determined time points. The dye released into the PBS buffer medium from HEMA-LA-dye-g-SiO₂ and HEMA-SA-dye-g-SiO₂ was pursued and measured by UV/Vis spectroscopy over 58 days until the amount of dye released reached an equilibrium. The amount of released dye of both HEMA-LA-dye-g-SiO₂ and HEMA-SA-dye-g-SiO₂ was determined by observing the absorbance of the withdrawn samples at 25°C and 37°C, at predetermined intervals at 480 nm wavelength (Figures 2.8, 2.9), respectively. As expected, the amount of released dye of both polymers at 37°C was higher than at 25°C in the same period of time. As well as the amount of released dye of HEMA-SA-dye-g-SiO₂ was higher than compared with the same amount (200 mg) of HEMA-LA-dye-g-SiO₂ (Figure 2.10).

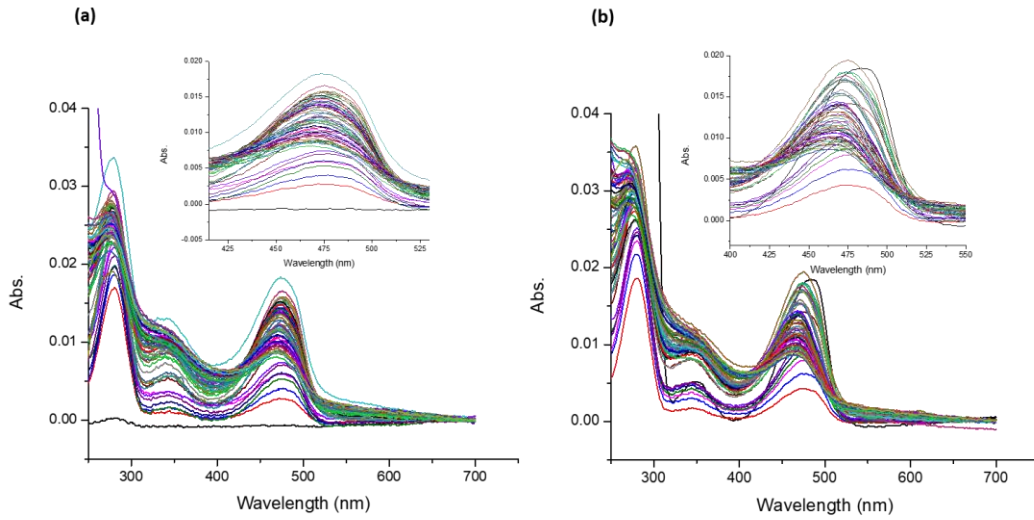


Figure 2.8: UV-vis spectra of SiO₂@P(HEMA-LA)-NBD-NH₂ at (a) 25°C and (b) 37°C for 58 days.

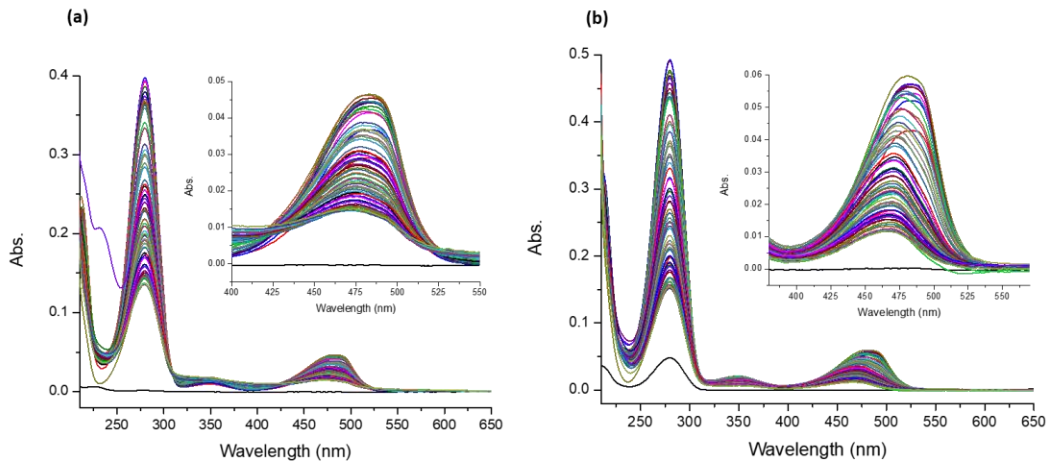


Figure 2.9: UV-vis spectra of SiO₂@P(HEMA-SA)-NBD-NH₂ at (a) 25°C and (b) 37°C for 58 days.

The cumulative release rate was calculated,³⁰⁻³²; it increases gradually within the time, and this trend will continue until reaching the equilibrium point

of dye release at pH value 7.4. HEMA-LA-dye-g-SiO₂ showed the maximal release of grafted dye (69.23%) at 25°C during the 1415 h (58 days) study period, compared to the HEMA-SA-dye-g-SiO₂ that have a maximal release (51.28%) the grafted dye at the same period of time and temperature. In other words, HEMA-LA-dye-g-SiO₂, and HEMA-SA-dye-g-SiO₂ provided a maximal amount of grafted NBD-dye (15.23, 9.97 μmol/g, respectively) at 25°C during the study period. On the other hands, the cumulative release rate of HEMA-LA-dye-g-SiO₂ showed the maximal release (82.62%) at a higher temperature (37°C) during the same period of study (58 days), compared with the HEMA-SA-dye-g-SiO₂ that showed a maximal release (65.17%) of the dye at the same period and temperature (Figure 2.10 a, b). Where the maximal amount of grafted NBD-dye that was released from HEMA-LA-dye-g-SiO₂, and HEMA-SA-dye-g-SiO₂ was 18.18, 12.67 μmol/g, respectively at 27°C during the 1415 h (58 days) study period.

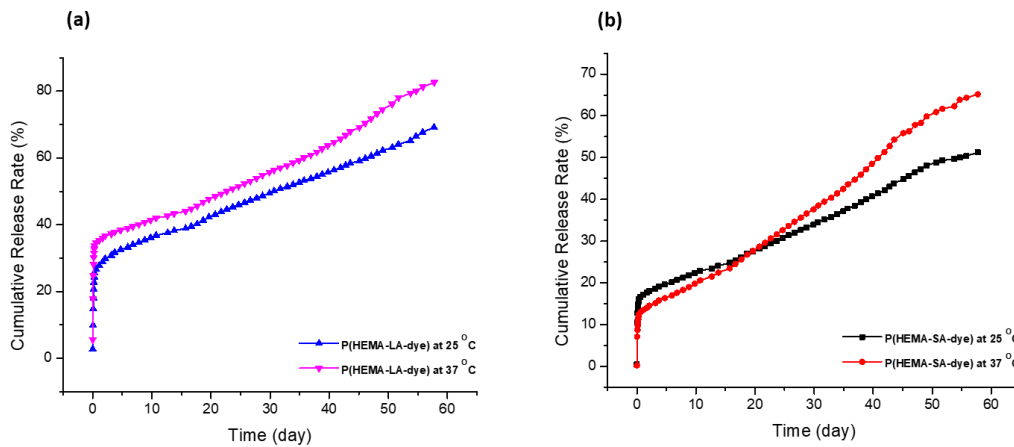


Figure 2.10: Cumulative release rate of (a) SiO₂@P(HEMA-LA-dye) and (b) SiO₂@P(HEMA-SA-dye), at 25°C and 37°C for 58 days.

Furthermore, both HEMA-LA-dye-g-SiO₂ and HEMA-SA-dye-g-SiO₂ were showed a high cumulative release rate of grafted dye at (37°C) compared with low temperature (25°C). By observing the cumulative release rate of the polymers, regardless of HEMA-LA-dye-g-SiO₂ or HEMA-SA-dye-g-SiO₂, there was an initial burst dye released within the first 24 hours at both 25°C and 37°C. The cumulative dye release from HEMA-LA-dye-g-SiO₂ at the first 24th hours was 5.87 μmol/g (26.68%) at 25 °C and 7.6 μmol/g (34.6%) at 37 °C. Beyond the burst period, after 24th hours, the cumulative dye release was gradually increased to reach a value of 15.23 μmol/g (69.23%) at 25°C in 1415th hour (58 days) and 18.18 μmol/g (82.62%) at 37°C in 1415th hour (58 days). On the other hand, the amount of released dye of HEMA-SA-dye-g-SiO₂ was lower in the same period of time. Within the 24th hour was 3.23 μmol/g (16.6%) at 25°C and 2.52 μmol/g (12.96%) at 37°C. After 24th hours the released dye was gradual to reach a value of 9.97 μmol/g (51.28%) at 25°C in 1415th hour (58 days) and 12.67 μmol/g (65.17%) at 37°C in 1415th hour (58 days). However, since the driving force of dye diffusion depends on the concentration gradient.³³ Therefore, the high concentration gradient of the dye between the surface of the nanoparticles and the PBS medium during the early stage of contact will lead to a higher initial burst and fast dye release rate (Figure 2.11).

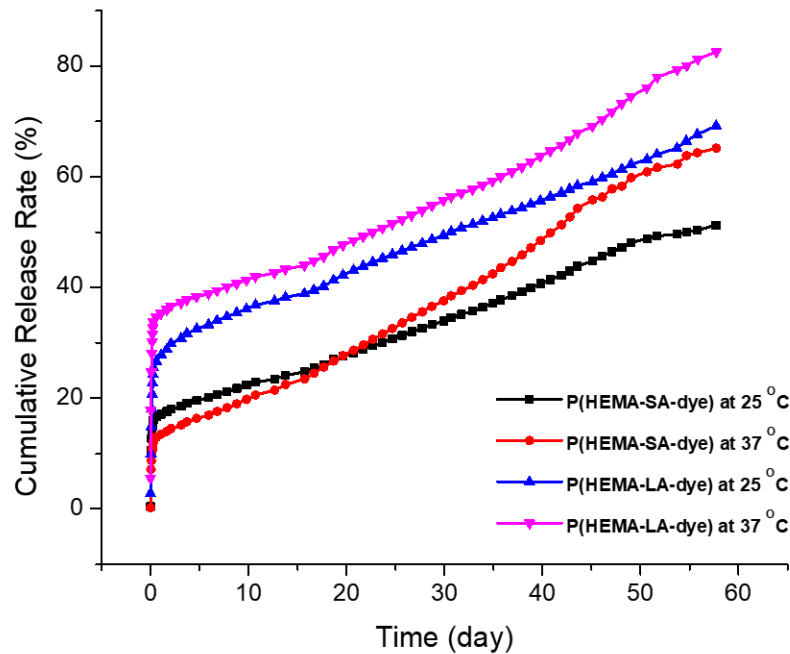


Figure 2.11: Cumulative release rate of $\text{SiO}_2@\text{P}(\text{HEMA-LA-dye})$, and $\text{SiO}_2@\text{P}(\text{HEMA-SA-dye})$, at 25°C and 37°C for 58 days.

One of the most attractive features of these polymers grafted on the nanoparticles, containing a hydrolytically sensitive ester linkage as drug carriers, is a thermos-responsive function to temperature changes. Overview, the cumulative release patterns observed for both two polymers grafted on the surface of nanoparticles showed a slow dye release during the first 20 days that could be assigned to release dye molecules that are adsorbed onto the surface of nanoparticles. Subsequently, the controlled release of released dye has occurred over a period of time. The release rates and extents of both polymers are different, although both exhibited very similar release profiles. The cumulative release rates

at 37°C at the end of the study period 1415 h (58 days) were higher than those at 25°C for the polymers regardless of HEMA-LA-dye-g-SiO₂ or HEMA-SA-dye-g-SiO₂, despite the cumulative release profiles at 37°C are the same as those at 25°C.

2.5 Conclusion:

In this research, the dye-loaded biodegradable PH-responsive polymers grafted on silica nanoparticles (SiO₂@PHEMA-LA-dye, SiO₂@PHEMA-SA-dye) were designed for usage in biomedical applications. These PH-responsive polymers have contained a hydrolytically sensitive ester linkage that can use as a drug delivery carrier. The polymers 2-((2-(propionyloxy) propanoyl)oxy)ethyl methacrylate (HEMA-LA) and 4-(2-(methacryloyloxy)ethoxy)-4-oxobutanoic acid (HEMA-SA) were successfully synthesized. Then, both were polymerized on the surface of silica nanoparticles using the RAFT polymerization and 4-cyanopentanoic acid dithiobenzoate (CPDB) as a chain transfer agent (CTA). However, two kinds of dyes were prepared and attached to the polymer grafted nanoparticles to investigate the controlled release rate of the polymer via usage in drug delivery applications. The synthesized dyes (NBD-aminohexanoic acid and NBD-hexylenediamine) were used as modal compounds to study the releasing rate behavior from the surface of silica nanoparticles at two different temperatures (25°C and 37°C) as a result of degradation of the polymers that containing a hydrolytically sensitive ester linkage using phosphate buffer solution (PBS, pH =

7.4). To achieve highly efficient targeting in specific sites, drug ligands (e.g., antibiotics) could be conjugated onto the surfaces of nanoparticles. PH-sensitivity could be combined with other stimuli like temperature to develop nanomaterials that have multifunctional drug delivery.

2.6 References:

- (1) Tiwari, G.; Tiwari, R.; Bannerjee, S.; Bhati, L.; Pandey, S.; Pandey, P.; Sriwastawa, B. *Int. J. Pharm. Investig.* 2012, 2 (1), 2.
- (2) Freiberg, S.; Zhu, X. X. *Int. J. Pharm.* 2004, 282 (1–2), 1–18.
- (3) Langer, R. 2003, 288 (4), 50–57.
- (4) Risbud, M. V.; Hardikar, A. A.; Bhat, S. V.; Bhonde, R. R. *J. Control. Release* 2000, 68 (1), 23–30.
- (5) Prabakaran, M.; Grailer, J. J.; Steeber, D. A.; Gong, S. *Macromol. Biosci.* 2008, 8 (9), 843–851.
- (6) Liu, J.; Huang, Y.; Kumar, A.; Tan, A.; Jin, S.; Mozhi, A.; Liang, X. J. *Biotechnol. Adv.* 2014, 32 (4), 693–710.
- (7) Manatunga, D. C.; de Silva, R. M.; de Silva, K. M. N.; de Silva, N.; Bhandari, S.; Yap, Y. K.; Costha, N. P. *Eur. J. Pharm. Biopharm.* 2017, 117, 29–38.

- (8) Stuart, M. A. C.; Huck, W. T. S.; Genzer, J.; Müller, M.; Ober, C.; Stamm, M.; Sukhorukov, G. B.; Szleifer, I.; Tsukruk, V. V.; Urban, M.; Winnik, F.; Zauscher, S.; Luzinov, I.; Minko, S. *Nat. Mater.* 2010, 9 (2), 101–113.
- (9) D'Souza, A. J. M.; Topp, E. M. J. *Pharm. Sci.* 2004, 93 (8), 1962–1979.
- (10) Thambi, T.; Deepagan, V. G.; Yoo, C. K.; Park, J. H. *Polymer (Guildf)*. 2011, 52 (21), 4753–4759.
- (11) Yang, H.; Wang, Q.; Huang, S.; Xiao, A.; Li, F.; Gan, L.; Yang, X. *ACS Appl. Mater. Interfaces* 2016, 8 (12), 7729–7738.
- (12) Smeets, N. M. B.; Patenaude, M.; Kinio, D.; Yavitt, F. M.; Bakaic, E.; Yang, F.-C.; Rheinstädter, M.; Hoare, T. *Polym. Chem.* 2014, 5 (23), 6811–6823.
- (13) Ishimoto, K.; Arimoto, M.; Ohara, H.; Kobayashi, S.; Ishii, M.; Morita, K.; Yamashita, H.; Yabuuchi, N. *Biomacromolecules* 2009, 10 (10), 2719–2723.
- (14) Hong, L.; Zhang, Z.; Zhang, Y.; Zhang, W. J. *Polym. Sci. Part A Polym. Chem.* 2014, 52 (18), 2669–2683.
- (15) Tous, E.; Ifkovits, J. L.; Koomalsingh, K. J.; Shuto, T.; Soeda, T.; Kondo, N.; Iii, J. H. G.; Gorman, R. C.; Burdick, J. a. *Biomacromolecules* 2011, 12 (11), 4127–4135.
- (16) Li, C.; Han, J.; Ryu, C. Y.; Benicewicz, B. C. *Macromolecules* 2006, 39 (9), 3175–3183.

- (17) Rungta, A.; Natarajan, B.; Neely, T.; Dukes, D.; Schadler, L. S.; Benicewicz, B. C. *Macromolecules* 2012, 45 (23), 9303–9311.
- (18) Li, J.; Wang, L.; Benicewicz, B. C. *Langmuir* 2013, 29 (37), 11547–11553.
- (19) Woodland, J. G.; Hunter, R.; Smith, P. J.; Egan, T. J. *Org. Biomol. Chem.* 2017, 15 (3), 589–597.
- (20) Borchmann, D. E.; Tarallo, R.; Avendano, S.; Falanga, A.; Carberry, T. P.; Galdiero, S.; Weck, M. *Macromolecules* 2015, 48 (4), 942–949.
- (21) Sanoj Rejinold, N.; Muthunarayanan, M.; Divyarani, V. V.; Sreerekha, P. R.; Chennazhi, K. P.; Nair, S. V.; Tamura, H.; Jayakumar, R. J. *Colloid Interface Sci.* 2011, 360 (1), 39–51.
- (22) Manatunga, D. C.; de Silva, R. M.; de Silva, K. M. N.; de Silva, N.; Bhandari, S.; Yap, Y. K.; Costha, N. P. *Eur. J. Pharm. Biopharm.* 2017, 117 (October), 29–38.
- (23) Keddie, D. J.; Moad, G.; Rizzardo, E.; Thang, S. H. *Macromolecules* 2012, 45 (13), 5321–5342.
- (24) Thomas, D. B.; Convertine, A. J.; Myrick, L. J.; Scales, C. W.; Smith, A. E.; Lowe, A. B.; Vasilieva, Y. A.; Ayres, N.; McCormick, C. L. *Macromolecules* 2004, 37 (24), 8941–8950.
- (25) Li, C.; Han, J.; Ryu, C. Y.; Benicewicz, B. C. *Macromolecules* 2006, 39 (9), 3175–3183.

- (26) Li, C.; Benicewicz, B. C. *Macromolecules* 2005, 38, 5929–5936.
- (27) Ojang, L.; Zhang, L.; Zhang, Z.; Zhou, N.; Cheng, Z.; Xiulin, Z. *J. Polym. Sci. Part A Polym. Chem.* 2010, 48 (9), 2006–2015.
- (28) Giacomelli, C.; Schmidt, V.; Borsali, R. *Macromolecules* 2007, 40 (6), 2148–2157.
- (29) Thilanga Liyanage, A. D.; Chen, A. J.; Puleo, D. A. *ACS Biomater. Sci. Eng.* 2018, 4 (12), 4193–4199.
- (30) Chandrasekaran, A. R.; Jia, C. Y.; Theng, C. S.; Muniandy, T.; Muralidharan, S.; Dhanaraj, S. A. *J. Appl. Pharm. Sci.* 2011, 1 (5), 214–217.
- (31) Leong, J.; Chin, W.; Ke, X.; Gao, S.; Kong, H.; Hedrick, J. L.; Yang, Y. Y. *Nanomedicine Nanotechnology, Biol. Med.* 2018, 14 (8), 2666–2677.
- (32) Liu, S. Q.; Wiradharma, N.; Gao, S. J.; Tong, Y. W.; Yang, Y. Y. *Biomaterials* 2007, 28 (7), 1423–1433.
- (33) Kim, M.; Kim, T. *Anal. Chem.* 2010, 82 (22), 9401–9409.

CHAPTER 3

ENGINEERING WATER-DISPERSIBLE BIMODAL POLYMER

GRAFTED SILICA NANOPARTICLES AS ANTIBIOTIC-CARRIERS ¹

¹Al-Ali, M.A. and Benicewicz B. C. To be submitted to Journal of Polymer Science.

3.1 Abstract:

The growing global interest in bacterial resistance to conventional antibiotics has attracted much attention in the pharmaceutical industry. Thus, novel strategies to implement the efficient integration of antibiotics with nanomaterials are required in the drug delivery systems. Bimodal polymer chains functionalized on silica nanoparticles surface was designed using surface-initiated reversible addition–fragmentation chain transfer (RAFT) polymerization. Two populations of polymer chains were grafted to create water-dispersible nanoparticles that have the advantage of serving as antibiotic-delivery vehicles in biomedical applications. For the first chain population, a pH-responsive controlled release of two monomers (HEMA-LA) and (HEMA-SA) containing a hydrolytically sensitive ester linkage, were functionalized on silica nanoparticles at high graft density and low molecular weight to use as antibiotic-delivery carriers. A low graft density of the high molecular weight water-dispersible poly(methacrylic acid) (PMAA) was grafted as the second population. Additionally, fluorescent dyes (NBD-X) were conjugated to the ends of pH-sensitive polymers (HEMA-LA, HEMA-SA) via the Steglich esterification reaction using (DCC/DMAP) catalyst, which is helpful to monitor the nanoparticles in biological systems. Water-dispersible PMAA grafted silica nanoparticles may provide an important platform for usage in biomedical applications.

3.2 Introduction:

Polymer grafted nanoparticles have gained much attention for a variety of biomedical applications.^{1,2} In particular, silica nanoparticles have received wide research attention because of their applications in drug delivery nanocomposites.³⁻⁵ Maintaining good water-dispersibility of polymer grafted nanoparticles is still a challenge for biomedical applications.⁶ One of the important applications of the reversible addition-fragmentation chain transfer (RAFT) polymerization is functionalizing different polymers on the surface of nanoparticles,⁷ such as acid-containing monomers that have a significant advantage in biomedical fields such as drug delivery.¹ RAFT polymerization has many advantages, such as engineering "bimodal nanoparticles" that can be used by grafting two different polymeric chains, forming a nanocomposite that has new characteristics.⁸ One particular approach is using a bimodal polymer brush that contains a high graft density of short molecular weight homopolymer chains and the second set of chains, which are grafted at low graft density high molecular weight.⁹ This important approach, widely used and versatile, enables us to independently control the molecular weights, synthesis, and graft densities of the individual polymeric populations that are grafted on the surface of nanoparticles.¹⁰

Stimuli-responsive polymers are a significant class that has been used in biomedical applications, such as poly(methacrylic acid) (PMAA) and other

polymers made from acid-containing monomers.¹¹ RAFT polymerization is a useful technique that can be used to polymerize such monomers, while other CRP techniques (e.g., ATRP) cannot be used due to catalyst poison issues.¹² A few years ago, several research groups reported the synthesis of PMAA on nanoparticle surfaces using the RAFT polymerization. For example, Feng et al.¹³ synthesized a quadruple-responsive nanocomposite that responds to temperature, pH, magnetic field, and NIR by incorporating iron oxide nanoparticles and gold nanorods into a dextran-based smart copolymer network that was prepared by sequential RAFT polymerization of methacrylic acid (MAA) and N -isopropyl acrylamide. Yilmaz et al.¹⁴ prepared a nanocomposite as a model anticancer drug via combined doxorubicin (DOX) with polymethacrylic acid (PMAA) grafted on the gold nanoparticles using the RAFT polymerization. Wang et al.¹⁵ engineered polymethacrylic acid (PMAA) functionalized silica nanoparticles and used them as a vehicle-delivery for antibiotics to bacterial cells.

In biomedical applications, specifically, grafted polymers on nanoparticles that can be used as antibiotic carriers, the dispersibility of the polymer grafted nanoparticles in water is considered a particular challenge.^{6,16} Therefore, the nature of the polymer grafted on nanoparticles is a significant issue that affects the final dispersibility of nanoparticles in the water. The dispersibility and biocompatibility of the nanoparticles can be achieved by grafting polymers on the nanoparticle's

surface.¹⁷ Therefore, designing water-dispersible polymer grafted nanoparticles that work as an antibiotic-carriers are highly desirable in biomedical application.¹⁸

In this work, we report on research of water-dispersible bimodal silica nanoparticles that consist of two different polymer populations prepared via RAFT polymerization. One of these two populations is a polymer of pH-sensitive antibiotic delivery carriers (HEMA-LA and HEMA-SA) grafted at a high graft density and low molecular weight of the polymer. The second chain population is the polymer of polymethacrylic acid (PMAA) grafted at a low graft density and high molecular weight, which imports water dispersibility to the nanoparticles.¹⁹ We believe that these bimodal grafted silica nanoparticles have great potential for bioapplications. Biocompatibility, controllable particle size, and an extensive chemistry toolbox of surface functionalization are some of the important attributes of these nanoparticles.²⁰ Additionally, polymer chains containing carboxylic acid moieties, such as poly(methacrylic acid), that are anchored on silica nanoparticles possess an important role in dealing with bacterial infections and as antibiotic delivery vehicles in the biomedical area.^{21,22}

3.3 Materials and Methods:

3.3.1 Materials:

Colloidal silica nanoparticles (SiO_2 , 30 wt% in MEK) were purchased from Nissan Chemical. 3-Aminopropyldimethylethoxysilane and dimethylmethoxy-n-octylsilane were purchased from Gelest, Inc (95%), and used as received. The reversible addition-fragmentation chain transfer (RAFT), 4-cyano-4-(phenylcarbonothioylthio)pentanoic acid (CPDB) were purchased from Boron Molecular and used as received. 2,2'-Azobis(2-methylpropionitrile) (AIBN, Aldrich, 98%), L-lactide (Sigma Aldrich, 95%), succinic anhydride (Acros Organics, 99%), and methacrylic acid (MAA, Alfa Aesar, 99%) were purchased and used as received. HEMA, 2-hydroxyethyl methacrylate (Sigma Aldrich, 99%) was purified by passing through a column of basic aluminum oxide (Alfa Aesar, 99%) to remove the inhibitor, methyl ether hydroquinone (MEHQ). All other reagents and solvents were used as received unless otherwise noted.

3.3.2 Instrumentation:

$^1\text{H-NMR}$ (Bruker Avance III-HD 300 MHz) spectrometer instrument was used to acquire the proton NMR spectra using CDCl_3 as a solvent and measured with tetramethylsilane (TMS) as an internal reference. Gel permeation chromatography (GPC) was used to measure the molecular weights (M_n) and dispersity index (\mathcal{D}). The GPC was equipped with a Varian 290-LC pump, a Varian 390-LC refractive

index detector, and three Styragel columns (HR1, HR3 and HR4, molecular weight range of 100-5000, 500-30000, and 5000-500000, respectively). Tetrahydrofuran (THF) was used as eluent at 30°C at a flow rate of 1.0 mL/min, calibrated with polystyrene and poly(methylmethacrylate) standards obtained from Polymer Laboratories. A thermogravimetric analyzer (TA) Instruments Q5000 was used to obtain TGA characterization. Samples were preheated to 100°C and kept at this temperature for 10 min to remove residual solvents for all the samples. After cooling to 50°C, the samples were reheated to 800°C at a heating rate of 10°C/min under nitrogen flow. FT-IR spectra were recorded using a BioRad Excalibur FTS 3000. UV-vis absorption spectra were taken on a Shimadzu UV-2450 spectrophotometer.

3.3.3 Methods:

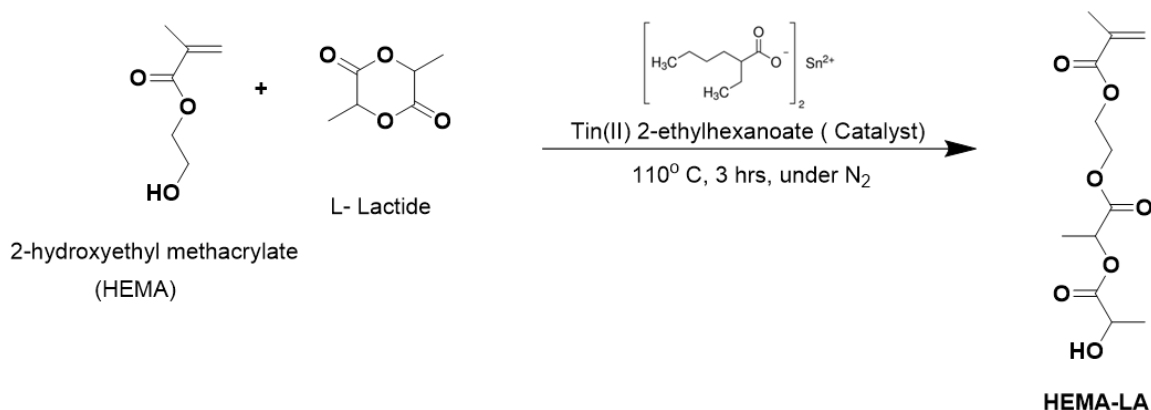
3.3.3.1 Synthesis of “Controlled Release” Monomers:

Methacrylate monomers (HEMA-LA, HEMA-SA) were synthesized via ring-opening reaction of the corresponding cyclic lactone compound, L-lactide, or succinic anhydride, respectively. The hydroxyethyl methacrylate (HEMA) was used as the initiator catalyzed by stannous 2-ethylhexanoate and DMAP, respectively.

3.3.3.1.1 Synthesis of 2-((2-(Propionyloxy) Propanoyl)oxy)ethyl Methacrylate

(HEMA-LA) (Scheme 3.1):

L-lactide (5.98 g, 41 mmol) was dried overnight under vacuum and placed in a 200 mL two-neck round bottom flask. Then, HEMA (5.6 mL, 46 mmol) and tin(II) 2-ethylhexanoate (105 μ L, 0.32 mmol) were added to the flask. The reaction mixture was deoxygenated by a repeated vacuum nitrogen cycle. The reaction was heated to 110°C under a sealed vacuum for 3 hours with stirring. Anhydrous chloroform (100 mL) was added to dissolve the crude product, which was washed with 1 M HCl. The organic phase of the chloroform was isolated after washing three times with deionized water. Finally, the residual chloroform was removed using a rotary evaporator operating under a vacuum, and the product was collected (yield: 75%, 8.55 g). $^1\text{H-NMR}$ (300 MHz, CDCl_3): $\delta = 1.38\text{--}1.63$ ppm (6H, CH-CH_3), $\delta = 1.94$ ppm (3H, $\text{CH}_2=\text{CCH}_3$), $\delta = 2.79$ ppm (1H, C-OH), $\delta = 4.26\text{--}4.39$ ppm (4H, $\text{OCH}_2\text{-CH}_2$), $\delta = 4.39\text{--}4.51$ ppm (1H, CH-(OH)CH_3), $\delta = 5.08\text{--}5.29$ ppm



Scheme 3.1: Synthesis of HEMA-LA monomer.

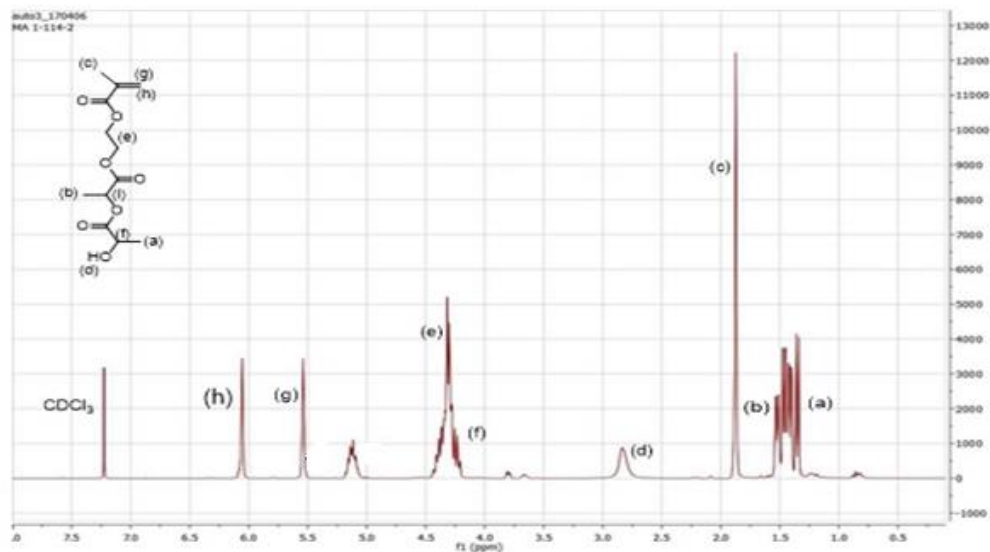


Figure 3.1: ^1H NMR (300 MHz, CDCl_3) spectrum of HEMA-LA monomer.

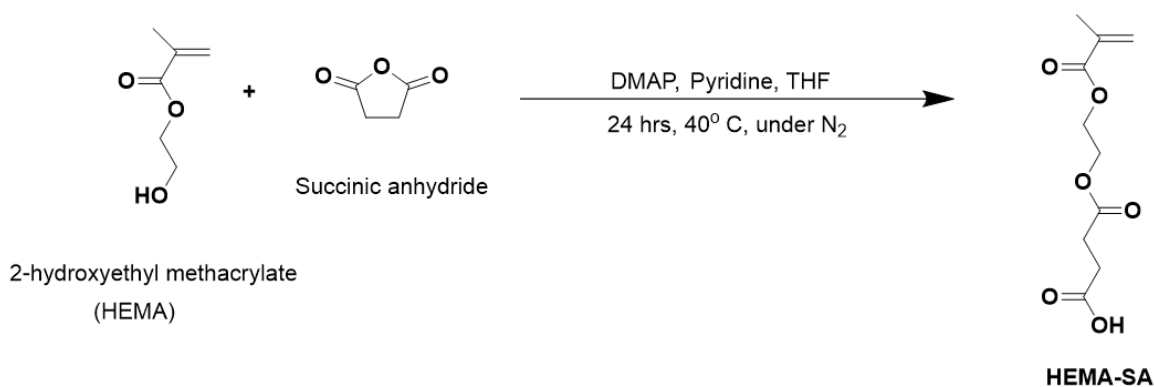
(q,1H), $(\text{C}=\text{O})\text{CH}(\text{C}-\text{O})$, $\delta = 5.58$ ppm (s,1H, $\text{CH}_2=\text{C}$), $\delta = 6.10$ ppm (s,1H, $\text{CH}_2=\text{C}$)

(Figure 3.1). HRMS (EI) (m/z) calcd for $\text{C}_{12}\text{H}_{18}\text{O}_7$: 274.1149; found: 274.1167.^{23,24}

3.3.3.1.2 Synthesis of 4-(2-(Methacryloyloxy)ethoxy)-4-oxobutanoic acid (HEMA-SA) (Scheme 3.2):

Anhydrous THF solution of 2-hydroxyethyl methacrylate (HEMA; 6.5 g, 50 mmol) was placed in a Schlenk flask (250 mL) with a magnetic stirring bar at room temperature under nitrogen. Succinic anhydride (6 g, 60 mmol), 15 mL of pyridine, and 4-dimethylaminopyridine (0.49 g, 4 mmol) were added to the Schlenk flask. Then, the reaction mixture was stirred for 24 h at 40°C under nitrogen. Thence, the reaction was cooled down to room temperature, and the solvent was evaporated under vacuum. DCM was added to dissolve the residue and washed three times with 0.1 M HCl solution. The organic phase of DCM was dried over anhydrous

magnesium sulfate overnight. MgSO_4 was filtered out, and the solvent was evaporated. The product (HEMA-COOH) was dried under vacuum at room temperature. A viscous liquid was obtained (6.4 g, yield 65%). ^1H NMR (300 MHz, CDCl_3): $\delta = 6.13$ (s, 1H, $\text{HCH}=\text{C}(\text{CH}_3)-$), 5.54 (s, 1H, $\text{HCH}=\text{C}(\text{CH}_3)-$), 4.36 (t, 4H, $-\text{OOC}(\text{CH}_2)_2\text{OCO}-$), 2.68 (t, 4H, $\text{HOOC}(\text{CH}_2)_2\text{COO}-$), 1.85 (s, 3H, $\text{H}_3\text{C}-\text{C}(\text{COO})\text{CH}_2$) (Figure 3.2). HRMS (EI) (m/z) calcd for $\text{C}_{10}\text{H}_{14}\text{O}_6$: 230.0842; found: 230.0873.^{25,26}



Scheme 3.2: Synthesis of HEMA-SA monomer.

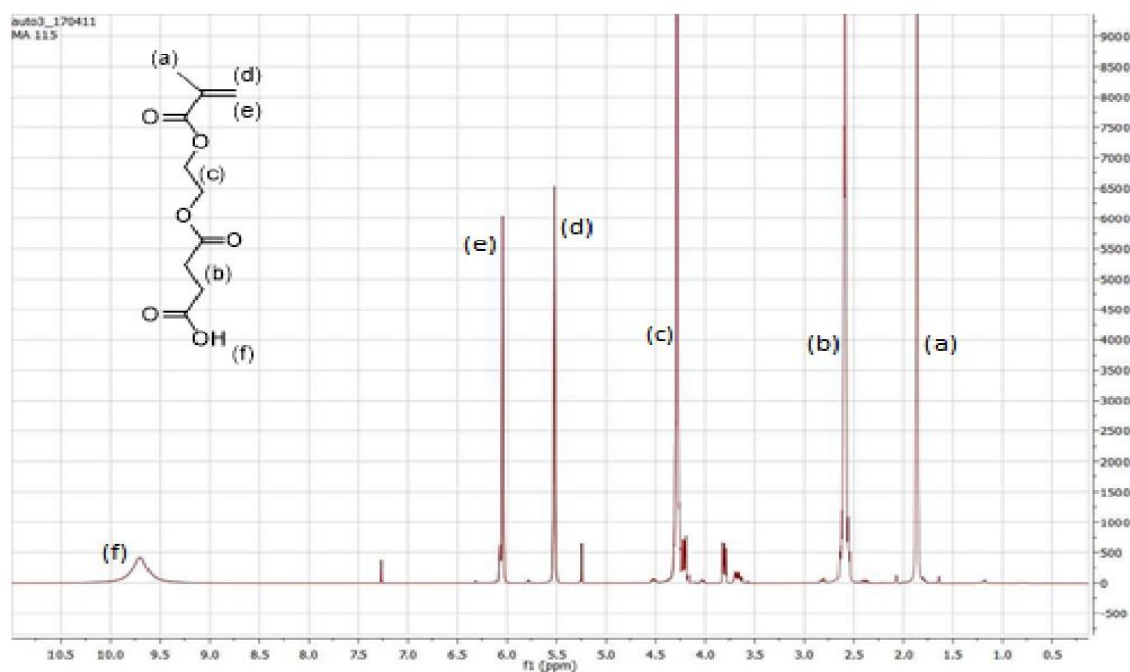


Figure 3.2: ^1H -NMR (300 MHz, CDCl_3) spectrum of HEMA-SA monomer.

3.3.3.2 Activation of 4-cyano-4-(thiobenzoylthio)pentanoic acid (CPDB):

4-Cyano-4-(thiobenzoylthio)pentanoic acid (CPDB) (3 g, 10.74 mmol), 2-mercaptothiazoline (1.54 g, 12.88 mmol), and dicyclohexylcarbodiimide (DCC) (2.66 g, 12.88 mmol) were placed in a 250 ml round bottom flask and dissolved in 40 ml of dichloromethane. Then, dimethylamino pyridine (DMAP) (0.13 g, 1.1 mmol) was added slowly to the solution and stirred (6 h) at room temperature. The solution was filtered, and the solids were removed. The solution was evaporated to remove the solvent. The activated CPDB was obtained as a red oil (3.1 g, 76% yield), which was purified via silica gel column chromatography (5:4 hexane: ethyl acetate).²⁷ ¹H NMR (300 MHz, CDCl₃): δ (ppm) 7.90 (d, 2H, aromatic ring), 7.56 (t, 1H, aromatic ring), 7.38 (t, 2H, aromatic ring), 4.58 (t, 2H, NCH₂CH₂S), 3.60-3.66 (m, 2H, (CN)C(CH₃)-CH₂CH₂CON), 3.31 (t, 2H, NCH₂CH₂S), 2.50-2.56 (m, 2H, (CN)C(CH₃)CH₂CH₂CON), 1.95 (s, 3H, (CH₃)C(CN)S). FT-IR: 1700 cm⁻¹ (C=O), 1160 cm⁻¹ (PhC=S), 1020 cm⁻¹ (NC=S). HRMS (EI) (m/z) calcd for C₁₆H₁₆N₂OS₄: 380.0193; found: 380.0203.

3.3.3.3 Attachment of Activated CPDB onto Silica Nanoparticles (SiO₂@CPDB):

3-Aminopropyldimethylethoxy silane (500 μL) was added to the 35 ml THF solution of 10.0 g silica nanoparticles. The solution was refluxed at 75°C overnight, after purging with N₂ more than 30 min. Then, the solution was cooled to the room temperature and precipitated into a large amount of hexanes. The nanoparticles

were recovered by centrifugation at 3,500 rpm for 8 minutes, and the solvent was decanted. Then, the precipitation-dissolution process was repeated for another two times and dispersed in 30 mL of dry THF. Next, the THF solution of the amine-functionalized nanoparticles was added dropwise into a THF solution of the activated CPDB at room temperature. Subsequently, the solution was stirred for 6 hours at r.t. Then, the solution was poured into (500 ml) of hexane, and the nanoparticles were collected using the centrifugation at 4000 rpm for 7 min. This precipitation-dissolution process was repeated until the supernatant solution was colorless. After that, the CPDB anchored nanoparticles were dried using the vacuum at r.t for 24 h. The grafting density (0.35 ch/nm^2) of CPDB anchored silica nanoparticles was determined using the calibration curve of the standard solutions of free CPDB via UV-vis spectrometry.⁹

3.3.3.4 RAFT Polymerization of “Controlled Release” Monomers from CPDB Functionalized Silica Nanoparticles:

A THF solution (10 ml) of monomer (HEMA-LA, or HEMA-SA), CPDB-anchored silica nanoparticles with desired graft density, AIBN (10 mM) was prepared in a dried Schlenk tube. The molar ratio of [CPDB]:[monomer]:[AIBN] was 1:500:0.1. The solution was degassed via three cycles of freeze–pump–thaw, then filled with nitrogen. The Schlenk tube was placed in an oil bath at 65°C for the desired time. Later, the polymerization was stopped by quenching the Schlenk

tube in ice water. The polymer-grafted silica nanoparticles were precipitated by pouring into 400 ml of hexanes and centrifuged at 4000 rpm for 7 min. The nanoparticles were dispersed back into 40 ml of THF. The molecular weight and polydispersity index of the polymers grafted onto silica nanoparticles were evaluated using GPC by dissolving (50 mg) of the nanoparticles in (3 ml) of THF and treating with (0.2 ml) aqueous HF (49%). Then, the solution was stirred overnight, and the cleaved polymer chains were analyzed by GPC.²⁸

3.3.3.5 Cleavage of CPDB agents from the polymeric chain ends of the Silica Nanoparticles:

The THF (40 ml) solution of dispersed polymer-grafted nanoparticles (SiO₂-g-HEMA-LA, SiO₂-g-HEMA-SA) was placed in a round flask. The initiator AIBN was added at the ratio 1:20 of ([CTA]:[AIBN]). The solution was heated at 65°C under nitrogen for 1 h. Then, the nanoparticles were precipitated by pouring the solution into 500 ml of hexane, and the nanoparticles were recovered by centrifuging at 3500 rpm for 8 min.⁹

3.3.3.6 Preparation of NBD-labelled Amino Acids (NBD-COOH):

6-Aminohexanoic acid (1.2 eq, 4.5 mmol) and NaHCO₃ (3 eq, 11.27 mmol) were dissolved in MeOH (30 mL) and stirred for 30 min at room temperature. A methanol solution (5 ml) of 4-chloro-7-nitrobenzofurazan (NBD-Cl; 1 eq, 3.76 mmol) was added dropwise to the solution of 6-aminohexanoic acid, which was

refluxed to 65°C. After two hours, the reaction mixture was cooled to room temperature and acidified to approximately pH 2 with 1M HCl. Subsequently, the mixture was extracted three times with EtOAc (25 mL). The organic layer of EtOAc was washed with brine solution and dried with MgSO₄ for two hours. The solution was filtered, and the solvent was removed out using a rotary evaporator. Then, the resultant NBD-labelled amino acid was recrystallized using an aqueous MeOH.²⁹ The product was yield as bright orange crystals (yield: 77%, 0.85 g). T_m= 156-158°C, UV (MeOH) λ_{max}: 335, 458. FT-IR ν_{max}/cm⁻¹ 1700 (strong, sharp C=O). MS (EI+) m/z: [M]⁺ 294.

3.3.3.7 Preparation of NBD-labelled hexamethylenediamine (NBD-NH₂):

There are two steps for the synthesis of hexamethylenediamine-NBD dye. First, N-Boc-hexamethylenediamine-NBD was prepared, which was converted to the hexylenediamine-NBD. 4-Chloro-7-nitrobenzofurazan (NBD-Cl) (1 eq, 1 g, 5 mmol) and mono-Boc hexamethylenediamine (1.1 eq, 1.19 g, 5.5 mmol) was dissolved in ethanol (30 mL). Pyridine was added (catalytic, 450 μL) and the solution was stirred for 30 min. The solution was concentrated and purified using column chromatography (toluene: ethyl acetate 7:3) to obtain the Boc-protected dye as a red foam. In the second step, the Boc-protected dye was dissolved in a 1:1 solution of trifluoroacetic acid (TFA): dichloromethane (DCM) and stirred for one hour at the room temperature. Subsequently, the solution was concentrated and

resuspended in acetonitrile. The final product was obtained as golden crystals after the solution was precipitated into cold diethyl ether (1.1 g, yield 78%).³⁰ UV (MeOH) λ_{max} : 336, 460. FT-IR $\nu_{\text{max}}/\text{cm}^{-1}$ 3380 (medium, sharp N-H). HRMS (EI) (m/z) calcd for $\text{C}_{12}\text{H}_{17}\text{N}_5\text{O}_3$: 279.1382; found: 279.3014.

3.3.3.8 Amino hexanoic acid-NBD conjugate on SiO_2 -g-HEMA-LA and hexamethylenediamine-NBD Conjugate on SiO_2 -g-HEMA-SA:

Polymer-g-silica nanoparticles (1 eq, 0.5 g) (HEMA-LA-g- SiO_2 or HEMA-SA-g- SiO_2) were dissolved in THF (50 mL) and placed in a 250 mL round flask. Then, dye-labeled (1.1 eq) (amino hexanoic acid-NBD, 0.59 g, 2 mmol or hexamethylenediamine-NBD, 0.66 g, 2.39 mmol), and dicyclohexylcarbodiimide (DCC) (1.3 equiv.) were dissolved and added to the flask. The mixture was stirred at room temperature for 9 h. The solution was filtered, and the solvent was poured into hexane (500 mL) to precipitate the nanoparticles. NP's were recovered via centrifugation at 4000 rpm for 7 min. Then, the precipitation-dispersion process was repeated until the supernatant layer after centrifugation was colorless to make sure there are no more free dyes.

3.3.3.9 Modification of CPDB RAFT agent with phosphate group:

Two synthetic steps were used to synthesize the CPDB-phosphate. 4-Cyano-4-(thiobenzoylthio)pentanoic acid (CPDB) (5 g, 17.89 mmol), 1,6-hexanediol (12.7 g, 107.38 mmol), and N, N'-dicyclohexylcarbodiimide (DCC) (4 g,

19.68 mmol) were placed in a 500 ml round bottom flask and dissolved in 100 ml of THF. The mixture was cooled to 0°C and flushed with N₂ for 15 min. A solution of 4-dimethylaminopyridine (DMAP) (0.1 g, 0.89 mmol) in 15 ml THF was added dropwise over 30 min. The solution was stirred overnight and then allowed to warm to room temperature. Next, the solids formed during the reaction were filtered off and the solution was concentrated by removing the solvent using a rotary evaporator. The product residue was dissolved in 100 ml DCM and washed three times with DI water. The DCM layer was isolated and dried with MgSO₄ for 2 hours. MgSO₄ was filtered off and the solvent was removed under a rotary vacuum. Then the residue was subjected to silica column chromatography (5:4, hexanes: ethyl acetate) and the product was recovered as a yellow oil (5.65 g, 83 % yield). ¹H NMR (300 MHz, CDCl₃): δ (ppm) 7.46 (d, 1H), 7.40 (t, 2H), 7.31 (t, 2H) (aromatic protons), 4.7 (s, 1H), (CH₂)OH, 4.20 (t, 2H), 4.11 (t, 2H), (C=O)CH₂(CH₂), 3.60 (t, 2H) (CH₂)CH₂(OH), 2.60 (t, 2H), (CN)C(CH₃)CH₂(CH₂CO), 2.34 (t, 2H), (CN)C(CH₃)(CH₂)CH₂(CO) 1.65–1.40 (O=CCH₂)(CH₂)₄(CH₂OH). FT-IR: 1700 cm⁻¹ sharp (C=O), 3500 cm⁻¹ broad (O-H).

The previous product (CPDB-OH) (4.5 g, 11.85 mmol) and triethylamine (1.44 g, 14.23 mmol) were dissolved in 50 ml of dry THF in a 250 ml round bottom flask. The solution was flushed with dry N₂ for 30 min, cooled to 0°C, and then phosphoryl chloride (6.36 g, 41.5 mmol) was added dropwise over one hour. The

solution was allowed to warm to room temperature and stirred overnight under an N₂ atmosphere. Then, DI water (100 ml) was added to the solution and stirred for two hours. Using a separatory funnel, the solution was transferred to an organic layer by adding DCM (100 ml) which was isolated and washed with three portions of DI water. The organic layer was isolated and dried with MgSO₄. The MgSO₄ was filtered off and the DCM solvent was removed under reduced pressure. The product was recovered as a thick pink to a red oil (3.9 g, 72% yield). ¹H NMR (300 MHz, CDCl₃): δ (ppm) 7.46 (d, 1H), 7.40 (t, 2H), 7.31 (t, 2H) (aromatic protons), 4.2 (s, 2H), (P=O)(OH)₂, 4.14 (t, 2H), (C=O)CH₂(CH₂), 4.05 (t, 2H) (CH₂)CH₂(O-P=O), 2.61 (t, 2H), (CN)C(CH₃)CH₂(CH₂CO), 2.33 (t, 2H), (CN)C(CH₃)(CH₂)CH₂(CO) 1.72 (s, 3H) (CN)C(CH₃), (1.70–1.43 (O=CCH₂)(CH₂)₄(CH₂OH). ³¹P NMR (300 MHz, CDCl₃): δ (ppm) 1.71, IR: 1700 cm⁻¹ sharp (C=O), 1200 cm⁻¹ (P=O). HRMS (ESI) [M+H] Calcd for C₁₉H₂₆NO₆PS₂: 459.0923; found 459.1031.

3.3.3.10 Functionalization of nanoparticles SiO₂-g-HEMA-LA-dye and SiO₂-g-HEMA-SA-dye with the second RAFT Agent (modified CPDB):

The modified CPDB-phosphate agent was attached to the surface of monomodal silica nanoparticles, which was synthesized previously. CPDB-phosphate was functionalized directly on the nanoparticles in a process similar to the one described for the first chain functionalization. THF solution (50 mL) of

monomodal nanoparticles (1 g) was placed in a two-necked round bottom flask. Then (0.37 g, 0.82 mmol, 5 ml) of CPDB-phosphate was added, and the solution was refluxed at 70°C overnight under nitrogen protection. Next, the reaction was cooled down to r.t. and poured into hexanes (500 ml). The nanoparticles were then recovered by centrifugation (3500 rpm for 7 min.). This redisperse–precipitation procedure was repeated two times until the supernatant layer after centrifugation was colorless. The second chains of the CPDB-anchored silica nanoparticles were dried and analyzed using UV-vis analysis to determine the graft density.

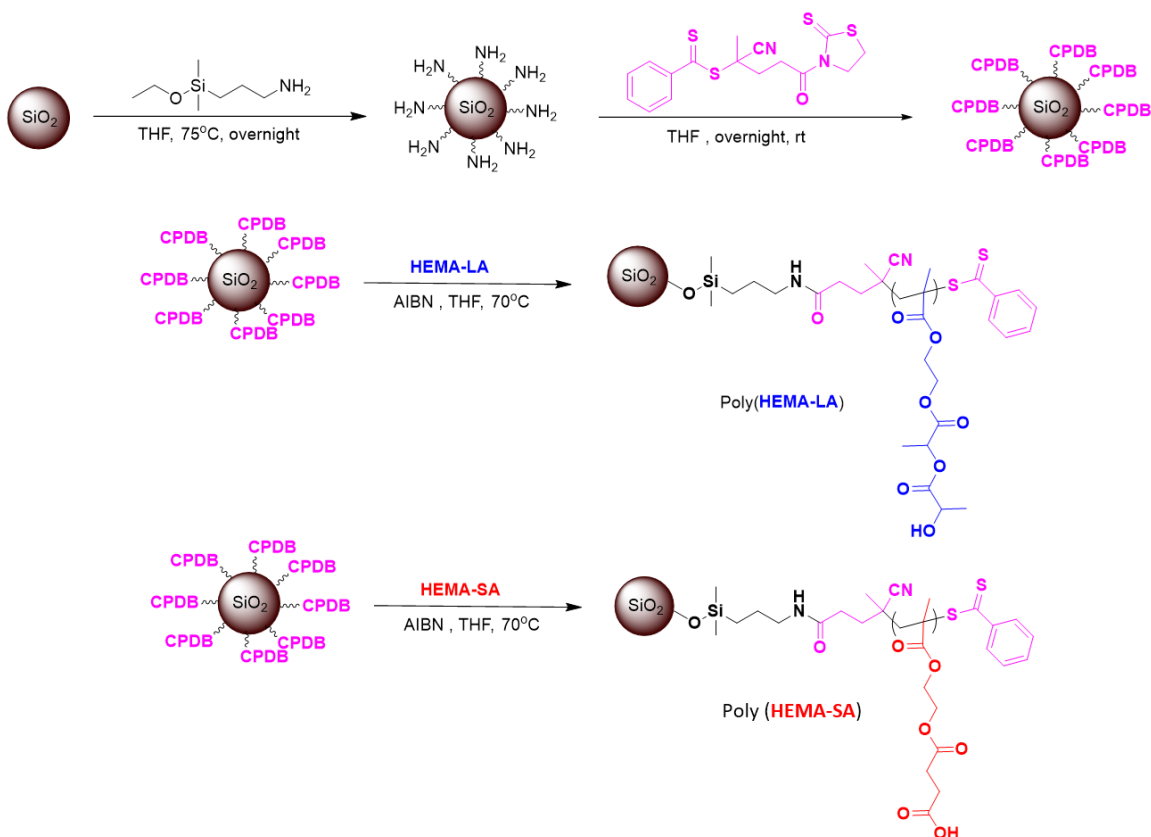
3.3.3.11 Graft Polymerization of Methacrylic acid (MAA) from SiO₂-g-(HEMA-LA-dye, CPDB) and SiO₂-g-(HEMA-SA-dye, CPDB) to synthesize the Second Brush:

The nanoparticles (SiO₂-g-(HEMA-LA-dye, CPDB) and SiO₂-g-(HEMA-SA-dye, CPDB)) (0.5 g by weight of silica) were dispersed in 20 mL THF and added to a Schlenk flask along with a predetermined amount of methacrylic acid (MAA) and AIBN (0.2 mL of 0.001 M THF solution). The Schlenk flask was degassed by three freeze-pump–thaw cycles, backfilled with nitrogen, and then placed in an oil bath at 65°C for the predetermined time, after which the polymerization was quenched in ice water. The nanoparticles were recovered by precipitating into hexanes and centrifugation at 4000 rpm for 7 minutes.

3.4 Results and Discussion:

Water-dispersible materials were designed using the bimodal brush approach implemented using the RAFT polymerization technique. The bimodal nanoparticles consisted of two polymer chain populations that were grafted on the surface of the nanoparticles. The first polymer population was a short brush, high graft density of the pH-responsive monomers (HEMA-LA, HEMA-SA). The second polymer population was a long brush, low graft density of a water-dissolvable polymer, which was methacrylic acid (MAA) in this study. The pH-responsive monomers (HEMA-LA, or HEMA-SA) were synthesized, as described previously. Briefly, both methacrylate monomers were synthesized by reacting hydroxyethyl methacrylate (HEMA) with the corresponding cyclic lactone compounds, L-lactide, or succinic anhydride, via ring-opening reaction in the presence of the catalysts, stannous 2-ethyl hexanoate,³¹ and DMAP,²⁵ respectively (Schemes 3.1, 3.2). Using the grafting-from approach and controlled radical RAFT polymerization technique, both monomers were grafted on the surface of silica nanoparticles (Scheme 3.3).

A kinetic study was conducted to test the compatibility of the grafted RAFT agent with the two monomers (HEMA-LA, HEMA-SA). Both monomers were easily polymerized with the grafted dithiobenzoate derivative RAFT agent, 4-cyanopentanoic acid dithiobenzoate (CPDB), at 65°C (Figure 3.3).



Scheme 3.3: Grafting-from Polymerization of HEMA-LA and HEMA-SA mediated by anchored CPDB on silica nanoparticles.

The plot between the consumption of monomer for HEMA-LA and the polymerization time showed a linear relationship while monomer consumption was linear for HEMA-SA at lower polymerization times (<10 hr). However, the molecular weight of both monomers gradually increased with increasing monomer conversion. Additionally, the polydispersity remained low (~1.3-1.4) for both monomers over the entire polymerization time. The first population of polymer chains of the bimodal nanoparticles was obtained using the RAFT polymerization of both HEMA-LA and HEMA-SA monomers via grafted CPDB

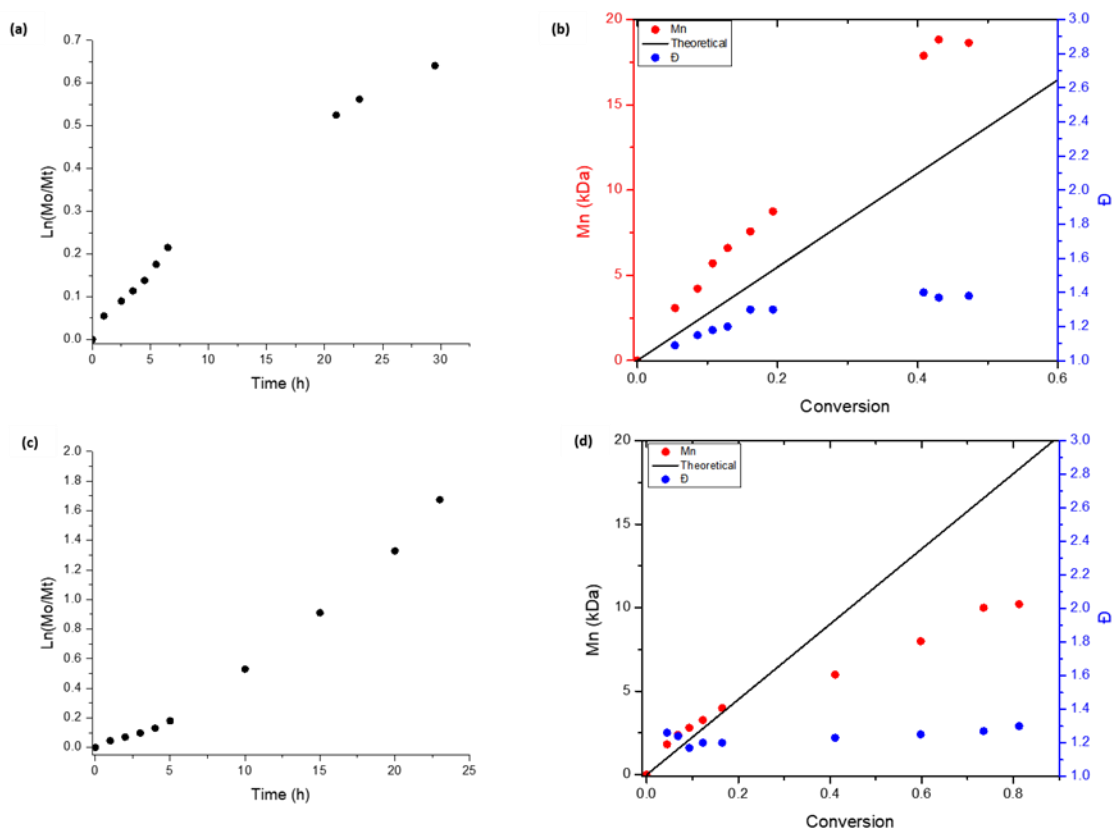


Figure 3.3 (a) Pseudo first-order kinetic plot of HEMA-LA. (b) Dependence of molecular weight of HEMA-LA (red circle), theoretical molecular weight (solid line), and the dispersity (blue circle) on the conversion for the surface-initiated RAFT polymerization of HEMA-LA on modified silica nanoparticles with CPDB density: 0.1 chains/nm² ([CPDB]/[HEMA-LA]/[AIBN]=500:1:0.1). (c) Pseudo first-order kinetic plot of HEMA-SA and (d) Dependence of molecular weight of HEMA-SA (red circle), theoretical molecular weight (solid line), and the dispersity (blue circle) on the conversion for the surface-initiated RAFT polymerization of HEMA-SA on modified silica nanoparticles with CPDB density: 0.1 chains/nm² ([CPDB]/[HEMA-SA]/[AIBN]=500:1:0.1).

silica nanoparticles (Scheme 3.3), using the feed ratio of [Monomer]/[CPDB]/[Initiator] of 1:500:0.1 at 65°C under inert gas conditions. First, a large amount of 3-aminopropyl dimethylethoxysilane was anchored to the surface of silica nanoparticles by refluxing the mixture at 75°C overnight under

nitrogen. Next, the surface anchored amine groups were reacted with an excess of mercaptothiazoline activated-CPDB (4-cyano-4-(phenylcarbonylthio)lthio) pentanoate) to obtain CPDB grafted silica nanoparticles.

Figure (3.4 a,b) shows the TGA traces of unmodified silica nanoparticles, CPDB-functionalized silica nanoparticles, and both polymer-grafted silica nanoparticles (PHEMA-LA, PHEMA-SA). The unfunctionalized nanoparticles exhibit a weight loss of approximately 4.7% over the temperature range of 50–800°C. Compared with the unmodified silica nanoparticles, the CPDB-anchor nanoparticles showed a slightly higher weight loss (5.2%) with temperature. This of course is due to the presence of organic material on the surface of nanoparticles. Finally, the polymer-grafted silica nanoparticles (PHEMA-LA, PHEMA-SA) exhibited a weight loss of approximately 70.3% and 75.7%, respectively over the same temperature range of 50–800°C. Thus, the TGA results provide further support that P(HEMA-LA) and P(HEMA-SA) had been successfully grafted on the surface of silica nanoparticles. From the measured graft density of the starting nanoparticles (0.237 ch/nm^2) and the measured weight gain measured by TGA, it is possible to calculate the molecular weight of the grafted chains. The molecular weights of PHEMA-LA and PHEMA-SA were calculated to be 31 kDa and 41 kDa, respectively, which are only slightly different from the measured molecular weights by GPC (32.5 kDa and 49 kDa) of the starting nanoparticles (0.237 ch/nm^2).

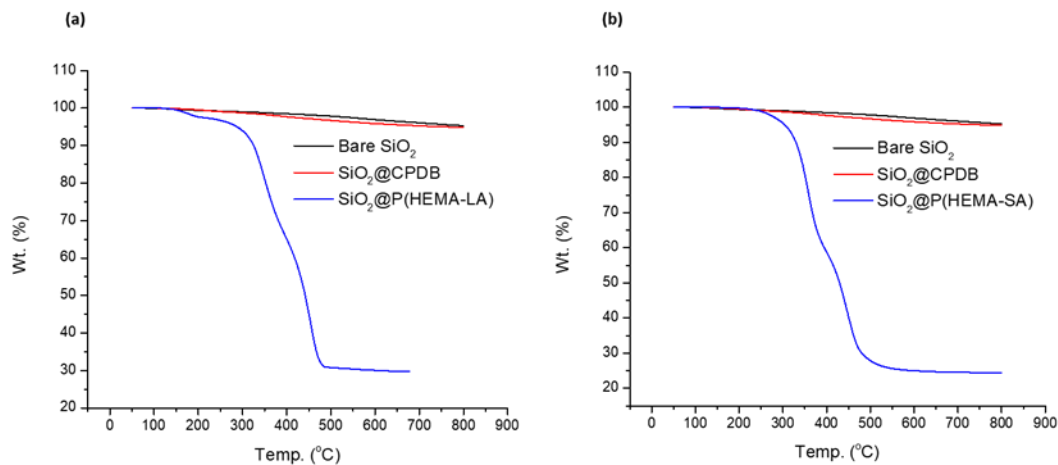


Figure 3.4: Thermogravimetric analysis of (a) SiO₂-g-P(HEMA-LA), and (b) SiO₂-g-P(HEMA-SA) nanoparticles.

Controlling the graft density of the RAFT agent on the surface of silica nanoparticles will depend on the ratio of silica nanoparticles to 3-aminopropyldimethylethoxysilane in the initial grafting process.^{32–35} After the exhaustive conversion of the amine groups to the RAFT agent, the graft density of the RAFT agent on the surface of the nanoparticles prior to polymerization was measured accurately using the UV absorption at 302.5 nm of the CPDB agent. Then, it was compared to a standard calibration curve of free CPDB to determine the concentration of the attached CPDB on the surface of silica nanoparticles before polymerization. Azobisisobutyronitrile (AIBN) was the initiator of all RAFT polymerizations used at a molar ratio (0.1) of initiator to RAFT (CPDB). Controlling the graft polymerization of the monomers HEMA-LA and HEMA-SA was dependent on both ratios [Initiator]/[CTA] and ([Monomer]:[CPDB]). Gelation

was observed when the molar ratio of initiator to the CPDB was >0.1 , as well as molar ratios of monomer to RAFT agent greater than 1000:1 when polymerization times were greater than 12 h. The polymer chains of HEMA-LA and HEMA-SA were cleaved from the surface of silica nanoparticles using 0.2 ml HF,³⁶ followed by GPC analysis to measure the molecular weight and polydispersity.

After functionalizing the first polymer chains on the surface of the nanoparticles using the RAFT polymerization, it was necessary to cleave the RAFT (chain transfer) agent,³⁷ which remained as an end group on the grafted chains prior to grafting the second population of polymer chains on the surface of the nanoparticles. The chain transfer agent was cleaved using the initiator (AIBN) via a radical cross-coupling mechanism. The efficient ratio for the cleavage reaction between AIBN: RAFT was 15:1 to 20:1. A color change was observed from pink to white polymer-coated nanoparticles when the reaction was complete and the particles were easily dispersed in THF. The cleavage reaction was confirmed by observing the disappearance of the CPDB peak using UV spectroscopy.

A major objective of this research was designing water-dispersible polymer grafted nanoparticles that could work as antibiotic-carriers, which is highly desirable in biomedical applications. Thus, labeling the end of repeat units of the polymers of HEMA-LA and HEMA-SA on the surface of the nanoparticles with fluorescent dyes is valuable in monitoring the hydrolysis of the pH-responsive

groups in biological cells or other systems.^{38,39} Two fluorescent dyes, NBD-COOH and NBD-NH₂, were synthesized and the UV-vis spectra showed absorption peaks at 460 nm compared with the absorption peak of commercially available dye, N-[2-{N-(7'-Nitrobenz- 2'-oxa-1',3'-diazol-4'-yl) amino} ethyl-carbonyloxy] succinimide (NBD-NHS) (Figure 3.5). These prepared NBD-dyes were synthesized and attached to the polymers on the surface of silica nanoparticles (HEMA-LA-g-SiO₂, HEMA-SA-g-SiO₂) using the DCC coupling reaction (Scheme 3.4). The dye-labeled pH-sensitive polymer grafted silica nanoparticles served as convenient surrogates to drug attached nanoparticles and were further investigated for the time-release properties.

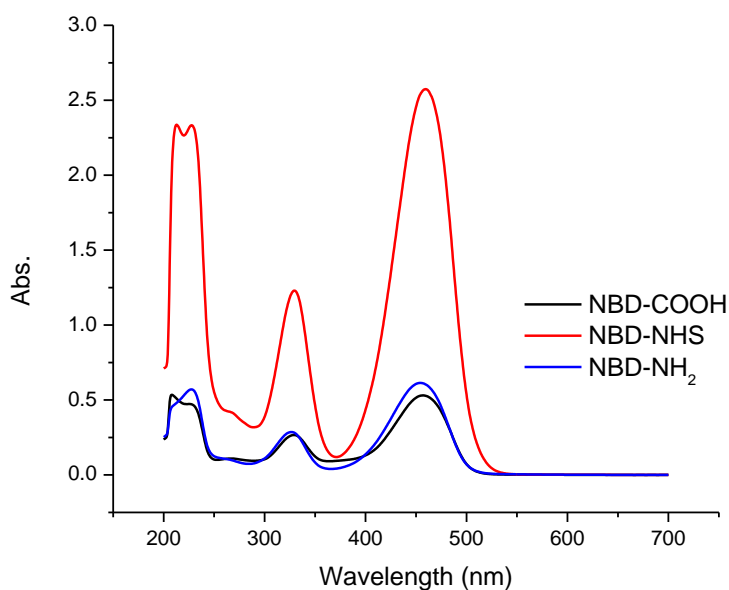
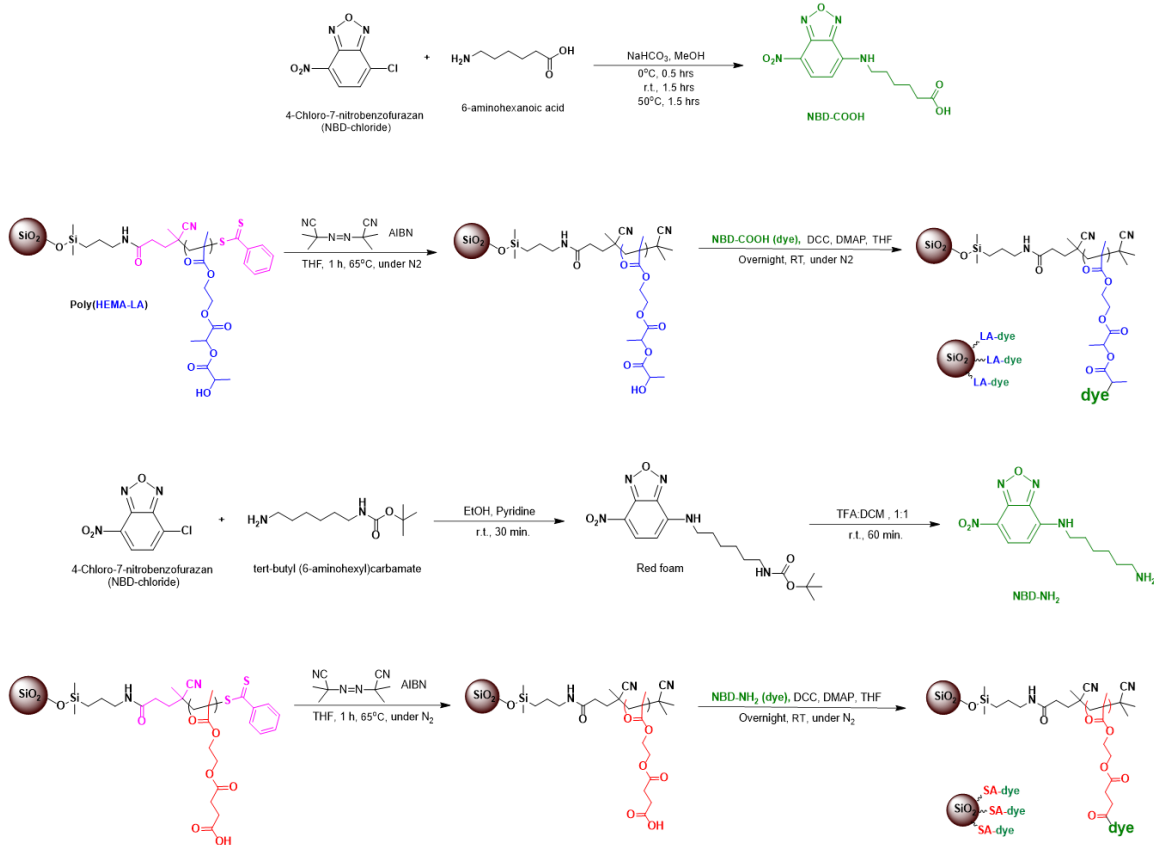


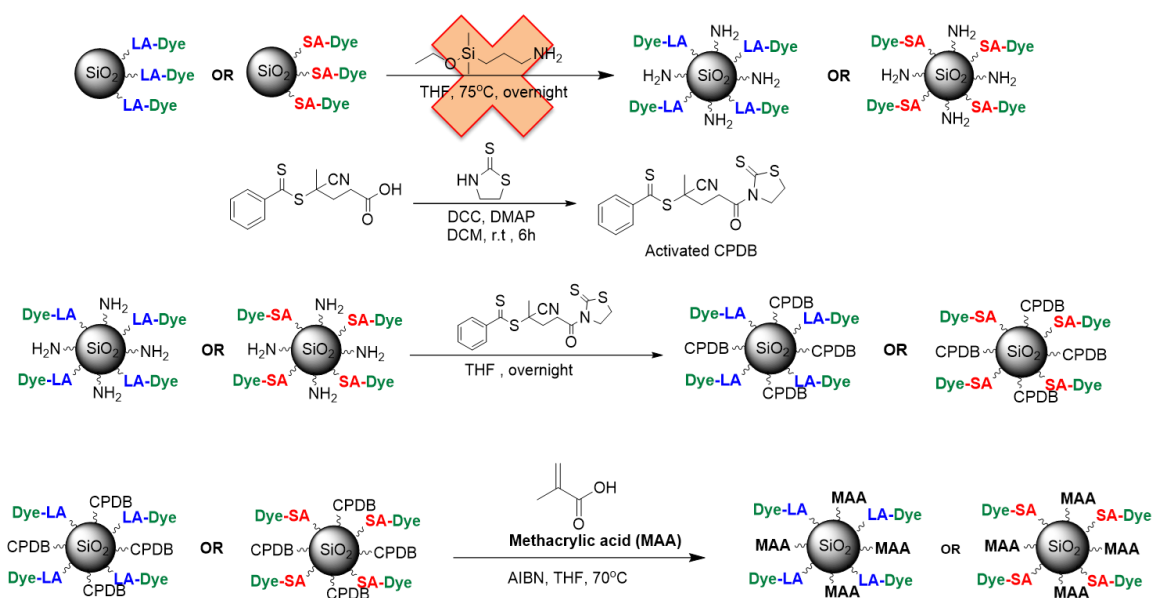
Figure 3.5: UV-vis spectra of prepared NBD-dyes NBD-COOH, NBD-NH₂ and commercially available dye, NBD-NHS.



Scheme 3.4: Synthesis and attachment of the fluorescence dyes on silica nanoparticles.

The next step after synthesizing the fluorescent-labeled monomodal silica nanoparticles was grafting the second population of polymer chains on the surface of nanoparticles to create the bimodal polymer brush architecture. Herein, the polymer of the methacrylic acid (MAA) was used in bimodal nanoparticles as a second polymer population to supply water solubility. The RAFT agent that is compatible with MAA is 4-cyano-4-(thiobenzoylthio) pentanoic acid (CPDB),⁴⁰ the same that was used in the grafting of the first population of chains. Pelet and Putnam have studied the kinetics for the polymerization of MAA with the CPDB

and found a linear relationship between the Mn and conversion and Mn increased linearly with the conversion.¹⁹ Therefore, the attachment of the second population of polymer chains on the surface of the monomodal of nanoparticles (SiO₂-g-HEMA-LA-dye, SiO₂-g-HEMA-SA-dye) was expected to proceed in a similar manner,⁹ as outlined in Scheme 3.5.

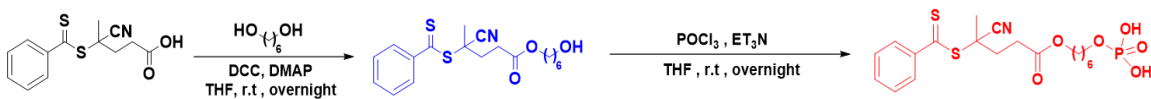


Scheme 3.5: The proposed approach to grafting the second population of polymer chains on the surface of the nanoparticles.

In this case, the first step of this proposed approach did not succeed. The fluorescent dyes that were attached to the first population prevented grafting the 3-aminopropyltrimethoxysilane on the surface of nanoparticles, where we postulate that the amine group on the 3-aminopropyltrimethoxysilane will react with nitrobenzoxadiazole on the NBD-dyes. This was confirmed via grafting

the 3-aminopropyldimethylethoxysilane as a second chain on the surface of non-fluorescent nanoparticles (SiO₂-g-HEMA-LA, SiO₂-g-HEMA-SA). Therefore, this proposed approach could not be followed.

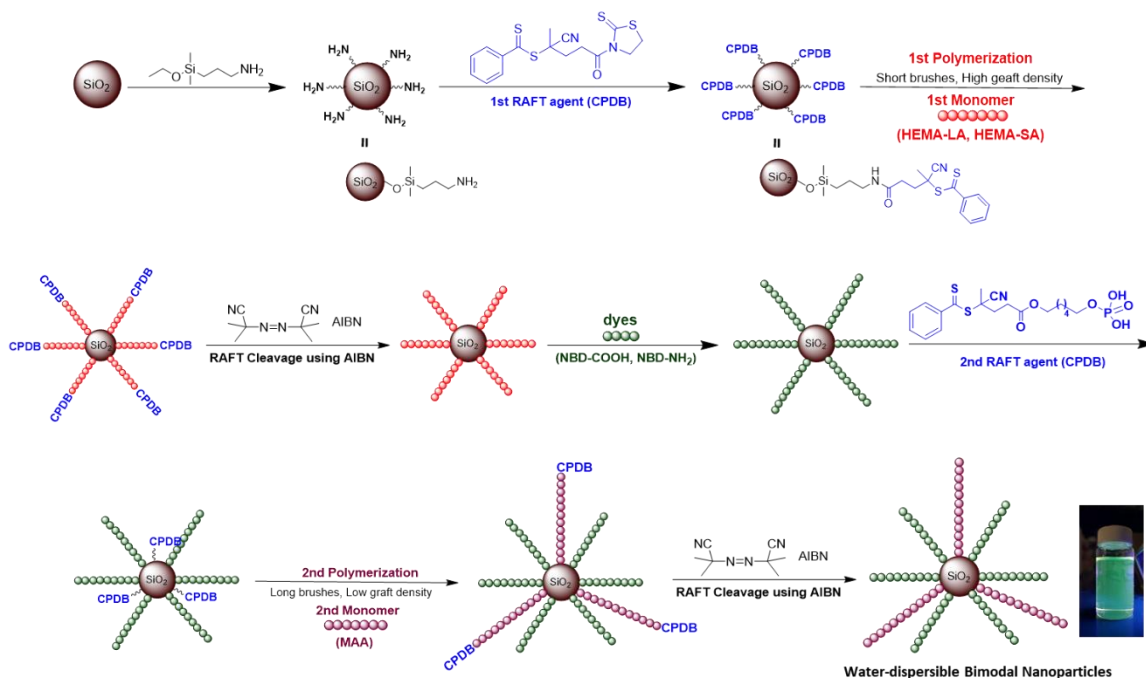
An alternative strategy for functionalizing the second population of polymeric chains on the surface of nanoparticles is grafting the RAFT agent directly on the surface of monomodal nanoparticles without using 3-aminopropyldimethylethoxysilane. This was accomplished via modification of the RAFT agent (Scheme 3.6), using a phosphate containing RAFT agent where the M-O-P bridges are more stable than M-O-Si bonds.⁴¹ CPDB was modified by reacting with 1,6-hexanediol to produce CPDB with a hydroxyl end group that was subsequently reacted with phosphorus oxychloride to obtain the modified RAFT agent. As with silane coupling agents control of the graft density of polymer chains on the surface of silica nanoparticles was achieved using various ratios of the modified CPDB to the SiO₂ nanoparticles. Increasing the feed ratio of modified CPDB will lead to increased graft density on the surface of silica nanoparticles.



Scheme 3.6: Modification of RAFT agent (CPDB) with a phosphate group.

The direct functionalization of CPDB on the surface of the polymer grafted-silica nanoparticles of (HEMA-LA, HEMA-SA) was more straightforward.

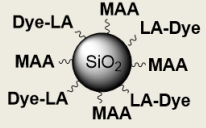
Furthermore, the modified RAFT agent was strongly attached to hydroxylated silica nanoparticles to produce CPDB anchored on the surface of silica nanoparticles^{42,43}, as shown in Scheme 3.7. Despite the grafting of the first polymer chain population, the modified CPDB easily diffused to the surface of the nanoparticles. These CPDB functionalized nanoparticles were washed several times by precipitation in hexane and redispersed in THF to remove unreacted modified CPDB. The grafting density of the second RAFT chains was determined as in the first polymer chains using UV-Vis spectrometry.⁴⁴ The polymerization of methacrylic acid (MAA) onto the nanoparticles was conducted using surface-initiated RAFT polymerization to form water-dispersible bimodal brush silica



Scheme 3.7: Synthetic strategy for synthesizing the bimodal grafted nanoparticles.

nanoparticles. Azobisisobutyronitrile (AIBN) was used as an initiator to start the polymerization using a ratio 1:250:0.1 [M]/ [CPDB]/ [AIBN]. Using GPC, the molecular weight and polydispersity of the second population of polymethacrylic acid (PMAA) were measured, as shown in Table 3.1.

Table 3.1: Grafting densities and molecular weights of bimodal nanoparticles, SiO₂@P(HEMA-LA-dye)-PMAA, and SiO₂@P(HEMA-SA-dye)-PMAA.

		GD (ch/nm ²)	M.w. (kDa)	Đ
	Long brush P(MAA)	0.201	90	1.35
	Short brush P(HEMA-LA- dye)	0.237	32.5	1.18
	Long brush P(MAA)	0.161	103	1.29
	Short brush P(HEMA-SA- dye)	0.237	49	1.21

Bimodal polymer grafted nanoparticles were synthesized using either HEMA-LA or HEMA-SA monomers combined with MAA, where the polymer composition of the short, dense brush was different, but the second brush population was the same polymer. For bimodal nanoparticles using HEMA-LA monomer, a short, dense brush was polymerized at 0.237 ch/nm² under controlled radical polymerization conditions with a molecular weight of 32.5 kDa and PDI of

1.18. A second long, dense brush population of MAA was polymerized at a density of 0.2 ch/nm² with a molecular weight of 90 kDa and polydispersity of 1.35. Also, a short, dense brush of HEMA-SA monomer was polymerized at 0.237 ch./nm² with a molecular weight of 49 kDa and PDI of 1.21. A second long, dense brush was polymerized using controlled radical polymerization at 0.161 ch/nm² with a molecular weight of 103 kDa and PDI of 1.29.

Bimodal polymer brushes were synthesized while preserving independent control over grafting density, molecular weight, and polydispersity using sequential RAFT polymerizations. GPC of the cleaved polymer chains showed two separate peaks representing each population of grafted polymer chains and confirmed the bimodal polymer brush composition (Figure 3.6).⁴⁵

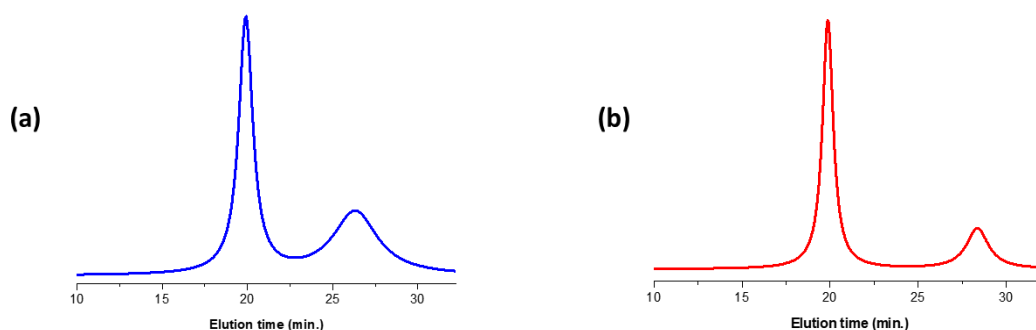


Figure 3.6: GPC analysis of bimodal grafted nanoparticles (a) SiO₂-g-P(HEMA-LA-dye)-PMAA, and (b) SiO₂-g-P(HEMA-SA-dye)-PMAA.

The composition of the water-dispersible bimodal nanoparticles was also investigated by thermogravimetric analysis (TGA). Figure 3.7 a, b shows the TGA traces of the unfunctionalized silica nanoparticles, monomodal silica nanoparticles SiO₂@PHEMA-LA-dye, SiO₂@PHEMA-SA-dye, and bimodal silica nanoparticles SiO₂@P(HEMA-LA-dye)-P(MAA), SiO₂@P(HEMA-SA-dye)-P(MAA). The ungrafted nanoparticles exhibit a weight loss of approximately 4.7% over the temperature range of 50–800°C. This weight loss is likely due to tightly bound water and surfactants on the surface of nanoparticles. The polymer-grafted silica monomodal nanoparticles (SiO₂@PHEMA-LA-dye, SiO₂@PHEMA-SA-dye) exhibited a weight loss of approximately 70.3% and 75.7%, respectively over the same range of temperature range 50–800°C. Finally, the bimodal silica nanoparticles, SiO₂@P(HEMA-LA-dye)-P(MAA), SiO₂@P(HEMA-SA-dye)-P(MAA), showed a higher weight loss of approximately 87.13% and 87.21%, respectively over the same range of temperature 50–800°C. Therefore, the TGA results provide further support that bimodal nanoparticles have been successfully grafted on the surface of silica nanoparticles. Using TGA analysis, molecular weights of the grafted chains were calculated and compared with the molecular weights measured by GPC. The molecular weights of PHEMA-LA-dye and PHEMA-SA-dye were calculated to be 31 kDa and 41 kDa, respectively, which are compared with the measured molecular weights by GPC (32.5 kDa and 49 kDa) of

the starting nanoparticles (0.237 ch/nm^2). The second population of polymeric chains (PMAA) grafted on the surface of silica nanoparticles $\text{SiO}_2@P(\text{HEMA-LA-dye})\text{-P}(\text{MAA})$, $\text{SiO}_2@P(\text{HEMA-SA-dye})\text{-P}(\text{MAA})$, exhibited a weight loss of approximately 17.1% and 11.5%, respectively different from the first grafted polymer of population chains $P(\text{HEMA-LA-dye})$, $P(\text{HEMA-SA-dye})$ over the same range of temperature range $50\text{--}800^\circ\text{C}$. Using TGA analysis, the molecular weights of the second grafted polymer of population chains were calculated to be approximately 105 kDa and 132 kDa, respectively which are slightly different compared with the measured molecular weights (90 kDa and 103 kDa) of nanoparticles using the GPC analysis in which the measured graft densities were (0.201 ch/nm^2 and 0.161 ch/nm^2) using the UV-vis absorption of the CPDB RAFT agents.

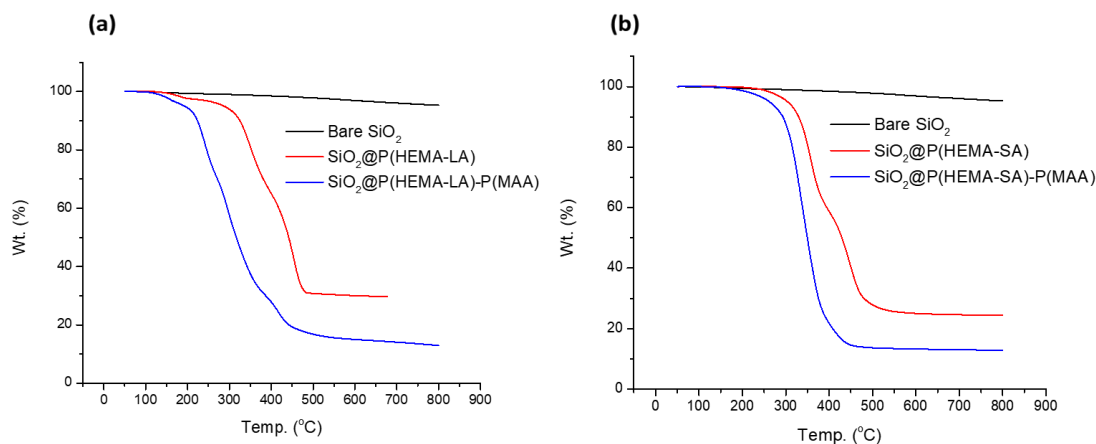


Figure 3.7: TGA analysis of (a) Bare SiO_2 , Monomodal NP's $\text{SiO}_2\text{-g-P}(\text{HEMA-LA})$, and Bimodal NP's $\text{SiO}_2\text{-g-P}(\text{HEMA-LA})\text{-P}(\text{MAA})$, (b) Bare SiO_2 , Monomodal NP's $\text{SiO}_2\text{-g-P}(\text{HEMA-SA})$, and Bimodal NP's $\text{SiO}_2\text{-g-P}(\text{HEMA-SA})\text{-P}(\text{MAA})$.

The direct grafting approach described herein avoided the side reactions that occurred in the initial synthetic strategy when attempting to attach a second population via amino silane attachment of the RAFT agent.⁹ The successful grafting of MAA on dye-labeled polymer coated-silica nanoparticles, which are particularly prone to agglomeration,^{46,47} resulted in well-dispersed nanoparticles in both THF and water and were stable for a long time. Thus, this approach of preparing bimodal nanoparticles presents a good platform for synthesizing bimodal water-dispersible polymer grafted silica nanoparticles that should allow for broad use in biomedical applications.

3.5 Conclusion:

We demonstrated a new technique using RAFT polymerization to synthesize water-dispersible bimodal polymer grafted nanoparticles. Bimodal silica nanoparticles were prepared by grafting two different populations of polymer chains on the surface of silica nanoparticles. Short, dense polymer brushes of pH-responsive monomers HEMA-LA, HEMA-SA were grafted on silica nanoparticles using surface-initiated RAFT polymerization for the first population. These polymer brushes could be used as antibiotic-delivery carriers. Prior to grafting the second polymer population, the activity of the RAFT agent at the polymer ends of the first population was removed via a radical cleavage reaction. The second RAFT agent was attached directly to the surface of silica

nanoparticles using a modified chain transfer agent that contained a phosphate group. This was necessary to avoid a side reaction between the amino silane coupling agent and the dye containing grafted polymer chains of the first population. Then, the water-dissolvable monomer MAA was polymerized to a high molecular weight at a graft density different than the first chain population. This approach also allowed for independent control of the molecular weight and the chemical composition of each chain population. The bimodal brush architecture was confirmed by GPC analysis of the cleaved polymer chains, which showed two separate peaks. The first large peak was assigned to the high molecular weight of the low graft density PMAA, and the second smaller peak was assigned to the lower molecular weight (HEMA-LA, HEMA-SA) at high graft density. This GPC analysis confirmed the composition of bimodal polymer grafted nanoparticles. The water-dispersible bimodal polymer grafted silica nanoparticles provide a platform to synthesize bio-nanoparticles as antibiotic vehicle carriers that could be used in bioapplications.

3.6 References:

- (1) Mout R.; Moyano D.; Rana S.; Rotello V. *Chem. Soc. Rev.* 2012, 41 (7), 2539–2544.
- (2) Danhier, F.; Ansorena, E.; Silva, J. M.; Coco, R.; Le Breton, A.; Préat, V. J. *Control. Release* 2012, 161 (2), 505–522.

- (3) Zhao, B.; Zhu, L. *Macromolecules* 2009, 42 (24), 9369–9383.
- (4) Fischer, S.; Salcher, A.; Kornowski, A.; Weller, H.; Förster, S. *Angew. Chemie - Int. Ed.* 2011, 50 (34), 7811–7814.
- (5) Mackay, M. E.; Tuteja, A.; Duxbury, P. M.; Hawker, C. J.; Van Horn, B.; Guan, Z.; Chen, G.; Krishnan, R. S. *Science* (80-.). 2006, 311 (5768), 1740–1743.
- (6) Wang, L.; Cole, M.; Li, J.; Zheng, Y.; Chen, Y. P.; Miller, K. P.; Decho, A. W.; Benicewicz, B. C. *Polym. Chem.* 2015, 6 (2), 248–255.
- (7) Wang, L.; Benicewicz, B. C. *ACS Macro Lett.* 2013, 2 (2), 173–176.
- (8) Vaia, R. A.; Maguire, J. F. *Chem. Mater.* 2007, 19, 2736–2751.
- (9) Rungta, A.; Natarajan, B.; Neely, T.; Dukes, D.; Schadler, L. S.; Benicewicz, B. C. *Macromolecules* 2012, 45 (23), 9303–9311.
- (10) Zhao, B.; He, T. *Macromolecules* 2003, 36 (23), 8599–8602.
- (11) Chen, H.; Hsieh, Y. Lo. *Biotechnol. Bioeng.* 2005, 90 (4), 405–413.
- (12) Matyjaszewski, K.; Xia, J. *Chem. Rev.* 2001, 101 (9), 2921–2990.
- (13) Feng, W.; Lv, W.; Qi, J.; Zhang, G.; Zhang, F.; Fan, X. *Macromol. Rapid Commun.* 2012, 33, 133–139.
- (14) Yilmaz, G.; Demir, B.; Timur, S.; Becer, C. R. *Biomacromolecules* 2016, 17 (9), 2901–2911.

- (15) Wang, L.; Chen, Y. P.; Miller, K. P.; Cash, B. M.; Jones, S.; Glenn, S.; Benicewicz, B. C.; Decho, A. W. *Chem. Commun.* 2014, 50 (81), 12030–12033.
- (16) Chen, H.; Xia, L.; Fu, W.; Yang, Z.; Li, Z. *Chem. Commun.* 2013, 49 (13), 1300–1302.
- (17) Yuan, J.; Lu, Y.; Schacher, F.; Lunkenbein, T.; Weiss, S.; Schmalz, H.; Müller, A. H. E. *Chem. Mater.* 2009, 21 (18), 4146–4154.
- (18) Qu, H.; Caruntu, D.; Liu, H.; O'Connor, C. J. *Langmuir* 2011, 27 (6), 2271–2278.
- (19) Pelet, J. M.; Putnam, D. *Macromolecules* 2009, 42 (5), 1494–1499.
- (20) De, M.; Ghosh, P. S.; Rotello, V. M. *Adv. Mater.* 2008, 20 (22), 4225–4241.
- (21) Cash, B. M.; Wang, L.; Benicewicz, B. C. *J. Polym. Sci. Part A Polym. Chem.* 2012, 50 (13), 2533–2540.
- (22) Pothayee, N.; Pothayee, N.; Jain, N.; Hu, N.; Balasubramaniam, S.; Johnson, L. M.; Davis, R. M.; Sriranganathan, N.; Riffle, J. S. *Chem. Mater.* 2012, 24 (11), 2056–2063.
- (23) Smeets, N. M. B.; Patenaude, M.; Kinio, D.; Yavitt, F. M.; Bakaic, E.; Yang, F.-C.; Rheinstädter, M.; Hoare, T. *Polym. Chem.* 2014, 5 (23), 6811–6823.
- (24) Ishimoto, K.; Arimoto, M.; Ohara, H.; Kobayashi, S.; Ishii, M.; Morita, K.; Yamashita, H.; Yabuuchi, N. *Biomacromolecules* 2009, 10 (10), 2719–2723.

- (25) Hong, L.; Zhang, Z.; Zhang, Y.; Zhang, W. J. *Polym. Sci. Part A Polym. Chem.* 2014, 52 (18), 2669–2683.
- (26) Tous, E.; Ifkovits, J. L.; Koomalsingh, K. J.; Shuto, T.; Soeda, T.; Kondo, N.; Iii, J. H. G.; Gorman, R. C.; Burdick, J. a. *Biomacromolecules* 2011, 12 (11), 4127–4135.
- (27) Li, C.; Han, J.; Ryu, C. Y.; Benicewicz, B. C. *Macromolecules* 2006, 39 (9), 3175–3183.
- (28) Li, J.; Wang, L.; Benicewicz, B. C. *Langmuir* 2013, 29 (37), 11547–11553.
- (29) Woodland, J. G.; Hunter, R.; Smith, P. J.; Egan, T. J. *Org. Biomol. Chem.* 2017, 15 (3), 589–597.
- (30) Borchmann, D. E.; Tarallo, R.; Avendano, S.; Falanga, A.; Carberry, T. P.; Galdiero, S.; Weck, M. *Macromolecules* 2015, 48 (4), 942–949.
- (31) Smeets, N. M. B.; Patenaude, M.; Kinio, D.; Yavitt, F. M.; Bakaic, E.; Yang, F. C.; Rheinstädter, M.; Hoare, T. *Polym. Chem.* 2014, 5 (23), 6811–6823.
- (32) Li, C.; Han, J.; Ryu, C. Y.; Benicewicz, B. C. *Macromolecules* 2006, 39 (9), 3175–3183.
- (33) Li, Y.; Benicewicz, B. C. *Macromolecules* 2008, 41 (21), 7986–7992.
- (34) Dukes, D.; Li, Y.; Lewis, S.; Benicewicz, B.; Schadler, L.; Kumar, S. K. *Macromolecules* 2010, 43 (3), 1564–1570.

- (35) Maillard, D.; Kumar, S. K.; Fragneaud, B.; Kysar, J. W.; Rungta, A.; Benicewicz, B. C.; Deng, H.; Brinson, L. C.; Douglas, J. F. *Nano Lett.* 2012, 12 (8), 3909–3914.
- (36) Ojang, L.; Zhang, L.; Zhang, Z.; Zhou, N.; Cheng, Z.; Xiulin, Z. *J. Polym. Sci. Part A Polym. Chem.* 2010, 48 (9), 2006–2015.
- (37) Chong, Y. K.; Moad, G.; Rizzardo, E.; Thang, S. H. *Macromolecules* 2007, 40 (13), 4446–4455.
- (38) Sahoo, Y.; Goodarzi, A.; Swihart, M. T.; Ohulchansky, T. Y.; Kaur, N.; Furlani, E. P.; Prasad, P. N. *J. Phys. Chem. B* 2005, 109 (9), 3879–3885.
- (39) Peng, H. S.; Chiu, D. T. *Chem. Soc. Rev.* 2015, 44 (14), 4699–4722.
- (40) Canning, S. L.; Neal, T. J.; Armes, S. P. *Macromolecules* 2017, 50 (16), 6108–6116.
- (41) Evans, G.; Duong, G. V.; Ingleson, M. J.; Xu, Z.; Jones, J. T. A.; Khimyak, Y. Z.; Claridge, J. B.; Rosseinsky, M. J. *Adv. Funct. Mater.* 2010, 20 (2), 231–238.
- (42) Li, Y.; Tao, P.; Viswanath, A.; Benicewicz, B. C.; Schadler, L. S. *Langmuir* 2013, 29, 1211–1220.
- (43) Li, J.; Khanchaitit, P.; Han, K.; Wang, Q. *Chem. Mater.* 2010, 22 (18), 5350–5357.

- (44) Zheng, Y.; Abbas, Z. M.; Sarkar, A.; Marsh, Z.; Stefik, M.; Benicewicz, B. C. *Polymer (Guildf)*. 2018, 135, 193–199.
- (45) Burdyńska, J.; Daniel, W.; Li, Y.; Robertson, B.; Sheiko, S. S.; Matyjaszewski, K. *Macromolecules* 2015, 48 (14), 4813–4822.
- (46) Tadano, T.; Zhu, R.; Muroga, Y.; Hoshi, T.; Sasaki, D.; Yano, S.; Sawaguchi, T. *Polym. J.* 2014, 46 (6), 342–348.
- (47) Wang, L.; Benicewicz, B. C. *ACS Macro Lett.* 2013, 2 (2), 3–6.

CHAPTER 4

DESIGNING “SWEET-NANOPARTICLES” AS A NOVEL
STRATEGY TO COMBAT ANTIBIOTIC-RESISTANT BACTERIA¹

¹Al-Ali, M.A. and Benicewicz B. C. To be submitted to Journal of Polymer Science.

4.1 Abstract:

The bacterial resistance of antibiotics has become one of the most important medical issues that pose a public health threat and, thus, needs urgent intervention around the world because of the widespread infectious diseases. In this work, we investigate a novel design of grafted nanoparticles that may be used to combat antibiotic-resistant bacteria. Herein, we explore the concept of “sweet-nanoparticles” via grafting bimodal polymer brushes on nanoparticles using reversible addition-fragmentation chain transfer (RAFT) polymerization. A sugar-containing monomer, 2-methacrylamido glucopyranose (MAG) was grafted as a low graft density, long brush on silica nanoparticles using 4-cyano-4-[(dodecylsulfanylthiocarbonyl)sulfanyl]pentanoic acid (CDSS) as a chain transfer agent. Two potential “controlled release” monomers 2-((2-((2-hydroxypropanoyl)oxy)propanoyl)oxy)ethyl methacrylate (HEMA-LA) and 2-(methacryloyloxy)ethyl succinate (HEMA-SA) containing potentially hydrolytically sensitive ester linkages were grafted individually as a high graft density, short brush using a different RAFT agent (4-cyano-4-(phenylcarbonothioylthio)pentanoic acid, CPDB). Conceptually, the addition of sugar-containing monomers in the long brushes should enhance bacterial uptake while delivering concentrated amounts of drugs via the short, controlled release monomers. The polymerization kinetics of the bimodal populations will be

described, and the structural characterization will be reported by $^1\text{H-NMR}$ spectroscopy and gel permeation chromatography (GPC). Then, the antimicrobial activities of these polymers will be investigating against clinically relevant Gram-positive and Gram-negative bacteria. Bimodal polymer grafted nanoparticles are envisioned for use as more efficient delivery vehicles for anti-bacterial applications.

4.2 Introduction:

Scientists describe the situation between antibiotics and bacteria as a global and ongoing medical condition.¹ Whenever new antibiotics emerge that kill some types of bacteria, the bacteria evolve to acquire new immunity that enables them to resist these antibiotics.² Bacterial resistance of β -lactam antibiotics has been widely spread around the world via antibiotic overuse and misuse.³ However, globally, it has become necessary to discover novel techniques to prevent antibiotic resistance in bacteria,⁴ since the global consumption of antibiotics is increasing incessantly.^{5,6} Therefore, the search for and development of new strategies and methods to try to eliminate bacteria that are resistant to traditional antibiotics has become imperative and urgent to avoid a global medical disaster. The use of nanoparticles has become one of the most promising strategies to combat bacterial resistance.⁷ Thus, designing polymer grafted nanoparticles for use as more efficient delivery vehicles for anti-bacterial applications is considered as the main

goal of this work. In particular, we propose to explore the use of bimodal polymer grafted brushes that contain two different polymer chain populations.⁸ One population would consist of a high graft density of short brushes that contain pH-responsive “controlled release” monomers to work as antibiotic-delivery carriers,⁹ and a second population of low graft density of long brushes that consist of sugar-containing monomer that work to enhance bacterial uptake for these "sweet" nanoparticles.

During the last 20 years, interest in carbohydrates (sugars) grafted on nanoparticles, which are referred to as glyconanoparticles,^{10,11} has increased dramatically due to their importance and expanded uses in the biomedical field.¹² Moreover, glyconanoparticles possess many properties, such as hydrophilicity, stability, and biodegradability, which make them attractive for a wide range of biomedical applications.¹³ Much research has been done using glyconanoparticles in biomedical applications. Cerisy et al. explained the mechanisms by which bacteria uptake and translocate sugars across the cell membrane.¹⁴ Disney et al. used carbohydrates to detect pathogens through the use of carbohydrate functionalized polymers as a detection method for bacteria.¹⁵ Disney et al. also developed an efficient bacterium capturing system by designing specific glyconanoparticle materials. Their results showed that the reusable antimicrobial magnetic glyconanoparticles have high efficiency and excellent performance

(more than 98%) for effective bacterial removal from water solutions by increasing bacterial capturing efficiencies.¹⁶

As part of the current approach, we considered the preparation of grafted glycopolymers on the surface of nanoparticles using one of the controlled polymerization techniques such as controlled radical,¹⁷⁻²⁰ and ring-opening metathesis polymerization.²¹ Glycomonomers have been synthesized by incorporating many olefinic groups, such as (meth)acrylates,^{18,22-24} (meth)acrylamides,^{17,25,26} and styrene derivatives²⁷ with monosaccharides such as glucose,^{17,18,20-23,28} galactose,^{24,29} and mannose,^{19,30} as well as disaccharides such as lactose.^{27,31,32} Reversible addition-fragmentation chain transfer (RAFT) polymerization is a desirable technique used to control the polymerization of many monomers that have relatively fast polymerization rates, such as (meth)acrylates and (meth)acrylamides and can be performed in many solvents without the use of metal catalysts.^{17,19,20,23,25,26,30}

This research is the first report that incorporates glycopolymers grafted on nanoparticles that serve as antibiotic-delivery carriers in a bimodal grafted silica nanoparticle architecture. Sugar-containing polymers grafted on the surface of silica nanoparticles were used to increase the bacterial uptake as compared with that of non-glyconanoparticles. Specifically, we investigated the polymerization of the trimethylsilyl (TMS)-protected monomer, α -2-deoxy-2-methacrylamido-

1,3,4,6-tetra(O-trimethylsilyl)D-glucopyranose (TMS-MAG) as a glycomonomer grafted on the surface of silica nanoparticles. This was combined with a second population of polymeric chains nanoparticles with stimuli-sensitive moieties that work as antibiotic delivery carriers to create a bimodal architecture exhibiting both controlled release and enhanced bacterial uptake properties.

4.3 Materials and Methods:

4.3.1 Materials:

Unless otherwise noted, all chemicals were purchased from Fischer and used as received. Colloidal silica nanoparticles (SiO₂, 30 wt% in MEK) were purchased from Nissan Chemical. 2,2'-Azobis(2-methylpropionitrile) (AIBN, 98%) was obtained from Aldrich. 2-Hydroxyethyl methacrylate (HEMA, Sigma Aldrich, 99%) was purified by passing through a column of basic aluminum oxide (Alfa Aesar, 99%) to remove the inhibitor, methyl ether hydroquinone (MEHQ). L-lactide (Sigma Aldrich, 95%), succinic anhydride (Acros Organics, 99%), D-glucosamine hydrochloride (Acros, 98+%), N,O-bis(trimethylsilyl)acetamide (BSA, Acros, 95%), methacryloyl chloride (Acros, 95%), and triethylamine (TEA, Acros, 99.7%) were used as received. Two different radical addition-fragmentation transfer (RAFT) chain transfer agents (CTA), 4-cyano-4-(phenylcarbonothioylthio)pentanoic acid (CPDB) and 4-cyano-4-[(dodecylsulfanylthiocarbonyl)sulfanyl]pentanoic acid (CDSS) were purchased

from Boron Molecular and used as received. 3-Aminopropyldimethylethoxysilane (95%) and dimethylmethoxy-n-octylsilane (95%) were purchased from Gelest, Inc, and used as received. Hydrochloric acid (Sigma-Aldrich, 37%) was diluted with DI water to a solution of 1.3 M before use.

4.3.2 Instrumentation:

^1H NMR spectra were recorded using a Bruker Avance III-HD 300 MHz spectrometer instrument using CDCl_3 as a solvent and measured with tetramethylsilane (TMS) as an internal reference. Gel permeation chromatography (GPC) was used to measure the molecular weights (M_n) and polydispersity index (Đ). The GPC was comprised of a Varian 290-LC pump, a Varian 390-LC refractive index detector, and three Styragel columns (HR1, HR3 and HR4, molecular weight range of 100-5000, 500-30000, and 5000-500000, respectively). Tetrahydrofuran (THF) was used as eluent at 30°C and a flow rate of 1.0 mL/min and calibrated with polystyrene or poly(methylmethacrylate) standards obtained from Polymer Laboratories. A Thermogravimetric Analyzer (TA) Instruments Q5000 was used to obtain TGA characterization. Samples were preheated to 100°C and kept at this temperature for 10 min to remove residual water and solvents for all the samples. After cooling to 50°C, the samples were reheated to 800°C at a heating rate of 10°C/min under nitrogen flow. FT-IR spectra were recorded using a BioRad

Excalibur FTS 3000. UV-vis absorption spectra were taken on a Shimadzu UV-2450 spectrophotometer.

4.3.3 Synthesis of “controlled release” monomers:

(HEMA-LA, HEMA-SA) monomers were synthesized using the ring-opening reaction of the symmetrical cyclic lactone compound, L-lactide, or succinic anhydride with hydroxyethyl methacrylate (HEMA) catalyzed by stannous 2-ethylhexanoate and DMAP, respectively.

4.3.3.1 Synthesis of 2-((2-(propionyloxy) propanoyl)oxy)ethyl methacrylate (HEMA-LA):

Hydroxyethyl methacrylate (HEMA, 5 g, 38.42 mmol) and tin(II) 2-ethylhexanoate (0.1 g, 0.27 mmol) were placed in a 100 mL one-neck round bottom flask. L-lactide (4.98 g, 34.57 mmol), dried overnight under vacuum, was added to the flask, and the mixture was deoxygenated by a repeated vacuum nitrogen cycle. Subsequently, the reaction mixture was stirred and heated to 110°C under vacuum for 3 hours. The crude product was dissolved in anhydrous chloroform (100 mL) and washed with 1 M HCl. Then, the organic phase was washed with deionized water, isolated, and residual chloroform removed using a rotary evaporator operating under vacuum. The colorless viscous liquid product, L-lactide, was obtained (yield: 85%, 8.95 g). ¹H-NMR (300 MHz, CDCl₃): δ = 1.38–1.63 ppm (t,6H) (CH–CH₃)₂, δ = 1.94 ppm (s,3H) (CH₂=CCH₃), δ = 2.79 ppm (s,1H) (C–OH), δ = 4.26–

4.39 ppm (t,4H) ($\text{OCH}_2\text{-CH}_2$), $\delta = 4.39\text{--}4.51$ ppm (q,1H) (CH-(OH)CH_3), $\delta = 5.08\text{--}5.29$ ppm (q,1H) (C=O)CH(C-O) , $\delta = 5.58$ ppm (s,1H) ($\text{CH}_2\text{=C}$), $\delta = 6.10$ ppm (s,1H) ($\text{CH}_2\text{=C}$). HRMS (EI) (m/z) calcd for $\text{C}_{12}\text{H}_{18}\text{O}_7$: 274.1149; found: 274.1167.^{33,34}

4.3.3.2 Synthesis of 4-(2-(methacryloyloxy)ethoxy)-4-oxobutanoic acid (HEMA-SA):

2-Hydroxyethyl methacrylate (HEMA; 5.00 g, 38.42 mmol) was placed in a 250 mL Schlenk flask and dissolved in anhydrous THF (100 mL) with a magnetic stirring bar at room temperature under nitrogen. Succinic anhydride (4.6 g, 46.1 mmol), pyridine (15 mL), and 4-dimethylamioopyridine (0.375 g, 3 mmol) were added. Then, the reaction mixture was stirred for 24 h at 40°C under nitrogen. Next, the solvent was evaporated under vacuum after cooling the reaction to room temperature. The residue was dissolved in DCM (100 mL) followed by washing three times with 0.1M HCl solution. The organic phase was dried over anhydrous magnesium sulfate overnight and filtered. After evaporation of the solvent, the remaining HEMA-SA product was dried under vacuum at room temperature. A viscous liquid was obtained (yield 84%, 7.45 g). ^1H NMR (300 MHz, CDCl_3): $\delta = 6.13$ (s, 1H, $\text{HCH=C(CH}_3\text{)-}$), 5.54 (s, 1H, $\text{HCH=C(CH}_3\text{)-}$), 4.36 (t, 4H, $\text{-OOC(CH}_2\text{)}_2\text{OCO-}$), 2.68 (t, 4H, $\text{HOOC(CH}_2\text{)}_2\text{COO-}$), 1.85 (s, 3H, $\text{H}_3\text{CC(COO-)-CH}_2$). HRMS (EI) (m/z) calcd for $\text{C}_{10}\text{H}_{14}\text{O}_6$: 230.0842; found: 230.0873.^{35,36}

4.3.4 Synthesis of α -2-deoxy-2-methacrylamido 1,3,4,6-tetra-(O-trimethylsilyl) D-glucopyranose (TMS-MAG):

The glycomonomer (TMS-MAG) was synthesized via two synthetic steps. Glucosamine hydrochloride (10.1 g, 46.84 mmol) was placed in a two neck flask (500 ml) and flushed with nitrogen, then 200 mL of dry pyridine was added. Bis(trimethylsilyl)acetamide (41.7 g, 205 mmol) was added using a funnel or a syringe over 10 minutes, and the mixture was stirred at rt for 12 hours. Subsequently, the mixture was poured into 1.5 L of ice-cold 0.1 M solution of K_2HPO_4 cooled to 0°C using an ice bath. Next, the solution was allowed to warm to rt, and the white solids that formed were filtered off. The white solids were collected and redissolved in 400 mL of DCM, after which the DCM solution was washed with water and brine solution, and finally, the solution was dried over $MgSO_4$ for 2 hours at rt. A colorless oil was obtained after DCM evaporation.

In the second step, the colorless oil was dissolved in DMF (400 mL), and 10 mL (70 mmol) of triethylamine (TEA) was added after the solution was cooled to 0°C using an ice bath. A solution of methacryloyl chloride (5.4 g, 51.65 mmol) in 50 mL of dry DCM was added to the previous solution of the colorless oil and TEA over 20 minutes. The mixture was stirred for 1 hour in an ice bath (0°C) followed by 3 hours at 25°C. The DCM solvent was evaporated under vacuum, and the remaining solution in DMF was cooled to 0°C before being poured into 1.5L of an

ice-cold 0.1M solution of K_2HPO_4 . The aqueous mixture was extracted with 3×200 mL of hexanes after it was allowed to reach rt. The organic layer in hexane was collected and washed with water and brine solution two times and finally dried over $MgSO_4$ overnight. The product was obtained after the $MgSO_4$ was filtered off, and the hexanes were evaporated to yield 7.8 g (91%) of an off-white crystalline material and which re-crystallized in cold hexanes.³⁷ 1H NMR (300 MHz, $CDCl_3$): δ (ppm): 5.85 (d, 1H, Hk), 5.65 (s, 1H, Hj), 5.40 (s, 1H, Hi), 5.10 (d, 1H, Hh), 4.10 (td, 1H, Hg), 3.60 – 3.75 (m, 5H, Hc,d,e,f,f'), 2.00 (s, 3H, Hb), 0.17 (s, 9H, TMS), 0.14 (s, 9H, TMS), 0.10 (s, 18H, TMS) (Figure 4.7). ^{13}C NMR (300 MHz, $CDCl_3$): δ (ppm): 168 (C=O, C11), 140 ((C–C(=C)–C), C10), 120 ((H₂C=), C9), 93 (C8), 74 (C7), 72.5, 72 (C6, C5), 62 (C4), 55 (C3), 19 ((CH₃), C2), 1.09, 0.83, –0.10, –0.28 (((CH₃)₃Si), C1) (Figure 4.8). HRMS (EI) (m/z) calcd for $C_{22}H_{49}NO_6Si_4$: 535.2638; found: 535.2692.

4.3.5 Activation of 4-cyano-4-(thiobenzoylthio)pentanoic acid (CPDB):

Dichloromethane solution of CPDB (2 g, 7.16 mmol), 2-mercaptothiazoline (0.94 g, 7.87 mmol), and dicyclohexylcarbodiimide (DCC) (1.77 g, 8.59 mmol) were placed in a 250 mL two-neck round bottom flask. Then, dimethylamino pyridine (DMAP) (0.087 g, 0.716 mmol) was added slowly to the solution. The solution was stirred for 6 h at room temperature. The solution was filtered to remove the solids. The solution was evaporated to remove the solvent and after silica gel column chromatography (5:4 hexane: ethyl acetate), activated CPDB was obtained as a red

oil (2.3 g, 84% yield). ^1H NMR (300 MHz, CDCl_3): δ (ppm) 7.90 (d, 2H, aromatic ring), 7.56 (t, 1H, aromatic ring), 7.38 (t, 2H, aromatic ring), 4.58 (t, 2H, $\text{NCH}_2\text{CH}_2\text{S}$), 3.60-3.66 (m, 2H, $(\text{CN})\text{C}(\text{CH}_3)\text{-CH}_2\text{CH}_2\text{CON}$), 3.31 (t, 2H, $\text{NCH}_2\text{CH}_2\text{S}$), 2.50-2.56 (m, 2H, $(\text{CN})\text{C}(\text{CH}_3)\text{CH}_2\text{CH}_2\text{CON}$), 1.95 (s, 3H, $(\text{CH}_3)\text{C}(\text{CN})\text{S}$). FT-IR: 1700 cm^{-1} ($\text{C}=\text{O}$), 1160 cm^{-1} ($\text{PhC}=\text{S}$), 1020 cm^{-1} ($\text{NC}=\text{S}$). HRMS (EI) (m/z) calcd for $\text{C}_{16}\text{H}_{16}\text{N}_2\text{OS}_4$: 380.0193; found: 380.0203.³⁸

4.3.6 Attachment of activated CPDB onto silica nanoparticles ($\text{SiO}_2@\text{CPDB}$):

Silica nanoparticles (15.0 g, 30 wt % in MEK) were dispersed in 50 mL THF and placed in a round bottom flask, and 3-aminopropyldimethylethoxy silane 400 μL was added. The solution was purged with N_2 for 1 h, and then the solution was refluxed in a 70°C oil bath overnight. The solution was then cooled to r.t and precipitated into hexanes (500 mL). The solution was centrifuged at 4000 rpm for 7 minutes and the solvent decanted. The precipitation-dissolution process was repeated for another two times. After that, the amine-functionalized nanoparticles were dispersed in 50 mL of dry THF and were added dropwise into a THF solution of activated CPDB (0.14 g, 0.185 M) at r.t and stirred for 6 hours. The solution was precipitated into a large amount of hexane (approx. 400 ml), and the nanoparticles were recollected by centrifugation at 4000 rpm for 7 min. This precipitation-dissolution process was repeated until the supernatant solution was colorless. Then, the nanoparticles were placed in a vacuum at r.t. The grafting density of

CPDB anchored silica nanoparticles (0.35 ch/nm^2) was determined using the UV-vis calibration curve made from standard solutions of free CPDB.⁸

4.3.7 RAFT polymerization of “controlled release” monomers from CPDB functionalized silica nanoparticles:

A THF solution (10 mL) of HEMA-LA or HEMA-SA, CPDB-anchored silica nanoparticles (1g) with desired graft density, was placed in a 50 ml dried Schlenk tube. AIBN (10 mM THF solution) was added to the Schlenk tube using a ratio between species of [CPDB]:[monomer]:[AIBN] =1:500:0.1. The solution was degassed by three freeze-pump-thaw cycles and filled with nitrogen. Then the Schlenk tube was placed in an oil bath at 65°C for the desired time. The polymerization was stopped by quenching the Schlenk tube in ice water. The polymer-grafted silica nanoparticles were precipitated by pouring into 400 ml of hexanes and centrifuged at 4000 rpm for 7 min, and the particles were dispersed back into THF. The polymer chains were cleaved by dissolving 50 mg of polymer-grafted nanoparticles in 3 mL of THF and treating with 0.2 ml aqueous HF (49%). The solution was stirred overnight and the cleaved polymer chains were analyzed by GPC.³⁹

4.3.8 Cleavage of CPDB agents from the polymeric chain ends of the Silica nanoparticles:

Polymer-grafted nanoparticles (1 g) of HEMA-LA-g-SiO₂ or HEMA-SA-g-SiO₂ were dispersed in 40 ml THF and solid AIBN (20 eq, 0.12 g) was added at the ratio of ([CTA]:[AIBN]= 1:20). The solution was heated at 65°C under nitrogen for 1 hr. The solution was poured into 400 ml of hexanes and centrifuged at 4000 rpm for 7 min to recover the nanoparticles.⁸

4.3.9 Preparation of NBD-labelled amino acids (NBD-COOH):

A solution of 6-aminohexanoic acid (1.2 eq, 0.39 g, 3 mmol) and NaHCO₃ (3 eq, 0.63 g, 7.5 mmol) in MeOH (40 mL) were stirred at room temperature for 30 min and then refluxed in a 65°C oil bath. Then, the 4-chloro-7-nitrobenzofurazan (NBD-Cl, 1 eq, 0.5 g, 2.5 mmol) was dissolved in MeOH (5 mL) and added dropwise to the solution. After two hours, the reaction mixture was cooled to room temperature and acidified to approximately pH 2 with 1M HCl. Subsequently, the mixture was extracted three times with EtOAc (25 mL), washed with brine, dried with MgSO₄ filtered, and the solvent removed using a rotary evaporator. The resultant NBD-labelled amino acid was then recrystallized from aqueous MeOH.⁴⁰ The product was isolated as bright orange crystals (yield: 82%, 0.6 g). T_m= 156-158°C, UV (MeOH) λ_{max}: 335, 458. FT-IR ν_{max}/cm⁻¹ 1700 (strong, sharp C=O). MS (EI+) m/z: [M]⁺ 294.

4.3.10 Preparation of NBD-labelled hexamethylenediamine (NBD-NH₂):

Hexamethylenediamine-NBD dye was synthesized in two steps, first preparing N-Boc-hexamethylenediamine-NBD that was converted to the desired product. Preparation of N-Boc-hexamethylenediamine-NBD: A solution of 4-chloro-7-nitrobenzofurazan (NBD-Cl) (1 eq, 0.75 g, 3.76 mmol) and mono-Boc-hexamethylenediamine (1 eq, 0.89 g, 4.31 mmol) was prepared in 40 mL ethanol. Pyridine (catalytic, 3400 μ L) was added to the stirred solution and allowed to stir for 30 min. The mixture was concentrated and purified by column chromatography (toluene: ethyl acetate 7:3) to obtain the product as a red foam. Preparation of hexamethylenediamine-NBD: At room temperature, the Boc-protected dye was dissolved in a 1:1 solution of trifluoroacetic acid (TFA): dichloromethane (DCM) and stirred for 1 h. Subsequently, the solution was concentrated and resuspended in acetonitrile. The final product was obtained as golden crystals (T_m = 149-152°C) after the solution was precipitated into cold diethyl ether (0.84 g, yield 80%).⁴¹ UV (MeOH) λ_{max} : 336, 460. FT-IR ν_{max}/cm^{-1} 3380 (medium, sharp N-H). HRMS (EI) (m/z) calcd for C₁₂H₁₇N₅O₃: 279.1382; found: 279.3014.

4.3.11 Aminohexanoic acid-NBD Conjugate on HEMA-LA-g-SiO₂ and Hexamethylenediamine-NBD conjugate on HEMA-SA-g-SiO₂:

Polymer-g-SiO₂ (1 eq.) (HEMA-LA-g-SiO₂, 0.53 g, 1.94 mmol or HEMA-SA-g-SiO₂, 0.5 g, 2.13 mmol), dye-labeled (1.1 eq) (aminohexanoic acid-NBD, 0.63 g, 2.13 mmol or hexamethylenediamine-NBD, 0.66 g, 2.39 mmol, respectively), and dicyclohexylcarbodiimide (DCC) (1.2 eq, 0.48 g or 0.53 g respectively) were dissolved in 40 mL of THF. (Dimethylamino) pyridine (DMAP) (0.1 eq, 0.194 mmole, or 0.217 mmole, respectively) was added slowly to the solution. Subsequently, the solution was stirred at room temperature for 6 h. Then, the solution was filtered, and the solvent was concentrated using a rotary evaporator. The solution was precipitated by pouring into 400 mL of hexane and centrifuged at 4000 rpm for 7 min to recover the nanoparticles. The precipitation-dissolution process was repeated twice until the supernatant layer after centrifugation was colorless to ensure the removal of free dyes.

4.3.12 Modification of CDSS RAFT agent with phosphate group:

Two synthetic steps were used to synthesize the CDSS-phosphate. 4-Cyano-4-(dodecylsulfanylthiocarbonyl) sulfanyl pentanoic acid (CDSS) (4 g, 9.9 mmol), 1,6-hexanediol (7 g, 59.45 mmol), and N, N'-dicyclohexylcarbodiimide (DCC) (2.25 g, 10.9 mmol) were placed in 500 ml round bottom flask and dissolved in 100 ml of THF. The mixture was cooled to 0°C and flushed with N₂ for 15 min. A solution

of 4-dimethylaminopyridine (DMAP) (0.06 g, 0.49 mmol) in 15 ml THF was added dropwise over 30 min. The solution was stirred overnight and then allowed to warm to room temperature. Next, the solids formed during the reaction were filtered off and the solution was concentrated by removing the solvent using a rotary evaporator. The product residue was dissolved in 100 ml DCM and washed three times with DI water. The DCM layer was isolated and dried with MgSO₄ for 2 hours. MgSO₄ was filtered off and the solvent was removed under a rotary vacuum. Then, the residue was subjected to silica column chromatography (5:4, hexanes: ethyl acetate). The product was recovered as a yellow oil (4.2 g, 84% yield). ¹H NMR (300 MHz, CDCl₃): δ (ppm) 4.70 (s, 1H) (CH₂OH), 4.12 (t, 2H) (O=CCH₂CH₂), 3.65 (t, 2H) (CH₂CH₂OH), 3.33 (t, 2H) (CH₂CH₂S), 2.64–2.60 (t, 2H) (CN-CCH₂CH₂), 2.38–2.33 (t, 2H) (CN-CCH₂CH₂C=O), 2.0–1.9 (t, 2H) (CH₂CH₂CH₂S), 1.80 (s, 3H) (CH₃C-CN), 1.65–1.40 (m, 8H) (OCH₂(CH₂)₄CH₂OH), 1.25–1.29 (s, 18H), 0.88 (t, 3H) (CH₃CH₂CH₂). ¹³C NMR (300 MHz, CDCl₃): δ (ppm) 217, 171.6, 119, 65.1, 62.7, 46.4, 37, 33.9, 32.6, 31.9, 29.8, 29.6, 29.5, 29.4, 29.3, 29.1, 28.9, 28.5, 27.7, 25.7, 25.4, 24.9, 22.7. FT-IR: 1700 cm⁻¹ sharp (C=O), 3500 cm⁻¹ broad (O-H). HRMS (EI) [M+H] Calcd for C₂₅H₄₅NO₃S₃: 503.2562; found 503.2573.

The second step of synthesizing CDSS-phosphate was accomplished using the following procedure. The previous product (CDSS-OH) (4 g, 7.94 mmol) and triethylamine (0.96 g, 9.52 mmol) were dissolved in 50 ml of dry THF using a 250

ml round bottom flask. The solution was flushed with dry N₂ for 30 min and cooled to 0°C, followed by the dropwise addition of phosphoryl chloride (4.26 g, 27.79 mmol) over one hour. The solution was allowed to warm to room temperature and stirred overnight under an N₂ atmosphere. Then, DI water (100 ml) was added to the solution and stirred for two hours. Using the separatory funnel, the solution was transferred to an organic layer by adding DCM (100 mL) which was washed with three portions of DI water. The organic layer was isolated and dried with MgSO₄. The MgSO₄ was filtered off and the DCM solvent was removed under reduced pressure. The product was recovered as a thick yellow to a brown oil (3.57 g, 77% yield). ¹H NMR (300 MHz, CDCl₃): δ (ppm) 6.29 (s, 2H) O-P(OH)₂, 4.12 (t, 2H) (O=CCH₂CH₂), 4.01 (t, 2H) (CH₂CH₂O-P), 3.33 (t, 2H) (CH₂CH₂S), 2.64–2.60 (t, 2H) (CN-CCH₂CH₂), 2.38–2.33 (t, 2H) (CN-CCH₂CH₂C=O), 2.0–1.9 (t, 2H) (CH₂CH₂CH₂S), 1.80 (s, 3H) (CH₃C-CN), 1.65–1.40 (m, 8H) (OCH₂(CH₂)₄CH₂OH), 1.25–1.29 (s, 18H), 0.88 (t, 3H) (CH₃CH₂CH₂). ¹³C NMR (300 MHz, CDCl₃): δ (ppm) 217, 171.7, 119, 67.4, 65.1, 46.4, 37.1, 33.9, 31.9, 29.8, 29.6, 29.4, 29.3, 29.1, 29, 28.4, 27.7, 25.4, 25, 24.8, 22.7. ³¹P NMR (300 MHz, CDCl₃): δ (ppm) 1.71. FT-IR: 1700 cm⁻¹ sharp (C=O), 1195 cm⁻¹ (P=O). HRMS (EI) [M+H]⁺ Calcd for C₂₅H₄₆NO₆PS₃: 584.2300; found 584.2298.

4.3.13 Functionalization of monomodal nanoparticles SiO₂-g-HEMA-LA-dye and SiO₂-g-HEMA-SA-dye by the second modified CDSS RAFT Agent:

The second modified CDSS-phosphate agent was attached to the surface of monomodal silica nanoparticles, as previously described. CDSS-phosphate was functionalized directly on the nanoparticles in a process similar to the one described for the first chain functionalization. THF solution (50 mL) of (1 g) monomodal nanoparticles was placed in a two-necked round bottom flask. Then, CDSS-phosphate (0.124 g, 0.21 mmol, 5 mL) was added, and the solution was refluxed at 70°C overnight under nitrogen protection. Next, the reaction was cooled to r.t. and poured into hexanes (500 mL). The nanoparticles were recovered by centrifugation (3500 rpm for 7 min.). This redispersion–precipitation procedure was repeated two times until the supernatant layer after centrifugation was colorless. The second chains of the CDSS-anchored silica nanoparticles were dried and analyzed using UV-vis analysis to determine the graft density.

4.3.14 Graft Polymerization of glycomonomer (TMS-MAG) from SiO₂-g-(HEMA-LA-dye, CDSS) and SiO₂-g-(HEMA-SA-dye, CDSS) to synthesize the second brush:

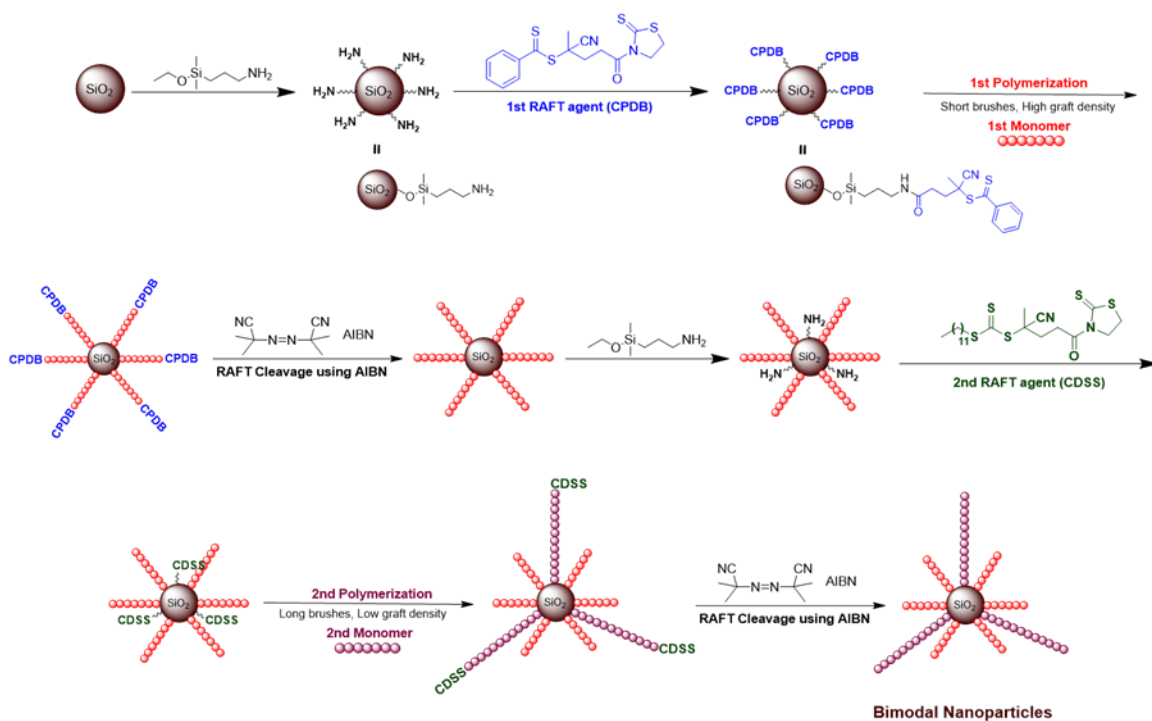
The nanoparticles (SiO₂-g-(HEMA-LA-dye, CDSS) and SiO₂-g-(HEMA-SA-dye, CDSS)) (0.5 g by weight of silica) were dispersed in 20 mL THF and added to a Schlenk flask along with predetermined the glycomonomer (TMS-MAG) and

AIBN (0.2 mL of 0.001 M THF solution). The mixture was degassed by three freeze-pump-thaw cycles, backfilled with nitrogen, and then placed in an oil bath at 65°C for 24 h after which the polymerization was quenched in ice water. The nanoparticles were recovered by precipitating into hexanes and centrifugation at 4000 rpm for 7 minutes.

4.4 Results and discussion:

4.4.1 Synthesis of bimodal nanoparticles:

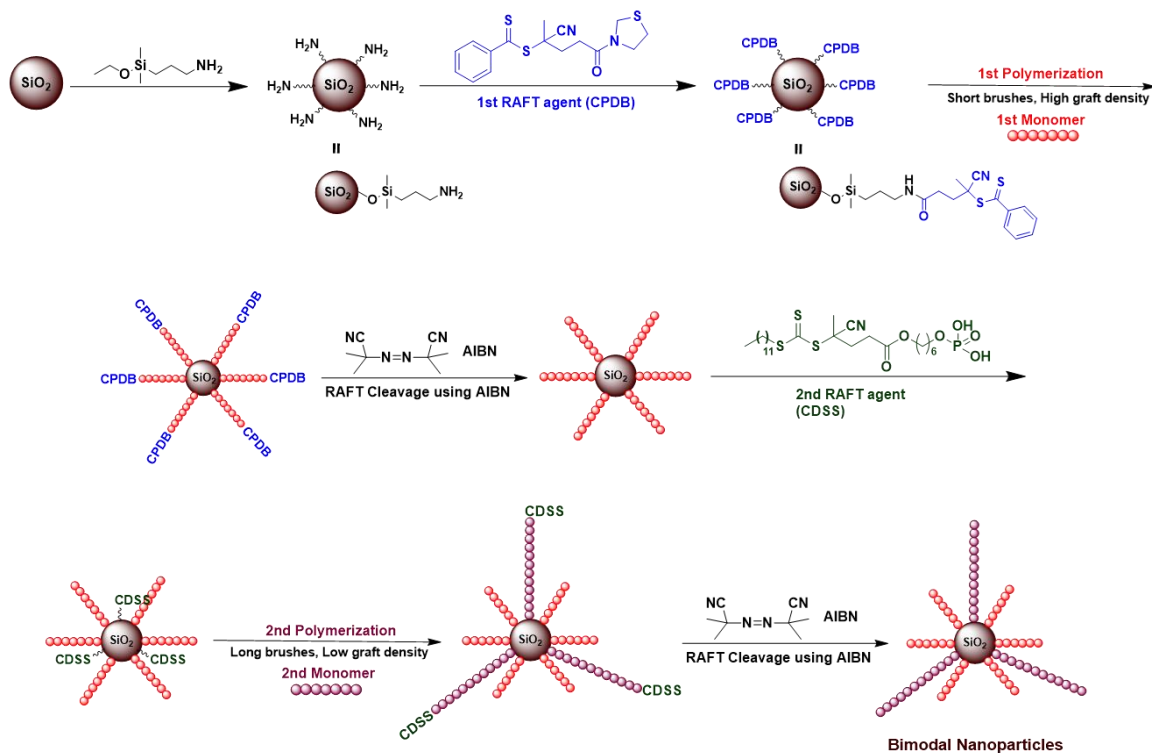
Designing bimodal nanoparticles using the RAFT agent technique for various monomers has been investigated for less than 10 years.^{8,42,43} Using the RAFT polymerization technique and the grafting-from approach, several researchers have previously shown this to be an effective method of synthesizing bimodal polymer brushes on various surfaces of nanoparticles.⁴⁴⁻⁴⁶ In the current work, we initially attempted to use a strategy shown in Scheme 4.1. This was modeled after our previous work on bimodal grafted nanoparticles.^{8,44,47} However, the attachment of the second round of aminosilane was not successful. We hypothesize that during the addition of the amine containing silane, the amine group also attached the ester groups in the first population of HEMA-LA and HEMA-SA grafted chains, leading to side reactions that prevented the grafting of the second population of polymer chains.



Scheme 4.1: Initially proposed synthesis of bimodal brush nanoparticles using two different RAFT agents.

To overcome this limitation, we re-designed the synthetic strategy. In this new successful strategy, we prepared high graft density, low molecular weight polymer chains of the pH-sensitive monomers HEMA-LA, HEMA-SA that contained a hydrolytically sensitive ester linkage on the surface of silica nanoparticles as the first polymeric population. The polymerization was conducted using 4-cyano-4-(phenylcarbonothioylthio) pentanoic acid (CPDB) as the first RAFT agent. For the second population of chains at low graft density and high molecular weight, the glycomonomer 2-methacrylamido glucopyranose (MAG), was polymerized using the 4-cyano-4-[(dodecylsulfanylthiocarbonyl)]

sulfanyl]pentanoic acid (CDSS) as a second RAFT agent. This chain transfer agent was modified to contain a phosphonate group that was grafted directly on the surface of silica nanoparticles and avoids using the 3-aminopropyltrimethoxysilane (Scheme 4.2).



Scheme 4.2: Proposed strategy to synthesis bimodal brush nanoparticles using two different RAFT agents.

4.4.2 Grafting first polymer population chains:

The monomers HEMA-LA, HEMA-SA that containing a pH-sensitive ester linkage were synthesized according to our previous work, using the ring-opening reaction of the corresponding cyclic lactone compound, L-lactide or succinic anhydride, with hydroxyethyl methacrylate (HEMA) catalyzed by stannous 2-

ethylhexanoate and DMAP, respectively. The graft densities of polymer chains on the surface of silica nanoparticles were controlled by varying the ratio of silica nanoparticles to 3-aminopropyltrimethoxysilane to prepare SiO₂-g-CPDB nanoparticles.^{38,48-50} As reported earlier, the 2-(2-cyanopropanyl dithiobenzoate) (CPDB) RAFT agent provided a controlled polymerization with both monomers HEMA-LA and HEMA-SA. Both have compatibly polymerized with CPDB using 1/500 as the feed ratio [CPDB]/[Monomer] for the polymerization under the standard conditions of 65°C and inert gas. The grafting density of the chains attached to the surface of silica nanoparticles prior to polymerization was measured using UV-Vis spectrometry. Azobisisobutyronitrile (AIBN) was used as the initiator for the polymerization with a ratio of 10:1 [CPDB]/[AIBN] for all polymerizations of both monomers (HEMA-LA, HEMA-SA). The molecular weights of the various P(HEMA-LA) and P(HEMA-SA) were evaluated using GPC by cleavage the polymeric chains from the surface of silica nanoparticles using hydrofluoric acid (HF).

4.4.3 CPDB RAFT agent cleavage:

After completing the first RAFT polymerization, the CPDB agent remains active on the chain ends and could be further polymerized upon the attempts to prepare a second chain population. Therefore, prior to the attachment of the second polymer population, it was necessary to cleave the first RAFT agent end

group from the first polymer population.⁵¹ Therefore, the cleavage reaction was achieved using a high ratio of the AIBN (monomer/initiator; 1/20) via a radical cross-coupling mechanism.⁵²⁻⁵⁴ As shown in Figure 4.1 for HEMA-LA and HEMA-SA grafted silica nanoparticles, UV spectroscopy was used to detect the CPDB peaks before and after the cleavage reaction.⁵⁵ Prior to cleavage, the nanoparticles were pink in color and showed absorbance at 302.5 nm. This peak disappeared from the UV spectrum after the cleavage reaction, and the color of the nanoparticles changed to white polymer-coated nanoparticles. The disappearance of the 302.5 nm absorbance peak provided evidence to the nearly quantitative removal of RAFT moieties.

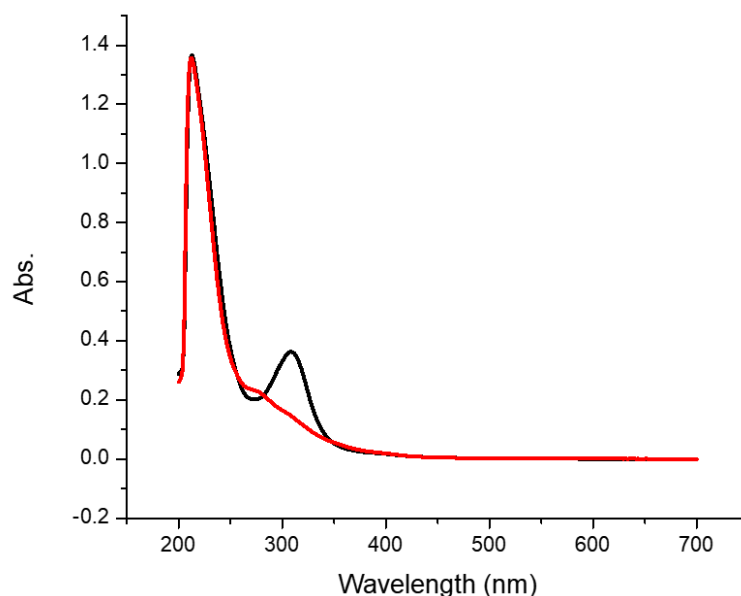


Figure 4.1: UV absorption spectra of polymer grafted nanoparticles with cleaved CDSS RAFT agent (red line), and with CDSS attached to the polymers on the surface of silica nanoparticles (black line).

4.4.4 NBD-dyes attachment

The main goal for synthesizing the bimodal brush nanoparticles is to provide a platform to use in biological applications. Therefore, it became necessary to develop a method to monitor the release of an attached group from the polymer grafted nanoparticles. Accordingly, labeling the polymer grafted nanoparticles with fluorescent dyes is advantageous in monitoring the presence, payload release and movement of bimodal nanoparticles in biological systems.⁵⁶ Two different dyes (aminohexanoic acid-NBD, hexamethylenediamine-NBD) were synthesized, as shown in our previous work. Both dyes were covalently conjugated to the polymer grafted nanoparticles SiO₂-g-HEMA-LA, SiO₂-g-HEMA-SA via the Steglich esterification reaction using (DCC/DMAP) catalyst to form the ester and amide bonds,⁵⁷ respectively (Scheme 4.3).

This method was successful for attaching the fluorescent dyes to the polymer grafted silica nanoparticles for release and tracking studies. The UV-vis analysis of the nanoparticles confirmed the existence of the absorption peak at ~460 nm for NBD dyes in both dye-labeled polymer grafted nanoparticles (SiO₂-g-P(HEMA-LA)-dye, SiO₂-g-P(HEMA-SA)-dye). In addition, the presence of a medium, sharp C=O stretching vibration peak at ~1731 cm⁻¹ using the FT-IR analysis, have ascribed to the formed ester group in SiO₂-g-P(HEMA-LA)-dye. Likewise, the presence of a strong, sharp C=O stretching vibration peak at ~1625



Scheme 4.3: Attaching (a) NBD-COOH dye to the SiO₂@P(HEMA-LA) and (b) NBD-NH₂ dye to the SiO₂@P(HEMA-SA).

cm⁻¹, has indicated to the amide group in SiO₂-g-P(HEMA-SA)-dye, as shown in Figure 4.2. Both UV-vis and FT-IR demonstrated the successful attachment of dyes to the polymer grafted nanoparticles. The dispersion and the fluorescence under UV-vis of the dye-labeled nanoparticles were shown in Figure 4.3.

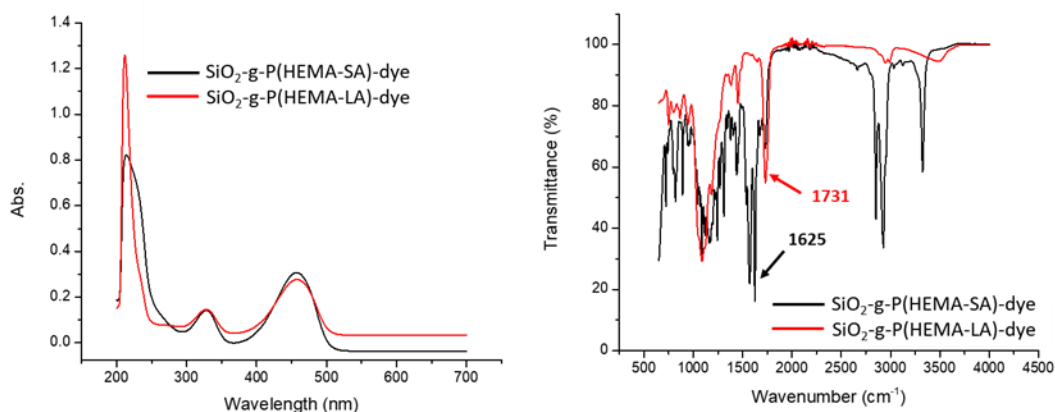


Figure 4.2: UV-vis, FT-IR spectrums of SiO₂-g-P(HEMA-LA)-dye (red curve), and SiO₂-g-P(HEMA-SA)-dye (black curve).



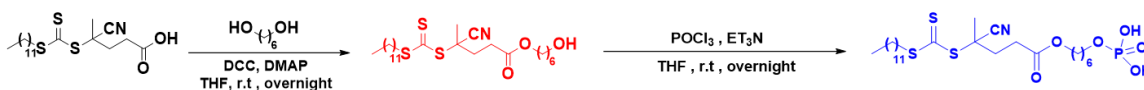
Figure 4.3: The dispersion of dye labeled polymer grafted nanoparticles (SiO₂-g-P(HEMA-SA)-dye) and the fluorescence under UV-vis light.

4.4.5 Grafting the second RAFT agent (CDSS-phosphate):

After attachment of the first population of polymer chains, the removal of the RAFT agent and the attachment of the dyes, the second population was synthesized by attachment of the second RAFT agent, 4-cyano-4-((dodecylsulfanylthiocarbonyl) sulfanyl)pentanoic acid (CDSS), which is different from the first chain transfer agent, 4-cyano-4-(phenylcarbonothioylthio)pentanoic acid (CPDB) that was used to synthesize the first polymer brush-grafted silica

nanoparticles. The modification of a novel phosphate-containing CTA agent for a RAFT polymerization was previously explored in our group.⁵⁸ The modified phosphate-CDSS was used to avoid using 3-aminopropyldimethylethoxysilane, which apparently reacted with the ester groups of dye-labeled side chains of the first population of bimodal nanoparticles.

Phosphate-containing CDSS agents are quite useful as a method for robust attachment on the surface of silica nanoparticles. The resultant Si-O-P bond is readily formed and hydrolytically stable. Synthesis of the phosphate-containing CDSS agent was performed in two synthetic steps (Scheme 4.4). In the first step, the esterification of the acid-containing CDSS RAFT agent was achieved using an excess of 1,6-hexanediol in dilute solution to prevent the formation of difunctional CDSS agents. In the second step, the unreacted alcohol moiety that resulted from the first step was converted to the phosphate using phosphoryl chloride (POCl₃).



Scheme 4.4: Synthesis of phosphate-containing CDSS agent.

The conversion of the alcohol to the phosphate moiety was confirmed via ¹H-NMR and ³¹P-NMR analysis. Clearly, we could observe the difference among ¹H-NMR spectrums of CDSS, CDSS-OH, and CDSS-phosphate. The chemical peaks of adjacent protons at -(C=O)-O-CH₂-(CH₂)₅ (δ = 4.1 ppm), (CH₂)₅-CH₂-OH

($\delta = 3.6$ ppm), were shifted to the downfield when going from alcohol functionality to phosphate moiety $-(C=O)-O-CH_2-(CH_2)_5$, $(CH_2)_5-CH_2-O-P$ ($\delta \sim 4.2-4.0$ ppm), as shown in Figure 4.4. Also, the presence of the phosphorus was confirmed by ^{31}P -NMR which showed a peak at $\delta \sim 1.7$ ppm. Furthermore, the successful conversion of the carboxylic acid in the RAFT agent (CDSS) to the phosphate moiety in the modified RAFT agent (CDSS-phosphate), was confirmed using the UV-vis analysis (no degradation of the trithiocarbonate moiety occurred), and FT-IR analysis (medium sharp peak at ~ 1200 cm^{-1} for $P=O$) (Figure 4.5).

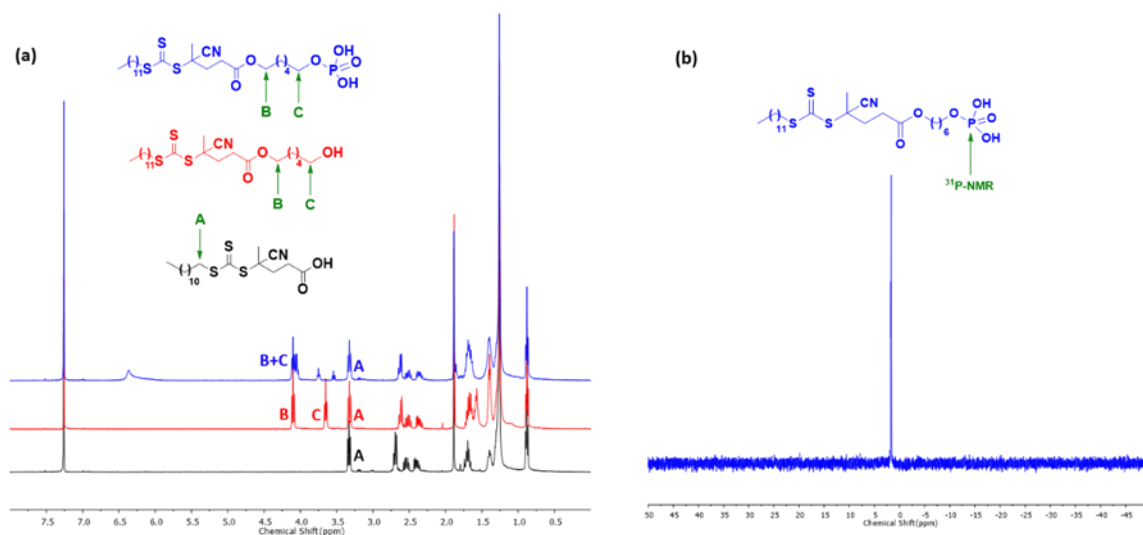


Figure 4.4: (a) 1H -NMR spectrums of CDSS RAFT agent, CDSS-OH, and CDSS-Phosphate and (b) ^{31}P -NMR spectrum of CDSS-Phosphate.

Next, the attachment of the second RAFT agent (CDSS-phosphate) on the surface of $SiO_2@P(HEMA-LA)$ or $SiO_2@P(HEMA-SA)$ was achieved using a similar approach as employed for the first RAFT polymerization. The synthetic RAFT agent CDSS-phosphate was able to diffuse to the surface of the silica nanoparticles

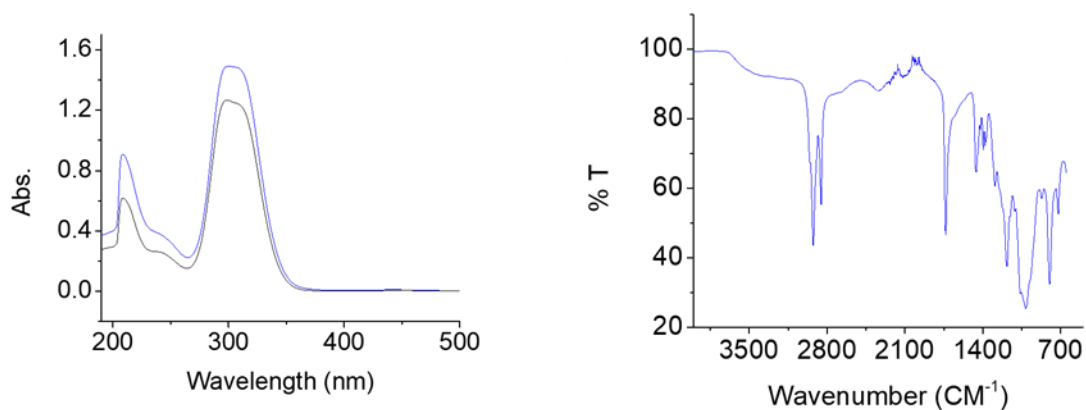


Figure 4.5: UV-vis, FT-IR spectrums of synthesized RAFT agent (CDSS-Phosphate).

even in the presence of the grafted brushes from the first polymer population. The grafting density of the second polymer brushes relied on the concentration of the CDSS-phosphate agent. Various graft densities (0.05–0.4 ch/nm²) of the second population were successfully achieved by controlling the ratio of RAFT agent (CDSS-phosphate) to the first brush grafted nanoparticles. The CDSS grafted nanoparticles were precipitated in hexanes and re-dispersed three times in THF to remove unreacted CDSS-phosphate. The attachment of the CDSS-phosphate RAFT agent on the surface of the nanoparticles was confirmed using the UV spectrum of the RAFT agent peak at 305 nm (Figure 4.6).

4.4.6 Synthesis and polymerization of the second monomer (TMS-MAG):

RAFT polymerization of the second polymer brush population was accomplished using the glycomonomer, trimethylsilyl-protected 2-deoxy-2-methacrylamido glucopyranose (TMS-MAG), as a second monomer, to give

bimodal nanoparticles. The glycomonomer (TMS-MAG) was synthesized, as shown in Scheme 4.5, in two steps.^{37,59}

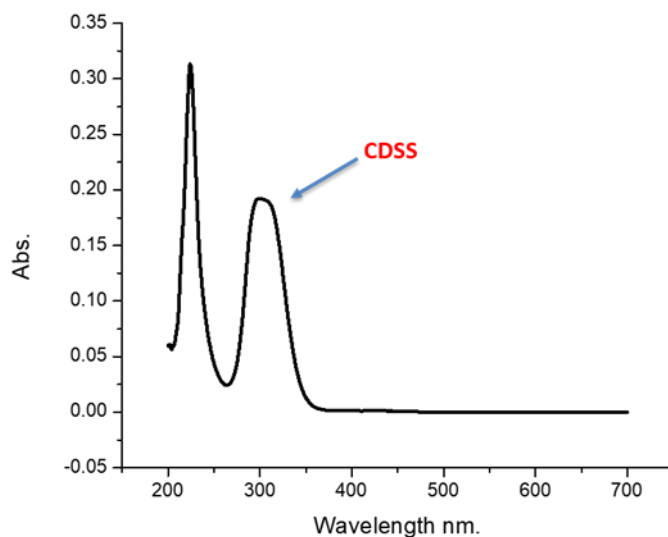
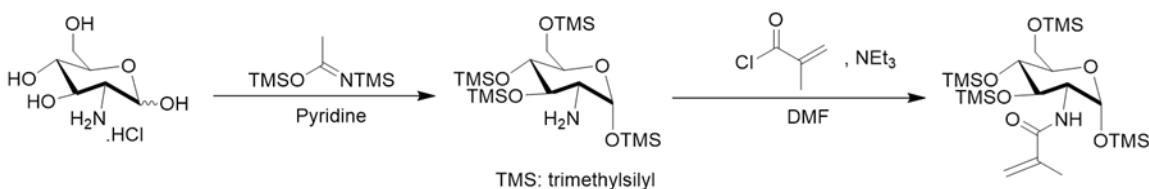


Figure 4.6: UV-vis of the CDSS-Phosphate grafted on the surface of monomodal nanoparticles.



Scheme 4.5: Synthesis of the glycomonomer TMS-MAG.

First, the glucosamine was protected via a trimethylsilylation reaction by reacting with N, O-bis(trimethylsilyl)acetamide in pyridine. Second, the TMS-MAG was synthesized by reacting to the TMS-protected glucosamine with methacryloyl chloride in DMF. Characterizations of the glycomonomer (TMS-MAG) show high purification via simple extractions with hexanes because of the

nonpolar nature of the product. The chemical shifts of Hh (doublet, 5.1 ppm) and Ca (93 ppm), as shown in the ^1H -NMR and ^{13}C NMR spectra of TMS-MAG in (Figures 4.7 and 4.8, respectively) confirmed the chemical structure.⁶⁰

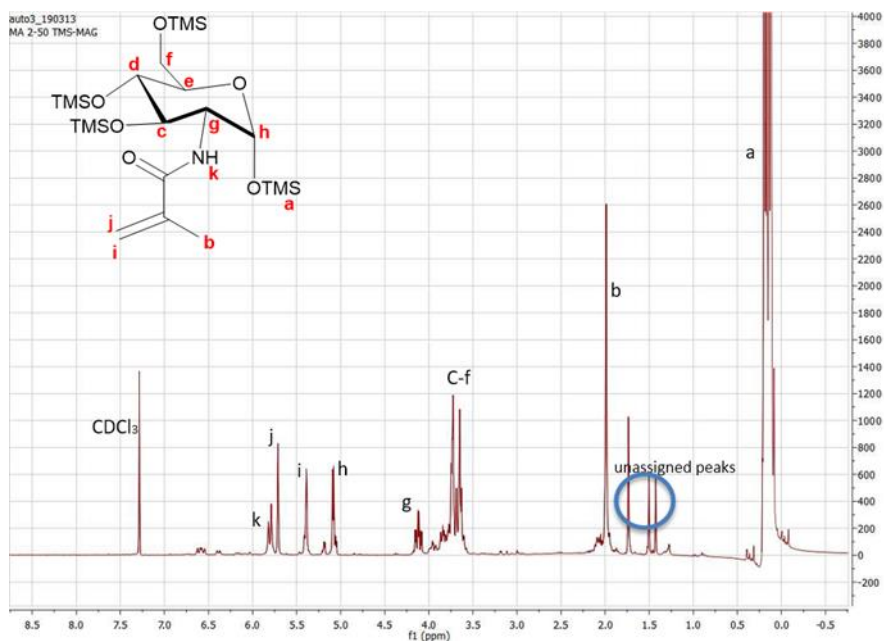


Figure 4.7: ^1H -NMR of the glycomonomer TMS-MAG.

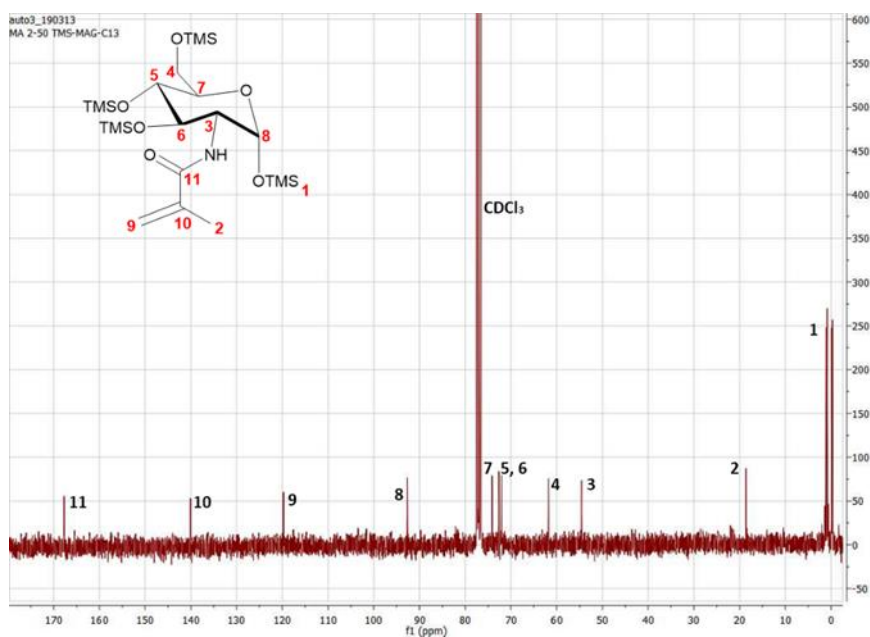


Figure 4.8: ^{13}C -NMR of the glycomonomer TMS-MAG.

In initial graft polymerization experiments, we observed the slow polymerization of TMS-MAG that led to the hypothesis that the propagation step of TMS-MAG is slow because of the steric hindrance around the methacrylamido reactive group caused by the surrounding trimethylsilyl groups. These results can be compared with the solution polymerization of the unprotected monomer (MAG), as reported by separate groups,¹⁷ where the polymerization was fast and high molecular weight polymers were obtained. The molecular weight of the second grafted polymer P(TMS-MAG) could be increased by maintaining the ratio of monomer (TMS-MAG) to RAFT agent at 500/1 to avoid gelation (Table 4.1).

Table 4.1: Polymerization of the glycomonomer (MAG-TMS) using CDSS as RAFT agent and AIBN as an initiator at 65°C.

Sample	Ratio (M/RAFT)	GD (ch/nm ²)	Time (h)	Conversion	Mn (kDa)	Đ
MA 2-149	500/1	0.21	9	0.4	22	1.26
MA 2-168	500/1	0.19	12	0.65	31	1.31
MA 2-143	500/1	0.145	24	0.81	44	1.36
MA 2-64	1000/1	0.152	24	Viscous liquid	-	-
MA 2-65	2000/1	0.152	24	Gelled up completely after 3 h	-	-

Gel permeation chromatography (GPC) was used to measure the molecular weight (M_n) and dispersity index (\mathcal{D}) of the second polymer brush of bimodal nanoparticles,⁶¹ indicating reasonable control over the second polymerization. The quantitative GPC results of both bimodal nanoparticles, $\text{SiO}_2\text{-g-P(HEMA-LA-dye)-P(TMS-MAG)}$, and $\text{SiO}_2\text{-g-P(HEMA-SA-dye)-P(TMS-MAG)}$ are summarized in Table 4.2.

Table 4.2: Molecular weights and grafting densities of bimodal nanoparticles, $\text{SiO}_2\text{@P(HEMA-LA-dye)-PMAG}$, and $\text{SiO}_2\text{@P(HEMA-SA-dye)-PMAG}$.

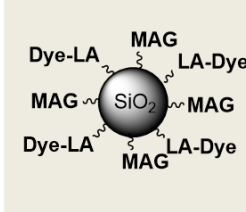
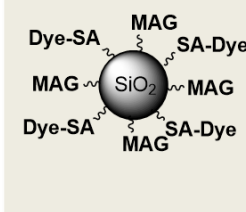
		GD (ch/nm ²)	M.W (kDa)	\mathcal{D}
	Short brush P(HEMA-LA-dye)	0.237	12	1.2
	Long brush P(MAG)	0.128	45	1.44
	Short brush P(HEMA-SA-dye)	0.237	15	1.24
	Long brush P(MAG)	0.156	38	1.39

Figure 4.9 a, b, shows the GPC traces of the bimodal polymer brushes on the nanoparticles compared to the GPC traces of the first brushes on the nanoparticles. The GPC trace for bimodal nanoparticles, $\text{SiO}_2\text{-g-P(HEMA-LA-dye)-P(TMS-MAG)}$, and $\text{SiO}_2\text{-g-P(HEMA-SA-dye)-P(TMS-MAG)}$, distinctly show

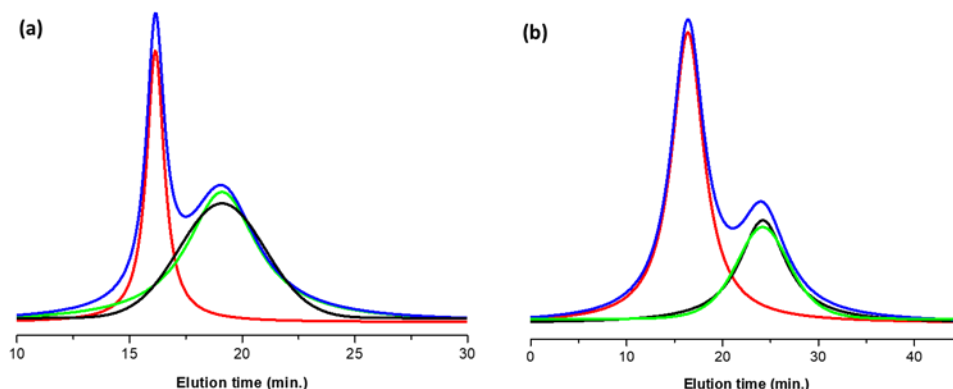


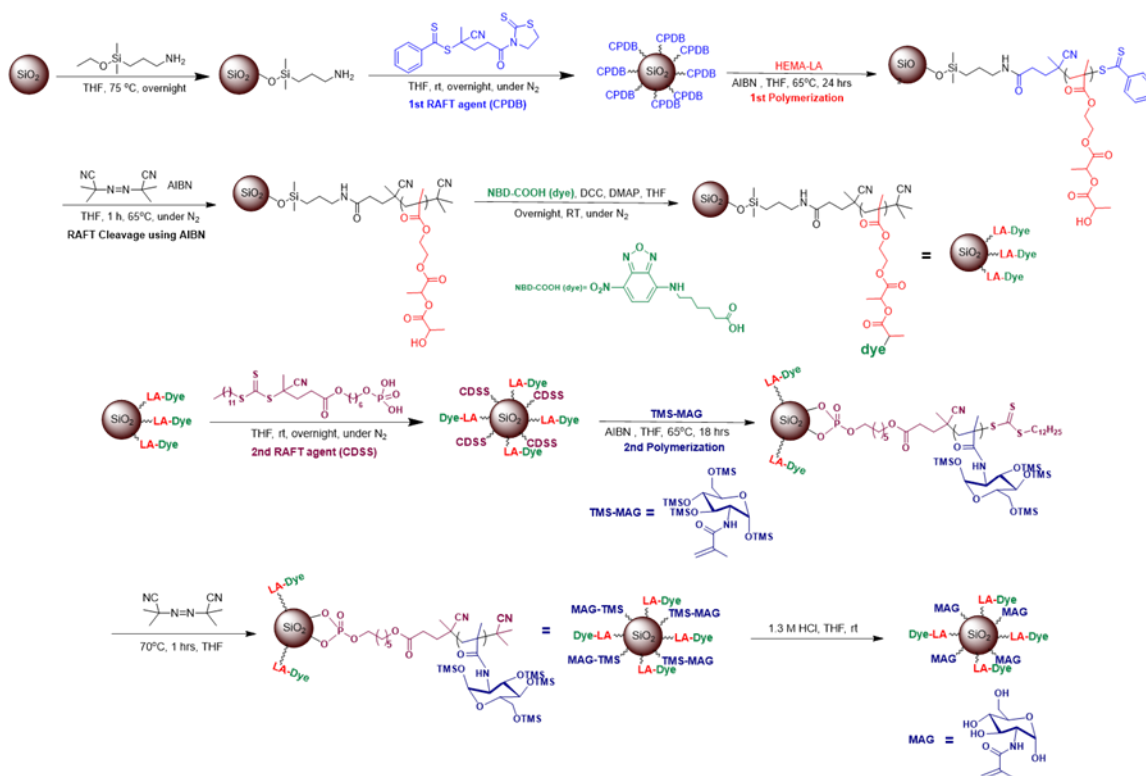
Figure 4.9: GPC traces of bimodal grafted silica nanoparticles **a)** bimodal grafted nanoparticles $\text{SiO}_2\text{-g-P(HEMA-LA-dye)-P(TMS-MAG)}$ (blue line), deconvoluted peaks of monomodal nanoparticles $\text{SiO}_2\text{-g-P(HEMA-LA-dye)}$ (green line), and $\text{SiO}_2\text{-g-P(TMS-MAG)}$ (red line), measured monomodal grafted nanoparticles $\text{SiO}_2\text{-g-P(HEMA-LA)}$ (black line). **b)** bimodal grafted nanoparticles $\text{SiO}_2\text{-g-P(HEMA-SA-dye)-P(TMS-MAG)}$ (blue line), deconvoluted peaks of monomodal nanoparticles $\text{SiO}_2\text{-g-P(HEMA-SA-dye)}$ (green line), and $\text{SiO}_2\text{-g-P(TMS-MAG)}$ (red line), measured monomodal grafted nanoparticles $\text{SiO}_2\text{-g-P(HEMA-SA)}$ (black line).

that the cleaved polymers have a binary distribution of molecular weight. The appearance of these two distributions has confirmed the composition of bimodal nanoparticles.⁶² In both bimodal grafted nanoparticles, the higher peak of molecular weight distribution indicates the long polymer brushes on the surface of nanoparticles that have a short elution time. A short, dense brush of $\text{SiO}_2\text{-g-P(HEMA-LA-dye)}$ was polymerized under controlled radical polymerization conditions at 0.237 ch/nm^2 with a molecular weight distribution of 12 kDa and \bar{D} of (1.2). As well, the low distribution peak has the same average molecular weight

as the distribution in monomodal nanoparticles that have a long elution time. The second population of TMS-MAG was polymerized at a density of 0.128 ch/nm² with a molecular weight of 45 kDa and dispersity (Đ) 1.44. On the other hand, the short, dense brush of SiO₂-g-P(HEMA-SA-dye) was polymerized at 0.237 ch/nm² with a molecular weight of 15 kDa and Đ of 1.24. While a long, dense brush was polymerized at 0.156 ch/nm² under controlled radical polymerization with a molecular weight of 38 kDa and Đ of 1.39.

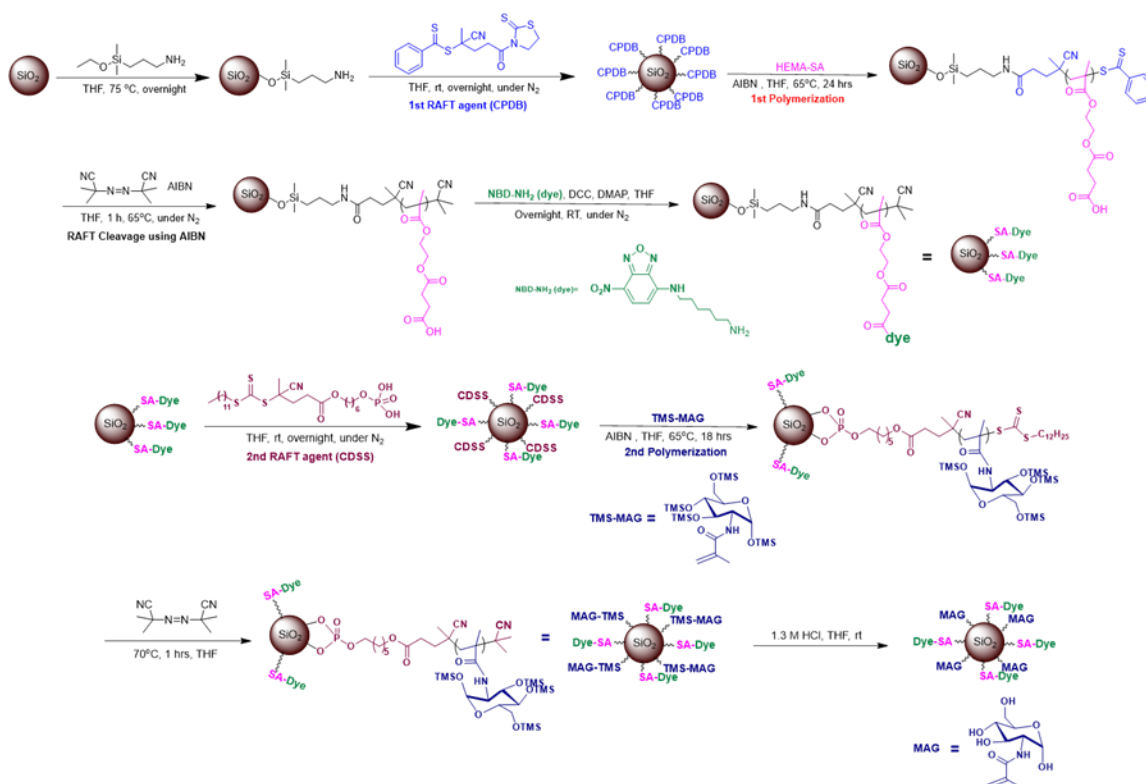
As the last step, deprotection of the glycopolymer was performed to remove the TMS groups from TMS-MAG polymer using the acid-catalyzed method in THF; 2 min of reaction at 25°C produced a quantitative and nearly instantaneous removal (>99%) of the TMS groups as confirmed by ¹H-NMR spectroscopy. On the basis of this scheme, we have successfully achieved the synthesis of bimodal sugar-monomer containing (or “sweet”) grafted nanoparticles containing two different sets of polymer chains. Bimodal grafted nanoparticles of high graft density, low molecular weight of HEMA-LA and HEMA-SA and low graft density, high molecular weight of a sugar-containing monomer (MAG) were synthesized.

The entire strategy for the synthesizing of “Bimodal Sweet Nanoparticles” using two different RAFT agents (CPDB, CDSS), via grafting-from approach, is described in Schemes 4.6, 4.7.



Scheme 4.6: Total synthesis of bimodal “sweet nanoparticles” SiO₂-g-P(HEMA-LA-dye)-P(MAG).

The bimodal RAFT polymerization grafting-from approach described above could be used to prepare several different types of bimodal polymer brush-anchored silica nanoparticles using different RAFT agents. Additionally, labeling the bimodal grafted nanoparticles with fluorescent dyes will be valuable to monitor the possible uptake by bacteria in biological systems. Figure 4.10 shows the fluorescence of the nanoparticles under UV light demonstrating that the particles retain this property even in the presence of other functionalities attached to the nanoparticle surface. The novel strategy described here opens up the



Scheme 4.7: Total synthesis of bimodal "sweet nanoparticles" SiO_2 -g-P(HEMA-SA-dye)-P(MAG).

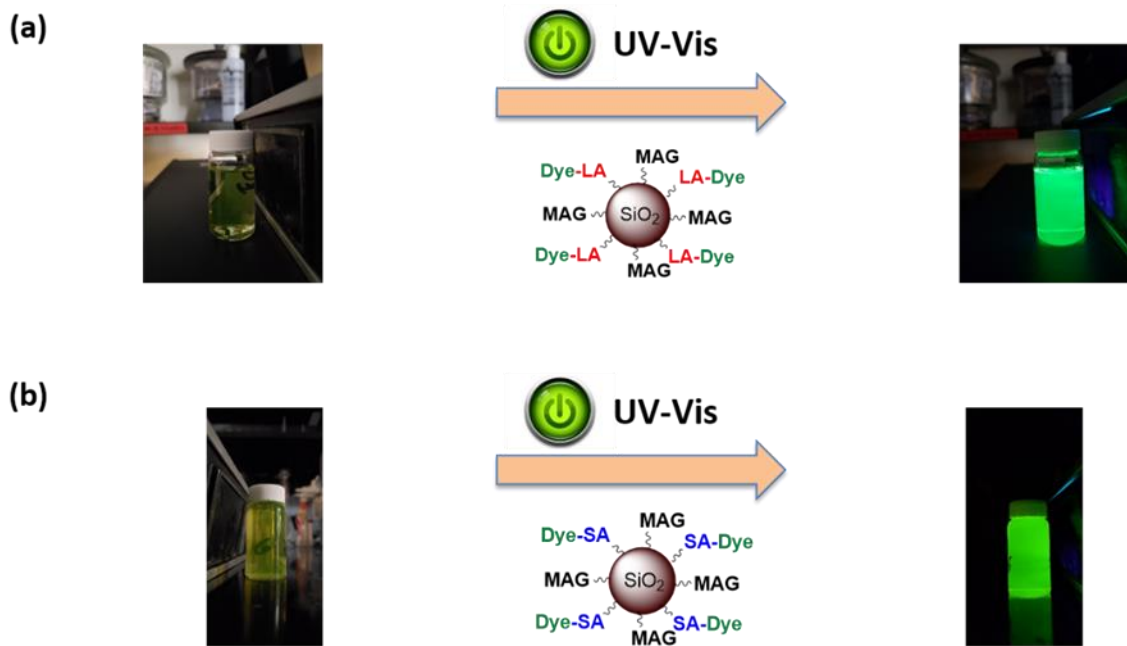


Figure 4.10: The fluorescence under UV light of the "Sweet Bimodal nanoparticles", (a) SiO_2 @P(HEMA-LA-dye)-PMAG, and (b) SiO_2 @P(HEMA-SA-

opportunity for designing a wide range of multifunctional nanoparticles and advanced polymer nanocomposites that could be used in various applications.

4.5 Conclusion:

We describe a novel synthesis of bimodal brush grafted nanoparticles that use two different RAFT agents (CPDB, CDSS) on the same nanoparticle. All of the previous reports of bimodal grafted nanoparticles were synthesized by grafting the same or different monomers using one RAFT agent, but in this research, we were able to polymerize two very different monomers using the grafting-from technique and two different chain transfer agents (CTA's), further expanding the types of functionality that can be installed on the surface of nanoparticles. These bimodal polymer grafted nanoparticles are envisioned for use as antibiotic delivery vehicles for biomedical applications. High graft density, low molecular weight of one of the "controlled release" monomers 2-((2-((2-hydroxypropanoyl)oxy)propanoyl)oxy)ethyl methacrylate (HEMA-LA) or 2-(methacryloyloxy)ethyl succinate (HEMA-SA) that contained hydrolytically sensitive ester linkages were initially grafted on the surface of the silica nanoparticles using 4-cyano-4-(phenylcarbonothioylthio) pentanoic acid (CPDB) as the first RAFT agent. The second polymer population of low graft density, high molecular weight chains made from a glycomonomer were grafted on the surface of silica nanoparticles using 4-cyano-4-[(dodecylsulfanylthiocarbonyl)

sulfanyl]pentanoic acid (CDSS) as the second RAFT agent. The bimodal grafted architecture was confirmed by GPC that showed two different peaks representing the two different polymer chain populations.

4.6 References:

- (1) Jansen, K.; Anderson, A. *Human Vaccines & Immunotherapeutic*. 2018, 14, 9, 2142-2149.
- (2) Hu, Y.; Wang, J.; Shen, Y. J. *Hazard. Mater.* 2020, 384 (September 2019), 121335.
- (3) Masadeh, M. M.; Mhaidat, N. M.; Alzoubi, K. H.; Hussein, E. I.; Al-Trad, E. I. *Infect. Drug Resist.* 2013, 6, 27–32.
- (4) Makarov, V.; Manina, G.; Mikusova, K.; Möllmann, U.; Ryabova, O.; Saint-Joanis, B.; Dhar, N.; Pasca, M. R.; Buroni, S.; Lucarelli, A. P.; Milano, A.; De Rossi, E.; Belanova, M.; Bobovska, A.; Dianiskova, P.; Kordulakova, J.; Sala, C.; Fullam, E.; Schneider, P.; McKinney, J. D.; Brodin, P.; Christophe, T.; Waddell, S.; Butcher, P.; Albrethsen, J.; Rosenkrands, I.; Brosch, R.; Nandi, V.; Bharath, S.; Gaonkar, S.; Shandil, R. K.; Balasubramanian, V.; Balganes, T.; Tyagi, S.; Grosset, J.; Riccardi, G.; Cole, S. T. *Science* (80-.). 2009, 324 (5928), 801–804.

- (5) Klein, E. Y.; Van Boeckel, T. P.; Martinez, E. M.; Pant, S.; Gandra, S.; Levin, S. A.; Goossens, H.; Laxminarayan, R. *Proc. Natl. Acad. Sci. U. S. A.* 2018, 115 (15), E3463–E3470.
- (6) Lu, C.; Quan, G.; Su, M.; Nimmagadda, A.; Chen, W.; Pan, M.; Teng, P.; Yu, F.; Liu, X.; Jiang, L.; Du, W.; Hu, W.; Yao, F.; Pan, X.; Wu, C.; Liu, D.; Cai, J. *Adv. Ther.* 2019, 2, 1900147.
- (7) Pelgrift, R. Y.; Friedman, A. J. *Adv. Drug Deliv. Rev.* 2013, 65 (13–14), 1803–1815.
- (8) Rungta, A.; Natarajan, B.; Neely, T.; Dukes, D.; Schadler, L. S.; Benicewicz, B. C. *Macromolecules* 2012, 45 (23), 9303–9311.
- (9) Abtew, E.; Ezra, A. F.; Basu, A.; Domb, A. J. *Biomacromolecules* 2019, 20 (8), 2934–2941.
- (10) Bernardi, A.; Jiménez-Barbero, J.; Casnati, A.; De Castro, C.; Darbre, T.; Fieschi, F.; Finne, J.; Funken, H.; Jaeger, K. E.; Lahmann, M.; Lindhorst, T. K.; Marradi, M.; Messner, P.; Molinaro, A.; Murphy, P. V.; Nativi, C.; Oscarson, S.; Penadés, S.; Peri, F.; Pieters, R. J.; Renaudet, O.; Reymond, J. L.; Richichi, B.; Rojo, J.; Sansone, F.; Schäffer, C.; Turnbull, W. B.; Velasco-Torrijos, T.; Vidal, S.; Vincent, S.; Wennekes, T.; Zuilhof, H.; Imberty, A. *Chem. Soc. Rev.* 2013, 42 (11), 4709–4727.

- (11) Marradi, M.; Chiodo, F.; García, I.; Penadés, S. *Chem. Soc. Rev.* 2013, 42 (11), 4728–4745.
- (12) de la Fuente, J. M.; Penadés, S. *Biochim. Biophys. Acta - Gen. Subj.* 2006, 1760 (4), 636–651.
- (13) Veerapandian, M.; Lim, S. K.; Nam, H. M.; Kuppannan, G.; Yun, K. S. *Anal. Bioanal. Chem.* 2010, 398 (2), 867–876.
- (14) Cerisy, T.; Iglesias, A.; Rostain, W.; Boutard, M.; Pelle, C.; Perret, A.; Salanoubat, M.; Fierobe, H. P.; Tolonen, A. C. *J. Bacteriol.* 2019, 201 (15), 1–13.
- (15) Disney, M. D.; Zheng, J.; Swager, T. M.; Seeberger, P. H. *J. Am. Chem. Soc.* 2004, 126 (41), 13343–13346.
- (16) Malakootikhah, J.; Rezayan, A. H.; Negahdari, B.; Nasser, S.; Rastegar, H. *Carbohydr. Polym.* 2017, 170, 190–197.
- (17) Smith, A. E.; Sizovs, A.; Grandinetti, G.; Xue, L.; Reineke, T. M. *Biomacromolecules* 2011, 12 (8), 3015–3022.
- (18) Muñoz-Bonilla, A.; Heuts, J. P. A.; Fernández-García, M. *Soft Matter* 2011, 7 (6), 2493–2499.
- (19) Hetzer, M.; Chen, G.; Barner-Kowollik, C.; Stenzel, M. H. *Macromol. Biosci.* 2010, 10 (2), 119–126.

- (20) Albertin, L.; Kohlert, C.; Stenzel, M.; Foster, J. R.; Davis, T. P.
Biomacromolecules 2004, 5 (2), 255–260.
- (21) Fraser, C.; Grubbs, R. H. Macromolecules 1995, 28 (21), 7248–7255.
- (22) Dai, X. H.; Dong, C. M.; Yan, D. J. Phys. Chem. B 2008, 112 (12), 3644–3652.
- (23) Liu, L. I.; Zhang, J.; Wenhui, L. V.; Luo, Y. A. N.; Wang, X. J. Polym. Sci.
Part A Polym. Chem. 2010, 48 (15), 3350–3361.
- (24) Suriano Fabian, Coulemblier Olivier, D. P. J. Polym. Sci. Part A Polym.
Chem. 2010, 48, 3271–3280.
- (25) Bernard, J.; Hao, X.; Davis, T. P.; Barner-Kowollik, C.; Stenzel, M. H.
Biomacromolecules 2006, 7 (1), 232–238.
- (26) Pearson Samuel, Allen Nathan, S. M. J. Polym. Sci. Part A Polym. Chem.
2009, 47, 1706–1723.
- (27) Ohno, K.; Tsujii, Y.; Miyamoto, T.; Fukuda, T.; Goto, M.; Kobayashi, K.;
Akaike, T. Macromolecules 1998, 31 (4), 1064–1069.
- (28) Dai, Xiao-Hui, D. C.-M. J. Polym. Sci. Part A Polym. Chem. 2008, 46
(September 2010), 817–829.
- (29) Ting, S. R. S.; Min, E. H.; Escalé, P.; Save, M.; Billon, L.; Stenzel, M. H.
Macromolecules 2009, 42 (24), 9422–9434.
- (30) Ting, S. R. S.; Granville, A. M.; Quémener, D.; Davis, T. P.; Stenzel, M. H.;
Barner-Kowollik, C. Aust. J. Chem. 2007, 60 (6), 405–409.

- (31) Dong, C. M.; Chaikof, E. L. *Colloid Polym. Sci.* 2005, 283 (12), 1366–1370.
- (32) Dong, C. M.; Faucher, K. M.; Chaikof, E. L. *J. Polym. Sci. Part A Polym. Chem.* 2004, 42 (22), 5754–5765.
- (33) Smeets, N. M. B.; Patenaude, M.; Kinio, D.; Yavitt, F. M.; Bakaic, E.; Yang, F. C.; Rheinstädter, M.; Hoare, T. *Polym. Chem.* 2014, 5 (23), 6811–6823.
- (34) Ishimoto, K.; Arimoto, M.; Ohara, H.; Kobayashi, S.; Ishii, M.; Morita, K.; Yamashita, H.; Yabuuchi, N. *Biomacromolecules* 2009, 10 (10), 2719–2723.
- (35) Hong, L.; Zhang, Z.; Zhang, Y.; Zhang, W. J. *Polym. Sci. Part A Polym. Chem.* 2014, 52 (18), 2669–2683.
- (36) Tous, E.; Ifkovits, J. L.; Koomalsingh, K. J.; Shuto, T.; Soeda, T.; Kondo, N.; Iii, J. H. G.; Gorman, R. C.; Burdick, J. a. *Biomacromolecules* 2011, 12 (11), 4127–4135.
- (37) Yin, L.; Dalsin, M. C.; Sizovs, A.; Reineke, T. M.; Hillmyer, M. A. *Macromolecules* 2012, 45 (10), 4322–4332.
- (38) Li, C.; Han, J.; Ryu, C. Y.; Benicewicz, B. C. *Macromolecules* 2006, 39 (9), 3175–3183.
- (39) Li, J.; Wang, L.; Benicewicz, B. C. *Langmuir* 2013, 29 (37), 11547–11553.
- (40) Woodland, J. G.; Hunter, R.; Smith, P. J.; Egan, T. J. *Org. Biomol. Chem.* 2017, 15 (3), 589–597.

- (41) Borchmann, D. E.; Tarallo, R.; Avendano, S.; Falanga, A.; Carberry, T. P.; Galdiero, S.; Weck, M. *Macromolecules* 2015, 48 (4), 942–949.
- (42) Natarajan, B.; Neely, T.; Rungta, A.; Benicewicz, B. C.; Schadler, L. S. *Macromolecules* 2013, 46, 4909–4918.
- (43) Zheng, Y.; Huang, Y.; Abbas, Z. M.; Benicewicz, B. C. *Polym. Chem.* 2016, 7 (34), 5347–5350.
- (44) Qiao, Y.; Yin, X.; Wang, L.; Islam, M. S.; Benicewicz, B. C.; Ploehn, H. J.; Tang, C. *Macromolecules* 2015, 48 (24), 8998–9006.
- (45) Virtanen, S.; Krentz, T.; Nelson, J.; Schadler, L.; Bell, M.; Benicewicz, B.; Hillborg, H.; Zhao, S. *IEEE Trans. Dielectr. Electr. Insul.* 2014, 21 (2), 563–570.
- (46) Li, Y.; Tao, P.; Viswanath, A.; Benicewicz, B. C.; Schadler, L. S. *Langmuir* 2013, 29, 1211–1220.
- (47) Feng, J.; Haasch, R. T.; Dyer, D. J. *Macromolecules* 2004, 37, 9525–9537.
- (48) Li, Y.; Benicewicz, B. C. *Macromolecules* 2008, 41 (21), 7986–7992.
- (49) Dukes, D.; Li, Y.; Lewis, S.; Benicewicz, B.; Schadler, L.; Kumar, S. K. *Macromolecules* 2010, 43 (3), 1564–1570.
- (50) Maillard, D.; Kumar, S. K.; Rungta, A.; Benicewicz, B. C.; Prud'homme, R. E. *Nano Lett.* 2011, 11, 4569–4573.

- (51) Chong, Y. K.; Moad, G.; Rizzardo, E.; Thang, S. H. *Macromolecules* 2007, 40 (13), 4446–4455.
- (52) Spaccini, R.; Pastori, N.; Clerici, A.; Punta, C.; Porta, O. J. *Am. Chem. Soc.* 2008, 130 (52), 18018–18024.
- (53) Liu, Z.; Zhang, J.; Chen, S.; Shi, E.; Xu, Y.; Wan, X. *Angew. Chemie* 2012, 124 (13), 3285–3289.
- (54) Moad, G.; Rizzardo, E.; Thang, S. H. *Aust. J. Chem.* 2012, 65 (8), 985–1076.
- (55) Lewis, R. W.; Evans, R. A.; Malic, N.; Saito, K.; Cameron, N. R. *Polym. Chem.* 2017, 8 (24), 3702–3711.
- (56) Reisch, A.; Klymchenko, A. S. *Small* 2016, 12 (15), 1968–1992.
- (57) Bhat, M. *Int. J. Curr. Eng. Technol.* 2014, 4 (4), 2711–2715.
- (58) Bell, M. H. *Ligand Engineering for Advanced Functional Composite Materials*, University of South Carolina, 2016.
- (59) Swapnil R Tale, Ligeng Yin, T. M. R. *Polym. Chem.* 2014, 5, 5160–5167.
- (60) Pearson, Samuel, Allen Nathan, S. M. H. *J. Polym. Sci. Part A Polym. Chem.* 2009, 47, 1706–1723.
- (61) Zheng, Y.; Huang, Y.; Abbas, Z. M.; Benicewicz, B. C. *Polym. Chem.* 2016, 7 (34), 5347–5350.
- (62) Bracchi, M. E.; Dura, G.; Fulton, D. A. *Polym. Chem.* 2019, 10 (10), 1258–1267.

CHAPTER 5
CONCLUSION AND FUTURE WORK

5.1 Conclusion:

The reversible addition-fragmentation chain transfer (RAFT) polymerization technique was used to functionalize polymer chains on the surface of silica nanoparticles. Monomodal and bimodal grafted silica nanoparticles were designed, synthesized and characterized to create an important platform for synthesizing nanoparticles for medical applications, especially novel strategies to combat bacterial resistance. Polymer grafted silica nanoparticles were synthesized and characterized with the goal to demonstrate new properties or functionality including: polymerization of “controlled release” monomers containing a hydrolytically sensitive ester linkage, engineering water-dispersible bimodal brush grafted silica nanoparticles as potentially antibiotic-carriers, and designing “Sweet-Nanoparticles” to enhance cell uptake of nanoparticles as part of a larger strategy to combat antibiotic-resistant bacteria.

Controlled release of polymer grafted silica nanoparticles containing a hydrolytically sensitive ester linkage was studied. Two monomers were synthesized and polymerized, 2-((2-(propionyloxy) propanoyl)oxy)ethyl methacrylate (HEMA-LA), and 4-(2-(methacryloyloxy)ethoxy)-4-oxobutanoic acid (HEMA-SA). We found the RAFT agent, 4-cyanopentanoic acid dithiobenzoate (CPDB), is compatible with the controlled radical polymerization of these monomers (HEMA-LA, HEMA-SA), with control of the molecular weight and

polydispersity. Labeled-dyes were synthesized and attached to the polymer grafted nanoparticles to monitor the release rate from the polymers. The release rates were investigated using phosphate buffer solution (PBS, pH = 7.4) at two different temperatures, 25°C and 37°C. The cumulative release rates of dye-loaded polymer grafted nanoparticles were studied over 58 days. SiO₂-g-P(HEMA-LA-dye) nanoparticles showed a dye release rate of approximately 69.23% at 25°C during the 58 days, which is an average of 18% greater than the release rate of SiO₂-g-P(HEMA-SA-dye) (51.28%). Additionally, SiO₂-g-P(HEMA-LA-dye) showed a higher release rate of approximately 82.62% at 37°C during the same period (58 days), compared with SiO₂-g-P(HEMA-SA)-dye) nanoparticles that showed a 65.17% release rate. Overall, the cumulative release rates of SiO₂-g-P(HEMA-LA-dye) nanoparticles were higher than the release rates of SiO₂-g-P(HEMA-SA-dye) at both temperatures. We ascribe these differences to the higher hydrolytic susceptibility of the lactide ester linkage compared to the “normal” esters of the succinic ester linkages.

Water-dispersible bimodal brush grafted silica nanoparticles were designed as a platform that could be used in biomedical applications as antibiotic-carriers. Bimodal grafted silica nanoparticles were synthesized using RAFT polymerization via grafting two different polymer chain populations. The first population, HEMA-LA or HEMA-SA, were functionalized on silica nanoparticles

at a high graft density and low molecular weight to use as antibiotic-delivery carriers. Subsequently, a water-dispersible monomer (methacrylic acid, MAA) was polymerized on the surface of nanoparticles at low graft density and high molecular weight for the second polymer chain population. GPC analysis confirmed the composition of the bimodal silica nanoparticle architecture. Two GPC peaks were observed, a large peak which appeared at low elution time that indicated the presence of high molecular weight and low graft density of P(MAA) chains. A second smaller peak appeared at higher elution time which represented the short brush, high graft density of the P(HEMA-SA-dye) or P(HEMA-LA-dye) chains.

Bimodal “sweet-nanoparticles” were synthesized using the grafting-from RAFT polymerization technique. This strategy created a novel platform to prepare various bimodal nanoparticles that could be used to enhance nanoparticle uptake and combat antibiotic-resistant bacteria. Additionally, we believe this is the first example of a synthesis of bimodal grafted nanoparticles using two different RAFT agents on the surface of silica nanoparticles. The first polymer chain population was polymerized on the surface of the silica nanoparticles using 4-cyano-4-(phenylcarbonothioylthio)pentanoic acid (CPDB) as a RAFT agent. Cyano-4-[(dodecylsulfanyl thiocarbonyl)sulfanyl]pentanoic acid (CDSS) was used as the second RAFT agent also anchored on the surface of the silica nanoparticles. The

first population was the high graft density and low molecular weight of P(HEMA-LA) or P(HEMA-SA). The second polymer chain population was the low graft density and high molecular weight polymer made from the glycomonomer, α -2-deoxy-2-methacrylamido 1,3,4,6-tetra-(O-trimethylsilyl) D-glucopyranose (TMS-MAG).

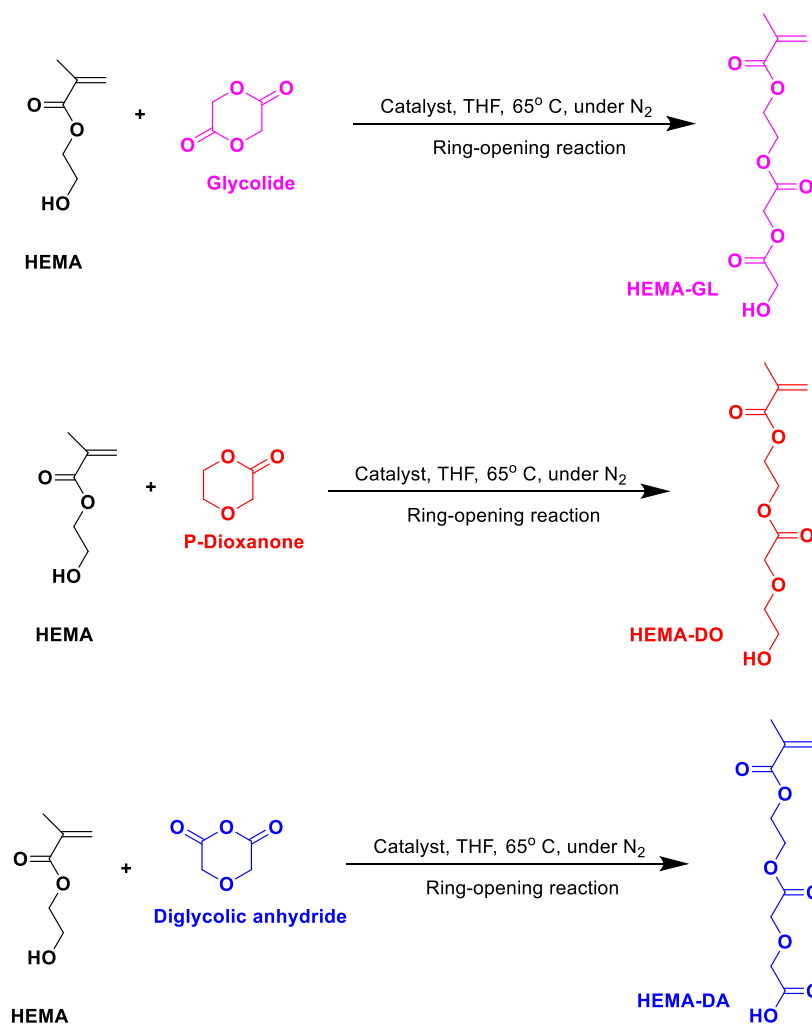
Furthermore, the composition of the bimodal brush grafted silica nanoparticle architecture was confirmed via GPC and TGA analysis. In the GPC analysis, the first peak at the low elution time was ascribed to PMAG chains of high molecular weight and low graft density. The second brush population indicated by the second GPC peak at higher elution times, was attributed to the P(HEMA-LA-dye) or P(HEMA-SA-dye) chains. TGA weight loss data correlated reasonably well with the GPC findings.

5.2 Future Work:

This thesis focused on the design, synthesis, and characterization of polymer grafted silica nanoparticles that are considered as an important platform towards designing functionalized nanoparticles that could be used in biomedical applications to combat bacterial resistance.

In this work, we polymerized two types of "controlled release" monomers (HEMA-LA, HEMA-SA) that have a reasonable release rate over 58 days. One suggestion for future research is the synthesis of different kinds of monomers that

will have a higher release rate over shorter times and to investigate their RAFT polymerization on the surface of silica nanoparticles. For instance, HEMA-GL, HEMA-DO, and HEMA-DA are derivatives formed by reacting hydroxyethylmethacrylate (HEMA) with different ring-opening compounds such as glycolide, p-dioxanone, and diglycolic anhydride, respectively (Scheme 5.1).



Scheme 5.1: Synthesis various kinds of monomers HEMA-GL, HEMA-DO, and HEMA-DA.

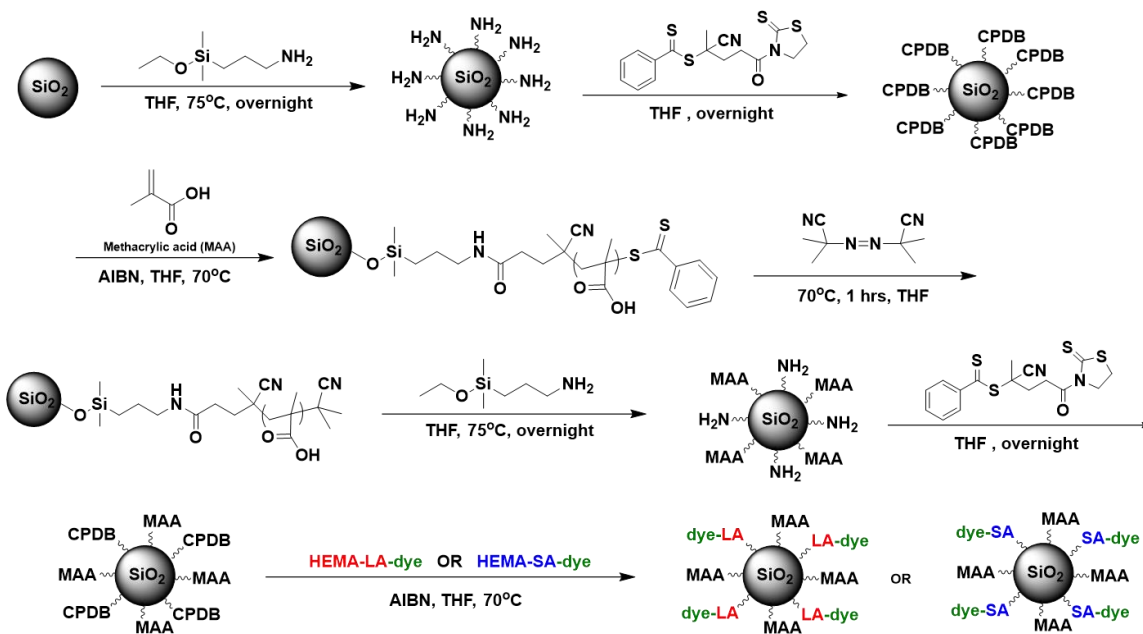
In each of these cases, the less sterically hindered and the glycolic acid linking structures are expected to increase the rate of ester hydrolysis. Comparing the cumulative release rate of HEMA-GL, HEMA-DO, and HEMA-DA with the release rate of HEMA-LA, HEMA-SA would provide further insights on tuning release rates useful for antibiotic-delivery vehicles in biomedical applications. In addition, antibiotics (instead of dyes) could be attached to the polymer (PHEMA-LA, or PHEMA-SA) that are grafted on the surface of silica nanoparticles. Once nanoparticles are grafted with polymer brushes that have antibiotics in each repeat unit, these samples will be used to study the effectiveness against bacteria using the "controlled release monomers" concept. Locally, the concentration and release of antibiotics should be much higher than many other types of drug delivery. With changes in pH conditions of the environment, it becomes possible to cleave the antibiotic from the polymer brush that is selective to the pH of the type of tissue.

One of the essential and significant roles behind synthesizing bimodal grafted nanoparticles and modifying the surface with various polymer chains is controlling the interface between the organic polymer matrix and the inorganic filler core. Moreover, achieving better properties of the polymer matrix will depend on the polymer chain populations that are grafted on the surface of nanoparticles. In many applications, water-dispersible bimodal brush grafted nanoparticles are needed where the grafting density and molecular weight of both

polymer chain populations are clearly different to enhance the various properties and dispersion in a polymer matrix. In the current work, we outlined the problem of using an aminosilane for the grafting of a second population when the first population had a sensitive ester group linkage. This was solved by using a modified RAFT agent, CPDB-phosphate group, to polymerize the methacrylic acid (MAA) as a second polymer population. In the future, another approach could be used to design water-dispersible bimodal nanoparticles by grafting the high molecular weight, low grafting density of MAA as a first polymer population and then grafting the low molecular weight, high grafting density of (HEMA-LA-dye, HEMA-SA-dye) as a second polymer population of the water-dispersible bimodal grafted nanoparticles as outlined in Scheme 5.2.

Bimodal polymer grafted silica nanoparticles were successfully synthesized via grafting two different RAFT agents (CPDB, CDSS). HEMA-LA and HEMA-SA were polymerized using CPDB as RAFT agent of the first, short brush polymer population while the second, long polymer population was made from the glycomonomer using CDSS as a RAFT agent. Thus, one of the important future works would be an investigation of the bacterial uptake of the sweet nanoparticles as the sugar coating could enhance the uptake of the nanoparticles.

Overall, this novel strategy of designing bimodal grafted nanoparticles could establish an exciting synthetic platform for various applications. Although



Scheme 5.2: The proposal new synthesis of bimodal nanoparticles SiO₂-g-P(MAA)-P(HEMA-LA-dye), and SiO₂-g-P(MAA)-P(HEMA-SA-dye).

we demonstrated a system where one of the polymer brushes of the bimodal grafted nanoparticles were dye-labeled polymers, antibiotics could be attached to the grafted-polymer instead of the dyes. This will lead to a design of bimodal grafted nanoparticles that could be used as more efficient delivery vehicles for anti-bacterial applications.

BIBLIOGRAPHY

- (1) Chiefari, J.; Chong, Y. K.; Ercole, F.; Krstina, J.; Jeffery, J.; Le, T. P. T.; Mayadunne, R. T. A.; Meijs, G. F.; Moad, C. L.; Moad, G.; Rizzardo, E.; Thang, S. H. *Macromolecules* **1998**, *31* (16), 5559–5562.
- (2) Ilgach, D. M.; Meleshko, T. K.; Yakimansky, A. V. *Polym. Sci. Ser. C* **2015**, *57* (1), 3–19.
- (3) Moad, Graeme, Ezio Rizzardo, and S. H. T. *Acc. Chem. Res.* **2008**, *41* (9), 1133–1142.
- (4) Moad, G.; Rizzardo, E.; Thang, S. H. *Aust. J. Chem.* **2005**, *58* (6), 379–410.
- (5) Moad, G.; Rizzardo, E.; Thang, S. H. *Aust. J. Chem.* **2012**, *65* (8), 985–1076.
- (6) Vazaios, A.; Lohse, D. J.; Hadjichristidis, N. *Macromolecules* **2005**, *38* (13), 5468–5474.
- (7) Li, C.; Benicewicz, B. C. *Macromolecules* **2005**, *38*, 5929–5936.
- (8) Hawker, C. J.; Bosman, A. W.; Harth, E. *Chem. Rev.* **2001**, *101* (12), 3661–3688.
- (9) Wang, J. S.; Matyjaszewski, K. *J. Am. Chem. Soc.* **1995**, *117* (20), 5614–5615.
- (10) Moad, G.; Rizzardo, E.; Thang, S. H. *Aust. J. Chem.* **2006**, *59* (10), 669–692.

- (11) Perrier, S. *Macromolecules* **2017**, *50* (19), 7433–7447.
- (12) Barner-Kowollik, C. *Handbook of RAFT Polymerization*; WILEY-VCH Verlag GmbH & Co., 2008.
- (13) Keddie, D. J.; Moad, G.; Rizzardo, E.; Thang, S. H. *Macromolecules* **2012**, *45* (13), 5321–5342.
- (14) Harvison, M. A.; Roth, P. J.; Davis, T. P.; Lowe, A. B. *Aust. J. Chem.* **2011**, *64* (8), 992–1006.
- (15) Moad, G.; Rizzardo, E.; Thang, S. H. *Polym. Int.* **2011**, *60* (1), 9–25.
- (16) Gregory, A.; Stenzel, M. H. *Prog. Polym. Sci.* **2012**, *37* (1), 38–105.
- (17) Roth, P. J.; Boyer, C.; Lowe, A. B.; Davis, T. P. *Macromol. Rapid Commun.* **2011**, *32* (15), 1123–1143.
- (18) Moad, G.; Chong, Y. K.; Mulder, R.; Rizzardo, E.; Thang, S. H. *ACS Symp. Ser.* **2009**, *1024*, 3–18.
- (19) Moad, G. *ACS Symp. Ser. 1187*, **2015**, 211–246.
- (20) Li, C.; Han, J.; Ryu, C. Y.; Benicewicz, B. C. *Macromolecules* **2006**, *39* (9), 3175–3183.
- (21) Fu, S. Y.; Feng, X. Q.; Lauke, B.; Mai, Y. W. *Compos. Part B Eng.* **2008**, *39* (6), 933–961.
- (22) Ranjan, R.; Brittain, W. J. *Macromolecules* **2007**, *40* (17), 6217–6223.

- (23) Barbey, R.; Lavanant, L.; Paripovic, D.; Schüwer, N.; Sugnaux, C.; Tugulu, S.; Klok, H. A. *Chem. Rev.* **2009**, *109* (11), 5437–5527.
- (24) Dai, Xiao-Hui, D. C.-M. *J. Polym. Sci. Part A Polym. Chem.* **2008**, *46* (September 2010), 817–829.
- (25) Brittain, W. J.; Minko, S. *J. Polym. Sci. Part A Polym. Chem.* **2007**, *45* (16), 3505–3512.
- (26) Schadler, L. S.; Kumar, S. K.; Benicewicz, B. C.; Lewis, S. L.; Harton, S. E. *MRS Bull.* **2007**, *32* (4), 335–340.
- (27) Deng, H.; McShan, D.; Zhang, Y.; Sinha, S. S.; Arslan, Z.; Ray, P. C.; Yu, H. *Environ. Sci. Technol.* **2016**, *50* (16), 8840–8848.
- (28) Li, W.; Dong, K.; Ren, J.; Qu, X. *Angew. Chemie - Int. Ed.* **2016**, *55* (28), 8049–8053.
- (29) Wang, L.; Chen, Y. P.; Miller, K. P.; Cash, B. M.; Jones, S.; Glenn, S.; Benicewicz, B. C.; Decho, A. W. *Chem. Commun.* **2014**, *50* (81), 12030–12033.
- (30) Wang, L.; Benicewicz, B. C. *ACS Macro Lett.* **2013**, *2* (2), 3–6.
- (31) Tamizharasi, S.; Rathi, V.; Rathi, J. C. *Syst. Rev. Pharm.* **2011**, *2* (1), 19–29.
- (32) Rungta, A.; Natarajan, B.; Neely, T.; Dukes, D.; Schadler, L. S.; Benicewicz, B. C. *Macromolecules* **2012**, *45* (23), 9303–9311.
- (33) Meldal, M. *Macromol. Rapid Commun.* **2008**, *29* (12–13), 1016–1051.

- (34) Kumar, S. K.; Krishnamoorti, R. *Annu. Rev. Chem. Biomol. Eng.* **2010**, *1* (1), 37–58.
- (35) Skvortsov, A. M.; Gorbunov, A. A.; Leermakers, F. A. M.; Fleer, G. J. *Macromolecules* **1999**, *32* (6), 2004–2015.
- (36) Tiwari, G.; Tiwari, R.; Bannerjee, S.; Bhati, L.; Pandey, S.; Pandey, P.; Sriwastawa, B. *Int. J. Pharm. Investig.* **2012**, *2* (1), 2.
- (37) Freiberg, S.; Zhu, X. X. *Int. J. Pharm.* **2004**, *282* (1–2), 1–18.
- (38) Langer, R. **2003**, *288* (4), 50–57.
- (39) Risbud, M. V.; Hardikar, A. A.; Bhat, S. V.; Bhonde, R. R. *J. Control. Release* **2000**, *68* (1), 23–30.
- (40) Prabakaran, M.; Grailer, J. J.; Steeber, D. A.; Gong, S. *Macromol. Biosci.* **2008**, *8* (9), 843–851.
- (41) Liu, J.; Huang, Y.; Kumar, A.; Tan, A.; Jin, S.; Mozhi, A.; Liang, X. J. *Biotechnol. Adv.* **2014**, *32* (4), 693–710.
- (42) Manatunga, D. C.; de Silva, R. M.; de Silva, K. M. N.; de Silva, N.; Bhandari, S.; Yap, Y. K.; Costha, N. P. *Eur. J. Pharm. Biopharm.* **2017**, *117*, 29–38.
- (43) Stuart, M. A. C.; Huck, W. T. S.; Genzer, J.; Müller, M.; Ober, C.; Stamm, M.; Sukhorukov, G. B.; Szleifer, I.; Tsukruk, V. V.; Urban, M.; Winnik, F.; Zauscher, S.; Luzinov, I.; Minko, S. *Nat. Mater.* **2010**, *9* (2), 101–113.

- (44) D'Souza, A. J. M.; Topp, E. M. *J. Pharm. Sci.* **2004**, *93* (8), 1962–1979.
- (45) Thambi, T.; Deepagan, V. G.; Yoo, C. K.; Park, J. H. *Polymer (Guildf)*. **2011**, *52* (21), 4753–4759.
- (46) Yang, H.; Wang, Q.; Huang, S.; Xiao, A.; Li, F.; Gan, L.; Yang, X. *ACS Appl. Mater. Interfaces* **2016**, *8* (12), 7729–7738.
- (47) Smeets, N. M. B.; Patenaude, M.; Kinio, D.; Yavitt, F. M.; Bakaic, E.; Yang, F.-C.; Rheinstädter, M.; Hoare, T. *Polym. Chem.* **2014**, *5* (23), 6811–6823.
- (48) Ishimoto, K.; Arimoto, M.; Ohara, H.; Kobayashi, S.; Ishii, M.; Morita, K.; Yamashita, H.; Yabuuchi, N. *Biomacromolecules* **2009**, *10* (10), 2719–2723.
- (49) Hong, L.; Zhang, Z.; Zhang, Y.; Zhang, W. *J. Polym. Sci. Part A Polym. Chem.* **2014**, *52* (18), 2669–2683.
- (50) Tous, E.; Ifkovits, J. L.; Koomalsingh, K. J.; Shuto, T.; Soeda, T.; Kondo, N.; Iii, J. H. G.; Gorman, R. C.; Burdick, J. a. *Biomacromolecules* **2011**, *12* (11), 4127–4135.
- (51) Li, C.; Han, J.; Ryu, C. Y.; Benicewicz, B. C. *Macromolecules* **2006**, *39* (9), 3175–3183.
- (52) Li, J.; Wang, L.; Benicewicz, B. C. *Langmuir* **2013**, *29* (37), 11547–11553.
- (53) Woodland, J. G.; Hunter, R.; Smith, P. J.; Egan, T. J. *Org. Biomol. Chem.* **2017**, *15* (3), 589–597.

- (54) Borchmann, D. E.; Tarallo, R.; Avendano, S.; Falanga, A.; Carberry, T. P.; Galdiero, S.; Weck, M. *Macromolecules* **2015**, *48* (4), 942–949.
- (55) Sanoj Rejinold, N.; Muthunarayanan, M.; Divyarani, V. V.; Sreerekha, P. R.; Chennazhi, K. P.; Nair, S. V.; Tamura, H.; Jayakumar, R. *J. Colloid Interface Sci.* **2011**, *360* (1), 39–51.
- (56) Manatunga, D. C.; de Silva, R. M.; de Silva, K. M. N.; de Silva, N.; Bhandari, S.; Yap, Y. K.; Costha, N. P. *Eur. J. Pharm. Biopharm.* **2017**, *117* (October), 29–38.
- (57) Thomas, D. B.; Convertine, A. J.; Myrick, L. J.; Scales, C. W.; Smith, A. E.; Lowe, A. B.; Vasilieva, Y. A.; Ayres, N.; McCormick, C. L. *Macromolecules* **2004**, *37* (24), 8941–8950.
- (58) Ojang, L.; Zhang, L.; Zhang, Z.; Zhou, N.; Cheng, Z.; Xiulin, Z. *J. Polym. Sci. Part A Polym. Chem.* **2010**, *48* (9), 2006–2015.
- (59) Giacomelli, C.; Schmidt, V.; Borsali, R. *Macromolecules* **2007**, *40* (6), 2148–2157.
- (60) Thilanga Liyanage, A. D.; Chen, A. J.; Puleo, D. A. *ACS Biomater. Sci. Eng.* **2018**, *4* (12), 4193–4199.
- (61) Chandrasekaran, A. R.; Jia, C. Y.; Theng, C. S.; Muniandy, T.; Muralidharan, S.; Dhanaraj, S. A. *J. Appl. Pharm. Sci.* **2011**, *1* (5), 214–217.

- (62) Leong, J.; Chin, W.; Ke, X.; Gao, S.; Kong, H.; Hedrick, J. L.; Yang, Y. Y. *Nanomedicine Nanotechnology, Biol. Med.* **2018**, *14* (8), 2666–2677.
- (63) Liu, S. Q.; Wiradharma, N.; Gao, S. J.; Tong, Y. W.; Yang, Y. Y. *Biomaterials* **2007**, *28* (7), 1423–1433.
- (64) Kim, M.; Kim, T. *Anal. Chem.* **2010**, *82* (22), 9401–9409.
- (65) Mout Rubul, Moyano Daniel, R. V. *Chem Soc Rev* **2012**, *41* (7), 2539–2544.
- (66) Danhier, F.; Ansorena, E.; Silva, J. M.; Coco, R.; Le Breton, A.; Préat, V. J. *Control. Release* **2012**, *161* (2), 505–522.
- (67) Zhao, B.; Zhu, L. *Macromolecules* **2009**, *42* (24), 9369–9383.
- (68) Fischer, S.; Salcher, A.; Kornowski, A.; Weller, H.; Förster, S. *Angew. Chemie - Int. Ed.* **2011**, *50* (34), 7811–7814.
- (69) Mackay, M. E.; Tuteja, A.; Duxbury, P. M.; Hawker, C. J.; Van Horn, B.; Guan, Z.; Chen, G.; Krishnan, R. S. *Science* (80-.). **2006**, *311* (5768), 1740–1743.
- (70) Wang, L.; Cole, M.; Li, J.; Zheng, Y.; Chen, Y. P.; Miller, K. P.; Decho, A. W.; Benicewicz, B. C. *Polym. Chem.* **2015**, *6* (2), 248–255.
- (71) Wang, L.; Benicewicz, B. C. *ACS Macro Lett.* **2013**, *2* (2), 173–176.
- (72) Vaia, R. A.; Maguire, J. F. *Chem. Mater.* **2007**, *19*, 2736–2751.
- (73) Zhao, B.; He, T. *Macromolecules* **2003**, *36* (23), 8599–8602.
- (74) Chen, H.; Hsieh, Y. Lo. *Biotechnol. Bioeng.* **2005**, *90* (4), 405–413.

- (75) Matyjaszewski, K.; Xia, J. *Chem. Rev.* **2001**, *101* (9), 2921–2990.
- (76) Feng, W.; Lv, W.; Qi, J.; Zhang, G.; Zhang, F.; Fan, X. *Macromol. Rapid Commun.* **2012**, *33*, 133–139.
- (77) Yilmaz, G.; Demir, B.; Timur, S.; Becer, C. R. *Biomacromolecules* **2016**, *17* (9), 2901–2911.
- (78) Wang, L.; Chen, Y. P.; Miller, K. P.; Cash, B. M.; Jones, S.; Glenn, S.; Benicewicz, B. C.; Decho, A. W. *Chem. Commun.* **2014**, *50* (81), 12030–12033.
- (79) Chen, H.; Xia, L.; Fu, W.; Yang, Z.; Li, Z. *Chem. Commun.* **2013**, *49* (13), 1300–1302.
- (80) Yuan, J.; Lu, Y.; Schacher, F.; Lunkenbein, T.; Weiss, S.; Schmalz, H.; Müller, A. H. E. *Chem. Mater.* **2009**, *21* (18), 4146–4154.
- (81) Qu, H.; Caruntu, D.; Liu, H.; O'Connor, C. J. *Langmuir* **2011**, *27* (6), 2271–2278.
- (82) Pelet, J. M.; Putnam, D. *Macromolecules* **2009**, *42* (5), 1494–1499.
- (83) De, M.; Ghosh, P. S.; Rotello, V. M. *Adv. Mater.* **2008**, *20* (22), 4225–4241.
- (84) Cash, B. M.; Wang, L.; Benicewicz, B. C. *J. Polym. Sci. Part A Polym. Chem.* **2012**, *50* (13), 2533–2540.
- (85) Pothayee, N.; Pothayee, N.; Jain, N.; Hu, N.; Balasubramaniam, S.; Johnson, L. M.; Davis, R. M.; Sriranganathan, N.; Riffle, J. S. *Chem. Mater.* **2012**, *24* (11), 2056–2063.

- (86) Smeets, N. M. B.; Patenaude, M.; Kinio, D.; Yavitt, F. M.; Bakaic, E.; Yang, F. C.; Rheinstädter, M.; Hoare, T. *Polym. Chem.* **2014**, *5* (23), 6811–6823.
- (87) Li, Y.; Benicewicz, B. C. *Macromolecules* **2008**, *41* (21), 7986–7992.
- (88) Dukes, D.; Li, Y.; Lewis, S.; Benicewicz, B.; Schadler, L.; Kumar, S. K. *Macromolecules* **2010**, *43* (3), 1564–1570.
- (89) Maillard, D.; Kumar, S. K.; Fragneaud, B.; Kysar, J. W.; Rungta, A.; Benicewicz, B. C.; Deng, H.; Brinson, L. C.; Douglas, J. F. *Nano Lett.* **2012**, *12* (8), 3909–3914.
- (90) Chong, Y. K.; Moad, G.; Rizzardo, E.; Thang, S. H. *Macromolecules* **2007**, *40* (13), 4446–4455.
- (91) Sahoo, Y.; Goodarzi, A.; Swihart, M. T.; Ohulchansky, T. Y.; Kaur, N.; Furlani, E. P.; Prasad, P. N. *J. Phys. Chem. B* **2005**, *109* (9), 3879–3885.
- (92) Peng, H. S.; Chiu, D. T. *Chem. Soc. Rev.* **2015**, *44* (14), 4699–4722.
- (93) Canning, S. L.; Neal, T. J.; Armes, S. P. *Macromolecules* **2017**, *50* (16), 6108–6116.
- (94) Evans, G.; Duong, G. V.; Ingleson, M. J.; Xu, Z.; Jones, J. T. A.; Khimyak, Y. Z.; Claridge, J. B.; Rosseinsky, M. J. *Adv. Funct. Mater.* **2010**, *20* (2), 231–238.
- (95) Li, Y.; Tao, P.; Viswanath, A.; Benicewicz, B. C.; Schadler, L. S. *Langmuir* **2013**, *29*, 1211–1220.

- (96) Li, J.; Khanchaitit, P.; Han, K.; Wang, Q. *Chem. Mater.* **2010**, *22* (18), 5350–5357.
- (97) Zheng, Y.; Abbas, Z. M.; Sarkar, A.; Marsh, Z.; Stefik, M.; Benicewicz, B. C. *Polymer (Guildf)*. **2018**, *135*, 193–199.
- (98) Burdyńska, J.; Daniel, W.; Li, Y.; Robertson, B.; Sheiko, S. S.; Matyjaszewski, K. *Macromolecules* **2015**, *48* (14), 4813–4822.
- (99) Tadano, T.; Zhu, R.; Muroga, Y.; Hoshi, T.; Sasaki, D.; Yano, S.; Sawaguchi, T. *Polym. J.* **2014**, *46* (6), 342–348.
- (100) Hudson, J. A. *Fighting antimicrobial resistance*; 2018; Vol. 32.
- (101) Hu, Y.; Wang, J.; Shen, Y. *J. Hazard. Mater.* **2020**, *384* (September 2019), 121335.
- (102) Masadeh, M. M.; Mhaidat, N. M.; Alzoubi, K. H.; Hussein, E. I.; Al-Trad, E. *I. Infect. Drug Resist.* **2013**, *6*, 27–32.
- (103) Makarov, V.; Manina, G.; Mikusova, K.; Möllmann, U.; Ryabova, O.; Saint-Joanis, B.; Dhar, N.; Pasca, M. R.; Buroni, S.; Lucarelli, A. P.; Milano, A.; De Rossi, E.; Belanova, M.; Bobovska, A.; Dianiskova, P.; Kordulakova, J.; Sala, C.; Brodin, P.; Christophe, T.; Waddell, S.; Butcher, P.; Albrethsen, J.; Rosenkrands, I.; Brosch, R.; Nandi, V.; Bharath, S.; Gaonkar, S.; Shandil, R. K.; Balasubramanian, V.; Balganes, T.; Tyagi, S.; Grosset, J.; Riccardi, G.; Cole, S. T. *Science (80-.)*. **2009**, *324* (5928), 801–804.

- (104) Klein, E. Y.; Van Boeckel, T. P.; Martinez, E. M.; Pant, S.; Gandra, S.; Levin, S. A.; Goossens, H.; Laxminarayan, R. *Proc. Natl. Acad. Sci. U. S. A.* **2018**, *115* (15), E3463–E3470.
- (105) Lu, C.; Quan, G.; Su, M.; Nimmagadda, A.; Chen, W.; Pan, M.; Teng, P.; Yu, F.; Liu, X.; Jiang, L.; Du, W.; Hu, W.; Yao, F.; Pan, X.; Wu, C.; Liu, D.; Cai, J. *Adv. Ther.* **2019**, 1900147, 1900147.
- (106) Pelgrift, R. Y.; Friedman, A. J. *Adv. Drug Deliv. Rev.* **2013**, *65* (13–14), 1803–1815.
- (107) Abtew, E.; Ezra, A. F.; Basu, A.; Domb, A. J. *Biomacromolecules* **2019**, *20* (8), 2934–2941.
- (108) Bernardi, A.; Jiménez-Barbero, J.; Casnati, A.; De Castro, C.; Darbre, T.; Fieschi, F.; Finne, J.; Funken, H.; Jaeger, K. E.; Lahmann, M.; Lindhorst, T. K.; Marradi, M.; Messner, P.; Molinaro, A.; Murphy, P. V.; Nativi, C.; Oscarson, S.; Penadés, S.; Peri, F.; Pieters, R. J.; Renaudet, O.; Reymond, J. L.; Richichi, B.; Rojo, J.; Sansone, F.; Schäffer, C.; Turnbull, W. B.; Velasco-Torrijos, T.; Vidal, S.; Vincent, S.; Wennekes, T.; Zuilhof, H.; Imberty, A. *Chem. Soc. Rev.* **2013**, *42* (11), 4709–4727.
- (109) Marradi, M.; Chiodo, F.; García, I.; Penadés, S. *Chem. Soc. Rev.* **2013**, *42* (11), 4728–4745.

- (110) de la Fuente, J. M.; Penadés, S. *Biochim. Biophys. Acta - Gen. Subj.* **2006**, *1760* (4), 636–651.
- (111) Veerapandian, M.; Lim, S. K.; Nam, H. M.; Kuppannan, G.; Yun, K. S. *Anal. Bioanal. Chem.* **2010**, *398* (2), 867–876.
- (112) Cerisy, T.; Iglesias, A.; Rostain, W.; Boutard, M.; Pelle, C.; Perret, A.; Salanoubat, M.; Fierobe, H. P.; Tolonen, A. C. J. *Bacteriol.* **2019**, *201* (15), 1–13.
- (113) Disney, M. D.; Zheng, J.; Swager, T. M.; Seeberger, P. H. *J. Am. Chem. Soc.* **2004**, *126* (41), 13343–13346.
- (114) Malakootikhah, J.; Rezayan, A. H.; Negahdari, B.; Nasser, S.; Rastegar, H. *Carbohydr. Polym.* **2017**, *170*, 190–197.
- (115) Smith, A. E.; Sizovs, A.; Grandinetti, G.; Xue, L.; Reineke, T. M. *Biomacromolecules* **2011**, *12* (8), 3015–3022.
- (116) Muñoz-Bonilla, A.; Heuts, J. P. A.; Fernández-García, M. *Soft Matter* **2011**, *7* (6), 2493–2499.
- (117) Hetzer, M.; Chen, G.; Barner-Kowollik, C.; Stenzel, M. H. *Macromol. Biosci.* **2010**, *10* (2), 119–126.
- (118) Albertin, L.; Kohlert, C.; Stenzel, M.; Foster, J. R.; Davis, T. P. *Biomacromolecules* **2004**, *5* (2), 255–260.
- (119) Fraser, C.; Grubbs, R. H. *Macromolecules* **1995**, *28* (21), 7248–7255.

- (120) Dai, X. H.; Dong, C. M.; Yan, D. J. *Phys. Chem. B* **2008**, *112* (12), 3644–3652.
- (121) Liu, L. I.; Zhang, J.; Wenhui, L. V.; Luo, Y. A. N.; Wang, X. J. *Polym. Sci. Part A Polym. Chem.* **2010**, *48* (15), 3350–3361.
- (122) Suriano Fabian, Coulemblier Olivier, D. P. *J. Polym. Sci. Part A Polym. Chem.* **2010**, *48*, 3271–3280.
- (123) Bernard, J.; Hao, X.; Davis, T. P.; Barner-Kowollik, C.; Stenzel, M. H. *Biomacromolecules* **2006**, *7* (1), 232–238.
- (124) Pearson Samuel, Allen Nathan, S. M. *J. Polym. Sci. Part A Polym. Chem.* **2009**, *47*, 1706–1723.
- (125) Ohno, K.; Tsujii, Y.; Miyamoto, T.; Fukuda, T.; Goto, M.; Kobayashi, K.; Akaike, T. *Macromolecules* **1998**, *31* (4), 1064–1069.
- (126) Ting, S. R. S.; Min, E. H.; Escalé, P.; Save, M.; Billon, L.; Stenzel, M. H. *Macromolecules* **2009**, *42* (24), 9422–9434.
- (127) Ting, S. R. S.; Granville, A. M.; Quémener, D.; Davis, T. P.; Stenzel, M. H.; Barner-Kowollik, C. *Aust. J. Chem.* **2007**, *60* (6), 405–409.
- (128) Dong, C. M.; Chaikof, E. L. *Colloid Polym. Sci.* **2005**, *283* (12), 1366–1370.
- (129) Dong, C. M.; Faucher, K. M.; Chaikof, E. L. *J. Polym. Sci. Part A Polym. Chem.* **2004**, *42* (22), 5754–5765.
- (130) Yin, L.; Dalsin, M. C.; Sizovs, A.; Reineke, T. M.; Hillmyer, M. A. *Macromolecules* **2012**, *45* (10), 4322–4332.

- (131) Li, C.; Han, J.; Ryu, C. Y.; Benicewicz, B. C. *Macromolecules* **2006**, *39* (9), 3175–3183.
- (132) Natarajan, B.; Neely, T.; Rungta, A.; Benicewicz, B. C.; Schadler, L. S. *Macromolecules* **2013**, *46*, 4909–4918.
- (133) Zheng, Y.; Huang, Y.; Abbas, Z. M.; Benicewicz, B. C. *Polym. Chem.* **2016**, *7* (34), 5347–5350.
- (134) Qiao, Y.; Yin, X.; Wang, L.; Islam, M. S.; Benicewicz, B. C.; Ploehn, H. J.; Tang, C. *Macromolecules* **2015**, *48* (24), 8998–9006.
- (135) Virtanen, S.; Krentz, T.; Nelson, J.; Schadler, L.; Bell, M.; Benicewicz, B.; Hillborg, H.; Zhao, S. *IEEE Trans. Dielectr. Electr. Insul.* **2014**, *21* (2), 563–570.
- (136) Feng, J.; Haasch, R. T.; Dyer, D. J. *Macromolecules* **2004**, *37*, 9525–9537.
- (137) Maillard, D.; Kumar, S. K.; Rungta, A.; Benicewicz, B. C.; Prud'homme, R. E. *Nano Lett.* **2011**, *11*, 4569–4573.
- (138) Spaccini, R.; Pastori, N.; Clerici, A.; Punta, C.; Porta, O. *J. Am. Chem. Soc.* **2008**, *130* (52), 18018–18024.
- (139) Liu, Z.; Zhang, J.; Chen, S.; Shi, E.; Xu, Y.; Wan, X. *Angew. Chemie* **2012**, *124* (13), 3285–3289.
- (140) Lewis, R. W.; Evans, R. A.; Malic, N.; Saito, K.; Cameron, N. R. *Polym. Chem.* **2017**, *8* (24), 3702–3711.

- (141) Reisch, A.; Klymchenko, A. S. *Small* **2016**, *12* (15), 1968–1992.
- (142) Bhat, M. *Int. J. Curr. Eng. Technol.* **2014**, *4* (4), 2711–2715.
- (143) Bell, M. H. *Ligand Engineering for Advanced Functional Composite Materials*, University of South Carolina, 2016.
- (144) Swapnil R Tale, Ligeng Yin, T. M. R. *Polym. Chem.* **2014**, *5*, 5160–5167.
- (145) Pearson, Samuel, Allen Nathan, S. M. H. *J. Polym. Sci. Part A Polym. Chem.* **2009**, *47*, 1706–1723.
- (146) Zheng, Y.; Huang, Y.; Abbas, Z. M.; Benicewicz, B. C. *Polym. Chem.* **2016**, *7* (34), 5347–5350.
- (147) Bracchi, M. E.; Dura, G.; Fulton, D. A. *Polym. Chem.* **2019**, *10* (10), 1258–1267.
- (148) Spanswick, J.; Matyjaszewski, K.; Spanswick, J. *Mater. Today* **2005**, *8* (3), 26–33.